The Hygrothermal Performance of Exterior Insulated Wall Systems

by

Trevor Trainor

A thesis

presented to the University of Waterloo

in fulfillment of the

thesis requirement for the degree of

Master of Applied Science

in

Civil Engineering

Waterloo, Ontario, Canada, 2014

Authors Declaration

I hereby declare that I am the sole author of this thesis. This is a true copy of the thesis, including any required final revisions, as accepted by my examiners.

I understand that my thesis may be made electronically available to the public.

Trevor M. Trainor

Abstract

As energy certification programs and mandatory governmental building codes demand better building energy performance, the development of durable, highly insulated wall systems has become a top priority. Wood framed walls are the most common form of residential wall in North America and the materials used are vulnerable to moisture damage. This damage typically occurs first at the wall sheathing in the form of mould, fungal growth and rot. Increased thermal resistance can lead to two potential issues related to moisture durability: 1) increased potential for air leakage condensation at the sheathing and 2) decreased ability of the wall to dry after a wetting event.

A natural exposure experimental study was performed at the University of Waterloo's BEGHUT test facility to evaluate the hygrothermal performance of exterior insulated wall systems utilizing 3 different insulation types. These walls had approximately 2/3 of their total thermal resistance interior to the sheathing and 1/3 exterior to the sheathing. These walls were compared to a standard construction wall and a highly insulated double stud wall system. The test walls were evaluated during as-built conditions and during imposed wetting conditions. Moisture was introduced into the walls in two phases. The air injection wetting phase was designed to evaluate air leakage condensation potential during winter conditions, and the wetting mat wetting phase simulated an exterior rain leak and was used to evaluate the drying potential of the test walls. Hourly temperature, relative humidity and moisture content measurements were taken at multiple locations within each test wall. This data was analyzed to determine the air leakage condensation potential and the drying capability of each test wall.

Results showed that the effective thermal resistance of the polyisocyanurate (PIC) insulation was significantly less than its nominal R-value rating under cold and moderate temperature conditions, and slightly higher under hot conditions. The effective thermal resistance of the extruded polystyrene (XPS) insulation was slightly less than its rated value under cold and moderate temperature conditions and significantly less under hot conditions. The rockwool (RW) insulation performed slightly above its rated thermal resistance under cold and moderate conditions and slightly less under hot conditions.

Results also showed that only the double stud wall was vulnerable to winter-time interstitial condensation during the as-built (air-sealed) condition. This was a result of the hygroscopic nature of the cellulose insulation and a large temperature gradient across the insulation cavity. During the air leakage wetting phase, all of the exterior insulated walls showed a significantly decreased risk of air leakage condensation compared to the Datum and Double stud walls. During and following the wetting mat wetting phase, the PIC and XPS walls showed significantly reduced drying capability, while the RW wall showed a small reduction in drying capacity compared to the Datum and Double stud walls.

It was concluded that adding insulation exterior to the wall sheathing can be an effective method to minimize air leakage condensation. The minimum ratio of exterior to interior insulation, however, must be suitable for the local climate and interior humidity conditions. Exterior insulation materials with low vapour permeability can significantly reduce the drying capacity of a wall system, but may be appropriate where exterior solar vapour drive is a concern or sufficient drying to the interior is available. Exterior insulation materials with high vapour permeability facilitate drying to the exterior and dry nearly as well as wall systems with no exterior insulation.

Acknowledgments

I would like to acknowledge the other contributors to this thesis:

Dr. John Straube, for his inspiration, mentorship and guidance.

Mike Fox for his collaboration on the design, construction and instrumentation of the test walls.

Fellow students Lorne, Rob and Emily for their help with construction.

My colleagues, Aaron, Jonathan, Alex and Chris for their technical help and advice.

My wife Erin for inspiring me and supporting me in everything I do.

My boys Neil, Dailey and Nolan for making my life so fun and exciting.

Table of Contents

List of Figures

List of Tables

1 Introduction

In Canada, buildings account for approximately 31% of all energy consumed. Residential energy use alone, costs Canadians $28.3 billion per year (NRCan, 2011). Due to the increased cost (both financially and environmentally) of harvesting, delivering and consuming this energy, reducing the energy footprint of buildings has become the focus of both governmentally mandated building codes and voluntary certification programs. Of all of the energy consumed in Canadian buildings, space conditioning accounts for more than half and presents the greatest opportunity for improvement. Improving the thermal resistance of the building enclosure is considered by many to be the most cost-effective method of reducing space conditioning demands.

Government codes and green building certification programs are now recognizing this opportunity. A revision to the 2012 Ontario Building Code requires an improvement in the thermal resistance of the building enclosure of 20- 25% relative to the previous code, (or equivalent improvements in mechanical systems). Voluntary programs such as R-2000, Energy Star and Passivhaus require even greater levels of thermal resistance for certification.

In their development of a national sustainable housing initiative (Equilibrium Home), the Canadian Mortgage Housing Corp. found that permanent fixed components such as walls are the most reasonable, cost-effective, low-maintenance and prudent investment in the pursuit of low energy homes (CMHC, 2007). The U.S. Department of Energy (DOE) agrees, stating that the top priority in pursuit of a cost-neutral, net-zero energy home design is to develop a durable high-R wall design for cold climates (Anderson & Roberts, 2008).

One major concern with increasing the thermal resistance of wall assemblies is that the durability of the building may be compromised. Wood framed walls are the most common form of residential wall in North America and the materials used are vulnerable to moisture damage. This damage typically occurs first at the wall sheathing in the form of mould, fungal growth and rot. Increased thermal resistance can lead to two potential issues related to moisture: 1) increased potential for air leakage condensation at the sheathing and 2) decreased ability of the wall to dry after a wetting event.

In wall designs where 100% of the insulation is within the framing cavity, the wall sheathing closely follows the exterior temperature conditions. The greater the thermal resistance within the framing cavity, the closer the sheathing temperature will be to the exterior temperature. In cold climates, this results in sheathing temperatures which are below the interior air dew point for a large percent of the year. Under these conditions, even small amounts of exfiltrating air can result in significant amounts of condensation on the interior surface of the sheathing. Without the proper conditions for drying, moisture can quickly accumulate within the wall cavity, leading to mould growth and deterioration of the framing materials.

In wall designs where insulation is placed exterior to the wall sheathing, the sheathing temperature lies somewhere in between the interior and exterior conditions. If the ratio of thermal resistance interior and exterior to the sheathing is properly designed for a given climate, the sheathing will remain above the dew point of the interior air for most of the winter and air leakage condensation potential will be greatly reduced.

By definition, a high-R wall will experience less heat flow through it than a standard wall design. This reduction of energy flow can adversely affect the ability of the wall system to dry out after a wetting event. With limited energy flow through the wall during the winter, these wall systems must be able to safely store moisture until warmer weather allows for drying to the exterior. In a wall system with 100% of insulation within the framing cavity, the sheathing is closely linked with the exterior conditions. With access to heat energy from the exterior and low resistance to vapour in that direction, drying can occur quickly.

In exterior insulated wall systems, less heat energy is available for drying to the exterior during warm weather. Also, depending on the vapour permeability of the exterior insulation layer, the flow of vapour to the exterior may be slowed significantly. This can result in a much slower rate of drying and cause the moisture sensitive materials to be wetter for a longer period of time.

Understanding and predicting heat energy and moisture movement into, within and through an assembly is of fundamental importance to predicting and improving the durability of highly insulated wall systems. Further research is needed to establish design guidelines for optimizing thermal and moisture performance considerations in various climate zones.

1.1 Scope

This thesis focuses on highly insulated (high-R) wall designs for low energy houses in the Canadian climate. For the purpose if this Thesis, a high-R wall system is a wall with a minimum thermal resistance of RSI 6.12 (R-35). The performance of these types of wall systems with respect to air leakage condensation potential and drying capacity will be discussed. Much of the information discussed and conclusions made will also apply to other wood-framed wall systems and other climate zones.

The walls that were part of the experimental program were RSI 6.2 nominal (R– 36) including approximately 1/3 of the thermal resistance on the exterior of the structure. All of the assemblies studied were composed of readily available and approved materials. Performance was studied under different imposed wetting conditions, and the natural climate conditions at Waterloo, Ontario, Canada.

1.2 Objective

The objective of this thesis is to improve the understanding of the moisture-related durability performance of exterior insulated, high-R, wood-framed wall systems. This knowledge will help the construction industry meet the increasing requirements for building energy efficiency mandated by building codes while minimizing the risk of moisture-related durability issues. The primary focus of the study will be on air leakage condensation potential and the ability of the wall system to dry after a wetting event. This information will be used to predict the long term durability of these wall systems and can then be used in conjunction with laboratory testing and computer modeling to develop design guidelines for various Canadian climate zones.

1.3 Approach

The approach for evaluating the hygrothermal performance of exterior insulated wall systems included a review of the theory and past research, as well as experimental field exposure testing.

In the experimental portion of this study, three different exterior insulated walls were compared to a standard residential wall, to a double-stud cellulose wall and to each other under field exposure conditions. The temperature, relative humidity, and moisture content of different components of the wall assemblies were measured and used to make these comparisons. Imposed periods of wetting were used for the evaluation of wall performance under air exfiltration and rain leakage conditions. The data collected from this field testing is also used to predict the relative durability of these assemblies.

2 Background

2.1 The History of Low Energy Housing

2.1.1 Introduction

Prior to the discovery and distribution of electricity, oil, gas and coal, all houses were inherently low energy homes. Because only small amounts of energy were available at the home site, only small amounts were consumed. Another characteristic of these homes was a very low level of comfort and convenience. Primitive homes were built of whatever materials were locally available, including stones, sticks, dirt, clay, snow and animal skins. These homes required very little energy, because they were very small, had few conveniences and many occupants. The occupants also had a very high tolerance for discomfort. When heat was required, it was usually provided by burning wood or other combustible materials in an open pit.

Some early civilizations also developed strategies such as sighting, orientation, thermal mass and shading to utilize energy from the sun to heat living spaces. Passive solar strategies do not involve low amounts of energy, but rather large amounts of free energy from the sun. These strategies have been demonstrated for thousands of years, by necessity, before the invention of mechanical heating systems. The famous roman bath houses of the first century BC were built with large south facing windows to let in the heat (Perlin, 2013), while the Anasazi Indians of North America utilized south-facing cliff dwellings that were shaded by the cliffs in the summer, but allowed direct sunlight in the winter (Lea, 2010).

With advancement in housing technology, including the invention of residential mechanical heating systems, much of this knowledge was lost or ignored in the mainstream housing industry. There were however visionary researchers and designers experimenting with these strategies in North America as far back as the 1930s and 40s, starting with an accidental discovery by architect George F. Keck. Keck was commissioned to build 'The House of Tomorrow' for the 1933 Chicago World's Fair. The house he designed was a three-story, 12-sided building with 90 percent plate glass walls. Keck chose the glass structure for its aesthetics, not its solar collecting properties. During construction, Keck noticed that it was warm inside the building, even before the installation of the heating system. He realized that the sunlight illuminating the interior also heated the concrete floor slab, which in turn, radiated heat after the sun set. It was also discovered that due to the extensive areas of un-insulated glass, heat loss was rapid. Keck went on to experiment with and build upon the discoveries he made in the House of Tomorrow. This work culminated in his first comprehensive solar design in 1940, a house for real estate developer Howard Sloan. It was an elongated home which gave all major rooms southern exposure and had a high projecting shed roof above the south facing clerestory windows. The Chicago Tribune dubbed this a 'Solar Home', the first time the term had been used. Howard Sloan then went on to build a 30-house development called Solar Park, the first completely sun-oriented residential community in the modern U.S. (Zonkel, 1998).

Other early leaders in the solar home movement include the team from the Massachusetts Institute of Technology (MIT) who created Solar 1 in 1939. Solar I was designed by Professor Hoyt C. Hottel, and is considered the first building in America to be intentionally heated using only the sun's energy. It was a single story house-like structure containing two rooms and functioned as an experimental lab. To heat the building, a sun heat trap, tilted at a 30 degree angle was placed on the roof under three layers of glass. The bottom of the heat trap was a sheet of copper painted black. Water circulated through tubes below the heat trap and was stored in metal tank located in the basement until needed (Denzer, 2013).

The architect Frank Lloyd Wright used passive solar principles in some of his designs. The most notable example of Wright's solar works was the Jacobs House, built in 1944 in Wisconsin, which was also known as the "Solar Hemicycle". This house was a two story semi-circular plan with a vast expanse of glass on the south elevation. The north, east and west sides of the house were bermed with earth for thermal resistance and to protect the house from the cold north winds. The lower level featured a concrete floor and limestone walls for thermal mass and a completely open floor plan (Aitken, 2011)

Outside of a few visionary researchers and designers who were experimenting with solar heating strategies, the homes built in North America before about 1930 were heated by the combustion of coal and/or wood. With the invention in the 1920s of the residential oil furnace, a new era in residential heating began. Due to the convenience and low cost of oil heat, by the 1960s the vast majority of homes in North America were heated with oil furnaces.

The modern era of low energy housing design began in 1973. Due to geo-political turmoil in the Middle-east, the OPEC (Organization of the Petroleum Exporting Countries) oil cartel -- which controlled 50% of world oil production -- raised oil prices by 70 percent overnight. In November 1973, all Arab oil-producing nations stopped shipping oil to the U.S. The OPEC oil embargo caused the price of oil to rise from $3.56 a barrel in October 1973 to $11.65 in January 1974 (Holladay, 2010). Since heating oil was the main source of space heating, this dramatic change in the price and availability of oil started a chain of events that continue today.

Due to the realization that oil will not always be cheap and plentiful, many parallel steps were taken to investigate and improve the energy required for heating homes in North America. Several government initiated programs helped kick-start the modern approach to low energy homes.

In 1974, Princeton University's Center for Energy and Environmental Studies received a federal grant to study residential heat loss. At the Center, a group that included Ken Gadsby, Gautam Dutt, David Harrje, and Frank Sinden performed research that has led to our current understanding of the importance of air-tightness and air pressure dynamics in residential heat loss.

This research lead the US government to implement the 'Weatherization assistance program' in 1976. The program provided funds to low income home owners and renters for air sealing measures to reduce home heating costs and conserve fuel oil. In 1977, the US government created an entire federal department, 'The Department of Energy', dedicated to studying energy use. In Canada, oil price increases lead the federal government to create a government-owned petroleum company in 1975 called PetroCanada and to create the National Energy Program in 1980.

During the 70s and 80s, two distinct approaches to low energy buildings developed: the passive solar approach and the super-insulation approach. Although these approaches had overlapping goals, time lines and technologies, they began as quite distinct concepts.

2.1.2 The Passive Solar Approach

The passive solar approach was an extension of the work of Keck and others. It was based on the philosophy that most, if not all heating loads for a house could be provided by the sun via direct gain through windows. One of the defining features of these passive solar houses was large areas of south-facing windows. Those who had previously attempted this approach soon realized that large amounts of solar radiation energy could be brought into the house with the use of extensive glazing and trapped via the greenhouse effect. South-facing window areas of 10 to 20% of floor area were commonly specified. They also learned that the practical challenges of this approach were to avoid overheating during the day and heat loss through the windows at night. To overcome these wide temperature swings, and to store solar energy for use at night and cloudy days, unique technologies were developed.

The primary approach was to increase the thermal mass within the house, through the use of concrete floor slabs, masonry interior walls, or added layers of gypsum. Surfaces exposed to direct sun were made dark-colored and of thermally massive materials. Another important aspect of passive solar design was the care taken to design both fixed and operable shades to minimize overheating in summer, spring and fall. To reduce night time heat loss, moveable insulating shutters were developed and deployed (Shurcliff, 1980).

More radical approaches, which impacted the design of the house more than passive direct gain systems, also were attempted. Invented in 1960's, the Trombe wall is a mass-wall situated behind a wall of windows, with an air-space to capture and store the sun's energy (Mazria, 1979). Vents are then opened to allow convection of the heat to the rest of the house during the day and closed to prevent heat loss at night. A similar concept uses vertical black-painted water-filled tanks for thermal storage. The Barra system consisted of a similar collector wall and utilized the thermosiphon effect to distribute the warm air through channels in the concrete slab floor (Barra et al., 1987).

Attempts to simplify the more radical approaches and overcome some of their less desirable constraints developed later. One example is the "solar slab" foundation as invented by Kachadorian in the 1970s, was built of concrete blocks with a poured slab over the top and paired with large amounts of south-facing windows. In this approach, the thermal mass the floor slab is used to store solar radiation let in by the windows and the air in the cavities of the hollow concrete blocks are used to transport the stored heat throughout the house when required. (Kachadorian, 2006)

Other storage systems attempted include water tanks in the attic (e.g., Saunder's "Cliff House"), large bins full of stones (so-called "rock bin storage") in the basement and sealed gravel or sand formed below a slab through which water was pumped (Shurcliff, 1978). The effectiveness of these energy storage strategies was limited and they were expensive, cumbersome and many relied on powered, often complex and unreliable, mechanical systems.

As experience in constructing and living in these passive solar heated buildings increased, it became clear that the most cost effective method of keeping the solar energy within the building was through high levels of enclosure thermal resistance, good windows (and/or thermal shutters) and air tightness. One example of a passive solar home that put this approach into practice was the "David Robinson House". Featured in the October, 1979 Issue of *Solar Age Magazine*, this house was built in Minnesota and was designed utilizing life cycle cost analysis to determine building enclosure thermal resistance levels. The home featured careful air sealing, R-30 walls with limited thermal bridging, an R-60 roof and R-16 insulation of the basement walls and below the slab (Holladay, 2010). This house featured 50% of the total window area facing south (double glazed) with triple glazing on the rest of the orientations and also employed an active solar heater and a heat recovery ventilator. This home was significant in that it demonstrated a shift in focus from maximizing solar gain, to minimizing thermal loss. While fundamental passive solar strategies are still considered one element of a low energy building design, the huge expanses of glazing and complex storage systems have been replaced with moderate amounts of south-facing glazing and thermal mass. In modern low energy building designs for cold climates, solar energy is considered a supplemental source of space heat energy, with the design focus on retaining heat within the building. The strategy of minimizing thermal loss has become known as the super-insulation approach.

2.1.3 The Super-insulation Approach:

While the passive solar approach focused on maximizing solar heat gain, the super-insulation approach focused on minimizing heat loss through the building enclosure. Practical research into super-insulated homes began in the early 1970's during the same time period as houses based on passive and active solar heating. Super-insulated houses were typified by a concern for airtight construction, thick layers of insulation, and modest south-facing window areas (usually in the range of less than 8% of floor area).

Considered by some to be the world's first super-insulated house, the "Lyngby House" was designed and built by researchers from the University of Denmark (Van Korsgaard and Esbensen) in 1974. The goal was to create a zero-energy house. This home included roof and wall insulation 12 to 16 inches thick and double glazed windows with insulating shutters. The home also utilized active flat plate thermal collectors (connected to an 8000 gallon storage tank), one of the first residential air-to-air heat exchangers and a solar space and water heating system. The active solar features of the house soon broke down and were abandoned. The lessons learned in this project, however started a shift in focus; away from active, high-tech solutions and towards the development of simple, passive low energy buildings ('Pioneer Award', 2013).

Another example of this new focus, was the "Lo-Cal" house. This design was developed by Wayne Schick at the University of Illinois at Urbana-Champaign in 1976 using computer simulations to predict the amount of energy that could be saved using high levels of insulation. This house employed double 2X4 walls, air-tight construction, a heat recovery ventilation system and triple glazed windows. The design had R-30 walls, R-60 ceilings and R-20 foundation insulation (McCulley, 2008). Although the house was never built, the simulation experiments demonstrated the energy savings that were possible using simple, passive designs and played an important role in legitimizing and popularizing the early super-insulated approach.

At the same time as the Scandinavian and American developments, a systematic study of energy-efficient buildings was carried out in Germany by H. Hörster, B. Steinmüller and others, with funding from the Federal Ministry of Research. Based on this study, the “Philips Experimental House” was designed using computer simulations and verified with field tests. Completed in 1975, the house had an R-40 building enclosure, coated, double pane windows with insulated shutters, a heat recovery ventilation system and active solar and heat pump technology. This building served as an experimental house for many years. The heating demand for this house was shown to be 20-30 kWh/m^2, which was 15 times less than the typical German housing stock at that time (Steinmuller 2007).

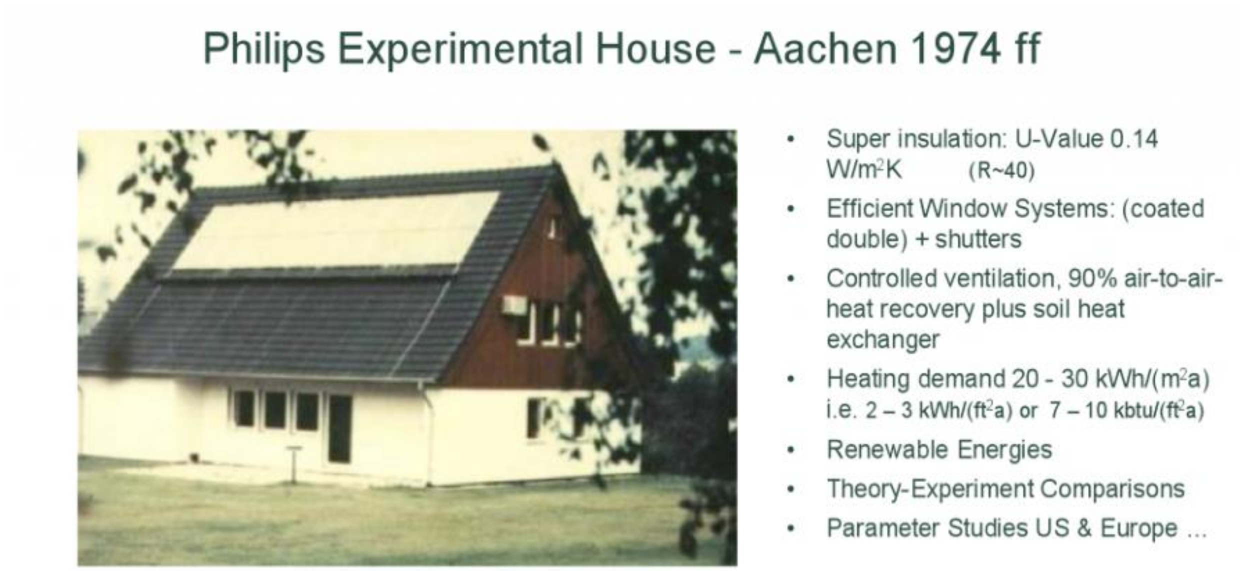

Figure 1- Phillips Experimental House (Passipedia.passive.de)

In 1978, “The Saskatchewan House” was designed and built by a group of Canadian researchers lead by Harold Orr and supported by the Canadian Government. The house featured R-40 double stud wall construction, R-60 ceilings, triple glazed windows and R-20 insulated shutters. The building had air-tight construction (1 ACH@50), a heat recovery ventilation system, a drain water heat recovery system and active solar collectors (Orr, 2013). By 1979, energy monitoring showed that the combination of super-insulation and the active and passive solar features reduced heating energy by 90% compared to a code compliant house of that era (Besant, Dumont & Schoneau, 1979).   The active solar heating system was found to be very expensive, and experienced reliability problems.   By 1983, a large study of 27 Saskatchewan houses built using the same energy-saving principles (without the active solar energy components), as The Saskatchewan House showed annual average heating loads of 63 kWh/m^2, a reduction of 70% compared to contemporary code-built houses, in a climate twice as cold as central Germany (Dumont, Orr & Hedlin, 1983), with modest additional costs.   The lessons learned in the design, construction and operation of the Saskatchewan house and similar local homes were massively influential, eventually leading to a national low energy building certification program, known as the R-2000 program in 1982. This program still exists today and has produced tens of thousands of low-energy homes.

Figure 2- The Saskatchewan House (Passivehouse.ca)

In 1979, “The Leger House” was built by Gene Leger in Massachusetts. This house featured double-wall construction, a heat recovery ventilation system, was extremely air tight and had no passive solar features. The house was heated with a natural-gas on-demand water heater and had an annual heating bill of under $40. The simplicity and low cost of the Leger house was in stark contrast to the passive solar designs of the time and this seemed to resonate with more developers and consumers. Many consider the success of Gene Leger‘s house as the resolution of the debate between passive solar design and super-insulation: The debate was resolved in favor of super-insulation (Nisson and Dutt, 1985).

Figure 3- The Leger House (Holladay, 2010)

Inspired by the success of the early super-insulation houses described above, physicist, Harvard professor and supporter of the passive solar approach, William Shurcliff issued a press release in 1979 defining what he thought the future of low energy homes should be (Nisson and Dutt, 1985). He essentially defined the super insulation approach as:

1) "Truly superb insulation, not just thick, but clever
2) Envelope of the house is practically air-tight
3) No provision for extra thermal mass
4) No provision for excessive south windows
5) No conventional furnace
6) No conventional heat distribution system
7) No weird architectural shapes necessary
8) No big added expense
9) Passive solar heating is modest
10) No need for humidifiers
11) No south side overheating "

As the 1970s was the decade for research and development in super-insulation techniques, the most important developments in the 1980s were related to the sharing this information and promoting the concepts of super-insulation to industry and the general public. As early as 1981, super insulation techniques were being featured in published books, trade journals and consumer magazines.

The Superinsulated Retrofit Book by Canadian researchers Brian Marshall and Robert Argue was published in 1981, giving practical advice and real examples on methods of retrofitting existing homes to improve energy efficiency. This book described the 'chainsaw retrofit' which involves constructing a new outer envelope including a continuous air barrier, thick layers of exterior insulation and new siding and roofing. Also included, were a third glazing layer on the windows and a heat recovery ventilation system. The same year, William Shurcliff released *Super Insulated Houses and Double Envelope Houses* (Shurcliff, 1981). This book described in some detail, the design and construction of successful super-insulated home projects throughout North America.

First published in July 1982, *Energy Design Update* was a super-insulation newsletter written by Massachusetts engineer Ned Nisson. Along with Princeton researcher Dautam Dutt, he also wrote *The Super Insulated Home Book* in 1985. This book provides actual construction details for several types of super-insulated wall systems, ventilation and air tightness strategies and vapor barriers.

The concepts of super-insulation were even featured in consumer magazines as early as 1981. An article in the May 1981 *Popular Science* magazine entitled 'Super Insulated Houses' (Ruby, 1981) featured construction details and energy use data for a double-stud home that was inspired by the Saskatchewan house.

2.1.4 Low-Energy Certification Programs

Beginning in the mid-1980s, government and other organizations interested in promoting low energy housing began to develop voluntary 'low-energy' certification programs. The R-2000 program, the Energy Star program and Passive House program are the three most influential of these programs in North America.

2.1.4.1 R-2000

The R-2000 Program was developed by Natural Resources Canada in conjunction with the Canadian Home Builders Association, based on the lessons learned in the Saskatchewan House project. The program kicked off in 1981, and included ratings for energy efficiency, indoor air quality and environmental impact.

The goal of the energy efficiency component of the program was to reduce energy use by 30% compared to a code-compliant home. Towards that goal, the standard required minimum levels of thermal resistance which exceed local building codes, set a maximum air leakage target, requiring air leakage measurements and defined maximum energy use as a function of climate. By 1995, the influence of the program could be seen in the national and provincial building codes of Canada, which increased the required thermal resistance to the R-2000 levels. In 2012, the R-2000 program received a major update. The new program is performance- based and requires a 50% decrease in energy use compared to the original program requirements. To meet this performance goal requires thermal resistance levels significantly higher than local building codes (NRCan, 2012)

2.1.4.2 Passive House

Another well regarded and influential residential certification program is the Passive House (or Passivhaus) standard, developed in Germany but applied throughout Europe, Scandinavia, and North America. The first Passive houses were designed by Bo Adamson and Wolfgang Feist based on the lessons learned from previous low energy homes such as the Philips House, the Lyngby House, the Lo-

Cal House and the Saskatchewan House (Steinmüller, 2008). A major development of over 100 houses was built in Darmstadt, Germany in 1990 and monitoring showed that they required 90% less space heating energy than code-compliant German houses of that time (Schneiders, 2003). The Passivhaus-Institute was created in 1996 to promote and control the building standard. The three core requirements of the Passive House certification are (Passive House Institute, 2014)

1) The building must be designed to have an annual heating demand as calculated with the Passivhaus Planning Package of not more than 15 kWh/m² per year (4746 btu/ft² per year) in heating and 15 kWh/m² per year cooling energy
2) Total primary energy consumption (primary energy for heating, hot water and electricity) must not be more than 120 kWh/m² per year (39 K btu/ft² per year)
3) The building must not have an air leakage rate of more than 0.6 times the house volume per hour ($n_{50} \leq 0.6$ / hour) at 50 Pa (N/m²) as tested by a blower door

Meeting the first requirement requires the building enclosure to have high levels of thermal resistance and usually significant amounts of passive solar gain. Depending on the climate, solar gains and internal gains, the thermal resistance levels required in cold climates far exceed any building code in North America, and often exceed levels used previously for super-insulated homes in cold climates. Because the same energy target is used in all climate zones, only a modest amount of insulation is required in moderate climate zones, such as Southern California and the Pacific Northwest (Walker and Less, 2013).

The Passive house standard is considered one of the most demanding housing certification from an energy use perspective and is seen as one of the most commercially successful programs, although far fewer homes have been registered in North America than the R-2000 program to date.

2.1.4.3 Energy Star

The Energy Star program was developed in 1992 by the U.S. by the Environmental Protection Agency (EPA) and the Department of Energy (DOE). Energy Star labeling was first applied to consumer electronics and appliances as an indication of the most energy efficient products in their category. Following the success of this program in the electronics and appliances markets, the Energy Star for new homes program was developed in 1995 and has had 2 major updates since then. The Canadian version is based on a prescriptive package of requirements, based on 2 climate categories (NRCan, 2014). Energy Star windows, heating equipment and appliances are required and minimal thermal resistance for building enclosure components are specified. An air leakage rate of about 2.5 air changes per hour at 50 Pa is required as well as an approved ventilation design. Some alternative methods and trade-offs are allowed under the program. Because the goal of a labeled house is only about a 15% improvement over a code-compliant house, these requirements are only slightly more restrictive than many local building codes. This results in a certification that is more easily attained and has become a popular choice, even among larger builders.

2.1.4.4 Net Zero Energy Buildings

A Net Zero Energy (NZE) building is defined as a building that uses only as much energy as is generated on site, using renewable energy sources. A NZE building may use the electrical grid for storage and retrieval of excess energy or it may employ an off-grid system, with batteries for storage and retrieval. Grid-tied systems have the advantage of limitless, and low-cost, storage and retrieval to get through periods of high energy use and/or low energy production. With an off-grid system, the cost and size of battery storage limits capacity, meaning that energy production and usage must be closely balanced on a day-to-day basis.

Many NZE buildings use only use electricity as their energy source, so that all energy required for the building is produced on site via photovoltaics and/or wind power. A grid-tied NZE building can, however, also use other energy sources such as natural gas or propane, as long as the electricity produced on-site off-sets the total sum of the electricity plus all other energy consumed at the home.

The U.S. Department of Energy (U.S. DOE) has studied the development of a proven, cost neutral, net zero energy (NZE) home design (Anderson & Roberts, 2008). In order to meet the objective of a practical NZE ready design, it is estimated that whole house energy must be reduced by 40% compared to the best current designs. To reach this goal, considerable research must be completed to develop and validate low risk, cost neutral building components and strategies. One of the top 5 priorities of this research program is to develop a durable high-R wall system for cold climates.

2.1.5 Summary

North American builders have had access to research data, construction techniques, and the materials necessary for building low energy houses since the mid-1980s. The effectiveness of these construction techniques has also been demonstrated over the past 30 years through programs such as R-2000, Energy Star and Passive House. These efforts have resulted in incremental changes to North American building codes which now require significantly greater thermal resistance and much more attention to air tightness than they did before 1980. As shown in Figure 4, these code changes have resulted in a decrease in heating energy consumption of approximately 20% over the past 20 years (RECS, 2012) in the U.S. Despite these improvements, much greater levels of thermal resistance are required to create truly low energy buildings in most climate regions of North America.

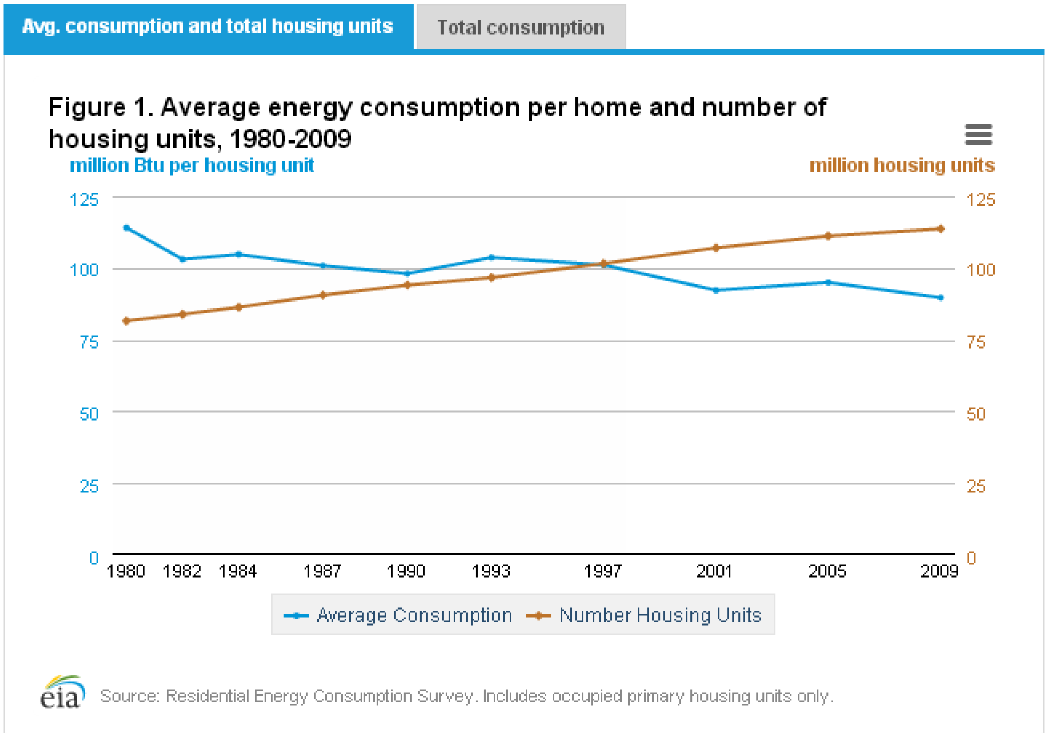

Figure 4- Average energy consumption per home from 1980 to 2009 (RECS, 2012)

2.2 The Role of Wall Systems in Low Energy Housing

The building enclosure system includes all of the elements of the building that separate the interior from the exterior. These include the floor, the roof, windows and doors and below grade and above grade wall systems.

To quantify the heat loss characteristics of each of these components in prototypical American homes, a study was performed by researchers from Lawrence Berkley National Laboratory (LBNL) (Huange et al, 1999). This study makes use of a database of existing residential building prototypes for different regions of the country (Ritschard et al. 1992). Parametric simulations were performed on these buildings using the DOE-2 building energy simulation program to calculate the seasonal heat loss attributable to the different building components: floors, walls, roof and windows. Heat loss due to air leakage was also simulated and reported as a separate component. Heat loss through windows can also be adjusted (reduced by 1/3) to account for solar heat gain through windows during the heating season.

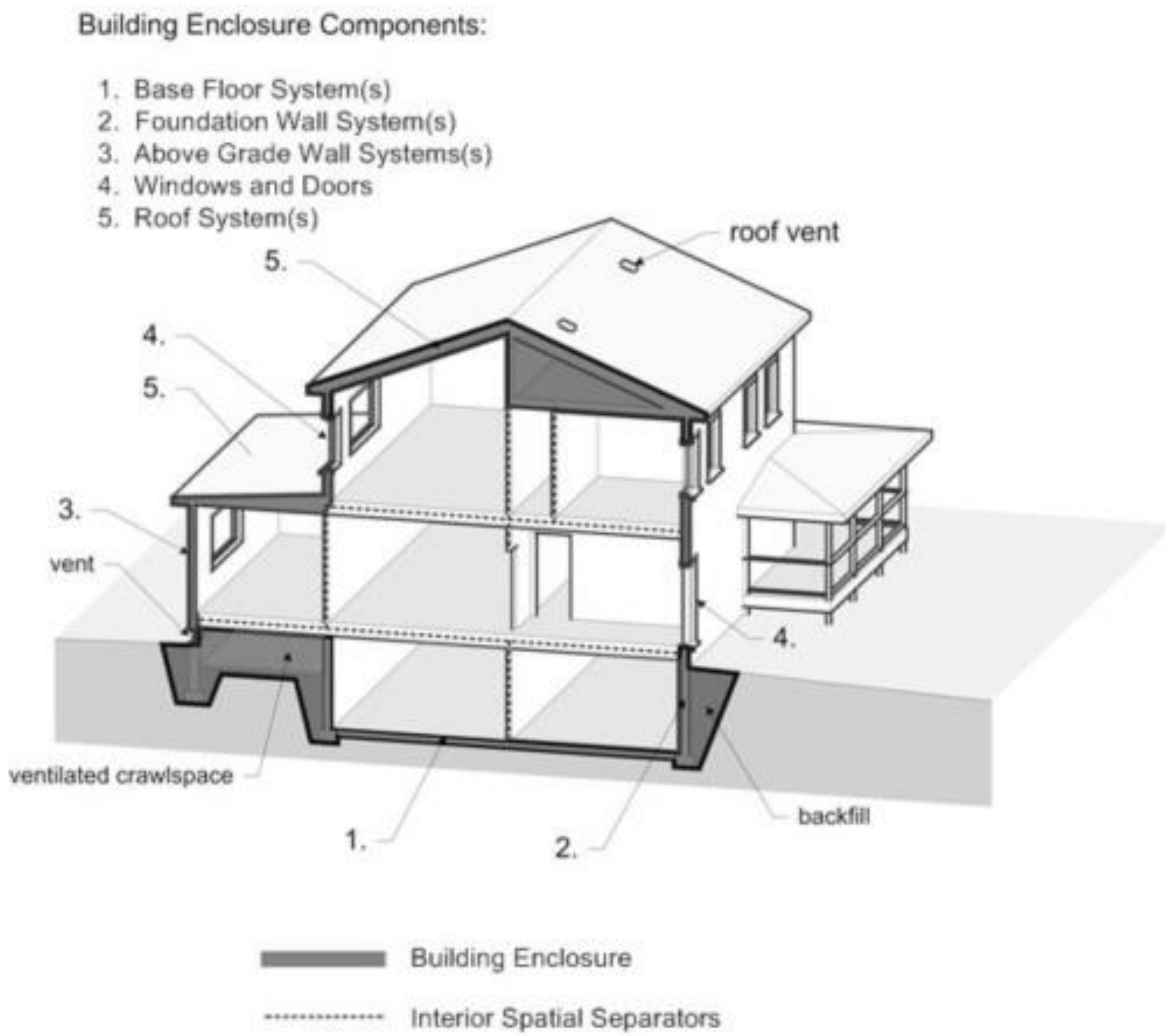

Figure 5- Building Enclosure Components (Straube, 2006)

The heat loss results of this study for the geographical area most closely representing the Canadian climate (North) can be seen in Figure 6. Using the insulation and air leakage characteristics of a prototypical home in the U.S. Northern region, air leakage is the largest source of heat loss, accounting for 32 % of total heat loss. Heat loss through the walls is the next largest contributor, accounting for 21% of total heat loss, while floors accounted for 18%, windows for 17% and the roof for 12%. This study showed that the walls were responsible for more heat loss than any other physical enclosure component. Although air leakage was not broken down by component, leakage through wall systems is obviously a major contributor to this category also. Historically, Canadian houses tend to be significantly more airtight than in the US (Fennell and Haehnel, 2005) and this tends to reduce the relative contribution of air tightness and increase the relative contribution of enclosure components.

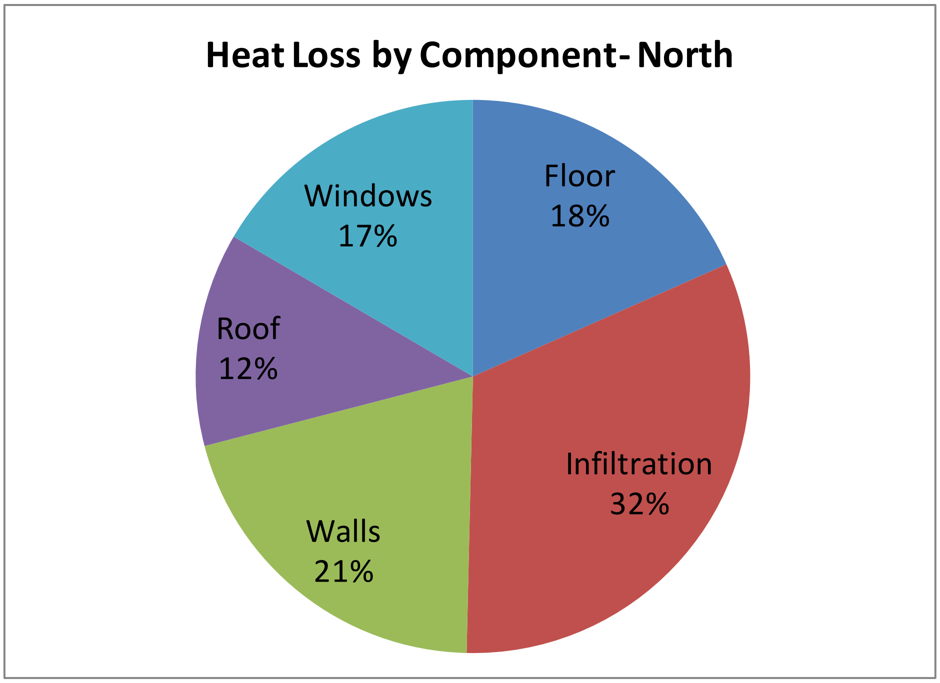

Figure 6- Seasonal heat Loss by Component (based on data from Huange et al, 1999)

The data from this study can also be used to demonstrate the effects of improvements in insulation strategies in the past 30 years. The housing units were broken down into two age categories: old (pre-1980) and new (post 1980). As shown in Figure 7, the newer houses show a significant decrease in the percentage of heat loss through the roof, (from 14.8% to 7.1% of total) and a much smaller decrease in the percentage of heat loss through the walls (from 21.4% to 19.1% of total) compared to the older houses. Although the nominal percentage changes are complicated by changes in the other elements over the same time period, a direct comparison between walls and roofs can be informative.

The difference between roof and wall heat loss changes (as a percentage of the total) over this period demonstrates that it is often easier to increase insulation levels at the roof/ceiling plane compared to wall systems. A large majority of single family homes have ventilated roof systems where there is ample room between the ceiling plane and the roof deck for increased levels of insulation.

In a traditional wood-framed wall system however, the thickness of the insulation layer is limited to the framing cavity depth. While innovative products such as spray polyurethane foam (SPF) insulation have a greater thermal resistance per inch (R-6) than traditional batt or loose fill insulations (R-4), major improvements in wall thermal resistance can not be achieved using this traditional approach. The standard framing cavity simply does not provide enough depth and the wood framing members allow too much heat flow to bypass the insulation. To reach effective thermal resistance values of R-35 or higher, innovative approaches to wall assembly design are required. Since the construction of new housing units represents only a small fraction of the total existing units, these innovative approaches should also ideally be applicable as a retrofit to existing buildings if they are to have a significant impact on the energy footprint of the housing stock.

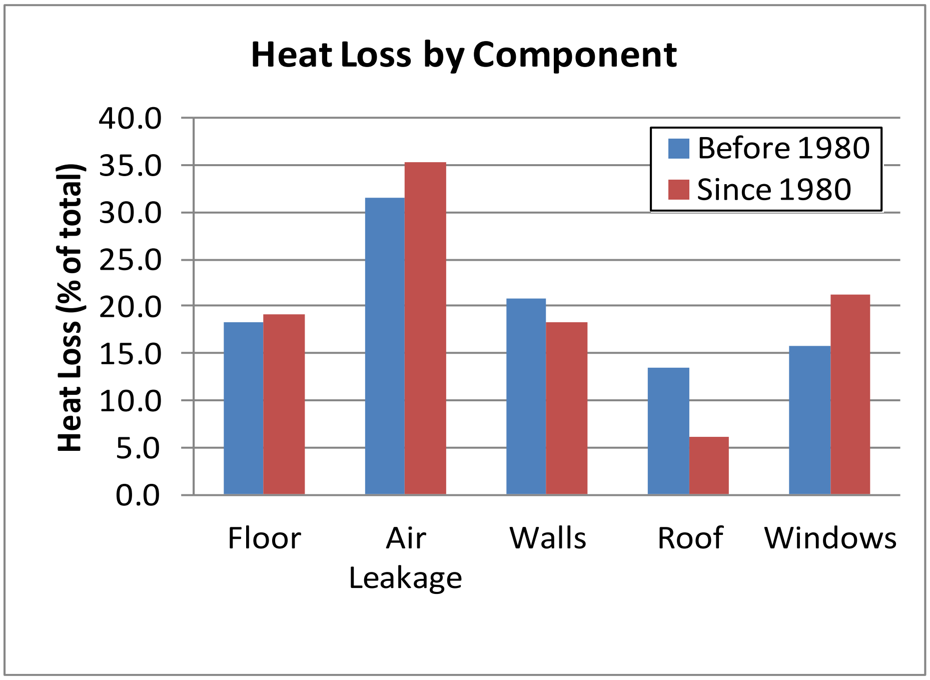

Figure 7 –Heat loss by component for houses built before and after 1980 (based on data from Huange et al, 1999)

In order to make significant improvements in the thermal resistance of residential wall systems, a dramatic change in design is required. With dramatic change however, comes significant risk. The building industry has experienced serious system failures in the past when changes were implemented without a complete understanding of the system by the designers and installers. The implementation of several building systems and materials such as Exterior Insulated Finish System (EIFs), Structural Insulated Panels and Oriented Strand Board (OSB) siding were marred by water-related durability failures (Lstiburek, 2006) and demonstrate the need for a complete understanding of the performance of a system before applying it broadly. To understand the performance and potential risks of any building enclosure system, it is important to define the functional layers of the system, and evaluate the ability of these layers to perform their required functions. The following two sections will define the required functional layers and provide a basis for evaluating potential performance.

2.3 The Wall as a System

2.3.1 Introduction

Like the other components of the building enclosure, above grade wall systems must provide four important functions (Straube and Burnett, 2005):

1) Support – against all internal and external forces applied to the enclosure
2) Distribute- goods and people into and out of the building and utilities throughout the building
3) Finish – to create durable and esthetically pleasing surfaces on the interior and exterior of the building
4) Control – the access of people and pests and environmental loadings such as precipitation, air flow, vapour flow, heat energy, sound and solar radiation.

To design an effective wall system, the most critical control layers must be identified and detailed appropriately. The most critical control layers, in order of importance are (Lstiburek, 2008):

a) Rain Control layer -
b) Air control layer
c) Vapour control layer
d) Thermal control layer

2.3.2 Rain Control Layer

This layer must prevent rain water from entering the wall assembly and damaging moisture sensitive materials. Siding or cladding acts as the primary rain shedding surface in a wall system, however the rain control layer is the last and most complete line of defense against the intrusion of rain water. This layer should be detailed with joints lapped in a shingle fashion and not rely on tapes or sealants to prevent water intrusion. In a typical residential wall system, the rain control layer is composed of building paper or polymeric house wrap but may, in unique and high-performance designs, be peel and stick membrane or a spray or trowel applied bituminous membrane. The greatest challenge is to maintain continuity at window and door penetrations. This requires careful detailing of flashings between the rain control layer and the window/door structure.

2.3.3 Air Control Layer

This layer must prevent the movement of air into or through the assembly. Controlling air flow is important for durability, energy saving, comfort and indoor air quality (IAQ). Air can carry significant quantities of water vapor, which can be deposited inside the assembly as condensation. The heat capacity of air also enables air to carry heat through the wall system, bypassing the resistance of the thermal control layer and increasing energy use and compromising comfort. Contaminants from outdoors or from within the wall assembly can ride along on the flow of air and thereby impact indoor air quality. A typical Canadian residential wall assembly relies on an interior layer of polyethylene behind the drywall as the air control layer. Taped and sealed sheathing membranes (e.g., housewraps) are one of the most common approaches taken in the United States. Other options include sealed gypsum wall board (the air-tight drywall approach), taped and sealed sheathing on the exterior of the framing members, and spray foam in the stud cavities combined with sealant at all joints.

The greatest challenge in maintaining continuity of the air control layer is sealing at wall-to-floor and wall-to-ceiling ceiling joints, penetrations for services, and window/door rough openings.

2.3.4 Vapour Control Layer

The function of this layer is to limit the flow of water vapour into or through the assembly by diffusion so as to avoid damaging quantities of condensation. Vapour diffusion is driven by vapour pressure differences across a material or air space and its rate is controlled by the vapour permeability of the material and the size of the vapor pressure differences. While it is not necessary to completely block the flow of water vapour diffusion in a wall assembly, it must be slowed considerably to prevent damaging levels of interstitial condensation by diffusion from the interior during cold weather and diffusion from the exterior during hot weather. Warm weather condensation can become especially important if the cladding can store significant amounts of absorbed rainwater (Straube et al., 2009 and Straube and Burnett, 1995). It is important to note that vapour flow is an important method of drying should the assembly get wet during construction or operation, and hence completely preventing diffusion also eliminates drying in the direction of the vapour barrier. In Canada, the vapour control layer is almost always applied to the interior side of the thermal control layer and is typically a polyethylene sheet. Other methods of controlling vapour flow are through the use of 'smart' vapour retarders that change permeability with relative humidity, by the application of vapour control paint to gypsum wall board, and through the use of vapor retarding insulating sheathing layers on the exterior of the structure.

2.3.5 Thermal Control Layer

The thermal control layer must control the flow of heat across the wall assembly. Controlling heat flow is important for occupant comfort and reducing space heating and cooling energy requirements. The layering and positioning of insulating materials can also be used to control the temperature of building components and affect the long-term durability of the assembly. In a typical Canadian wall assembly, the thermal control layer is composed of low-density batt insulation placed between the framing members. In this approach, the amount of insulation is limited by the thickness of the wall cavity and the framing members create many thermal bridges, reducing the effective thermal resistance of the assembly. In pursuit of energy reduction, the level of thermal resistance has been slowly increasing in Canadian buildings for the past 30 years. This improvement has primarily come from increasing the thickness of the insulation within the wall cavity. This was accomplished by changing the exterior walls from 2 X 4 to 2 X 6 construction, creating room for an additional 2 inches of cavity insulation. There have also been small improvements in the thermal resistance of the available cavity insulations. In order to reach aggressive energy reduction goals and net-zero energy buildings however, dramatic increases in thermal resistance are required.

2.3.6 Summary

The typical residential wood framed wall system, used in Canada for the past 30 years is illustrated in Figure 8 below.

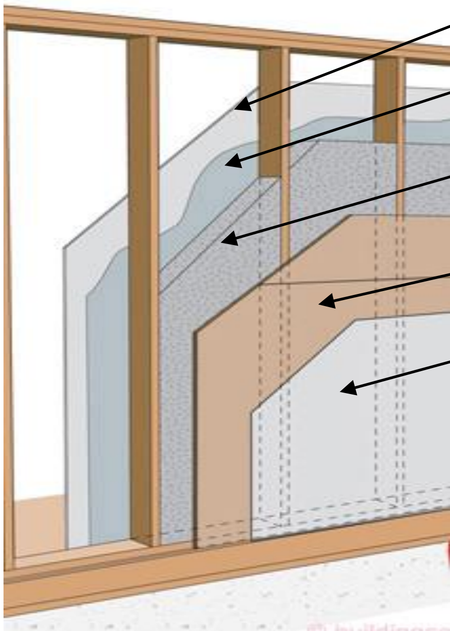

Figure 8- Typical Canadian wall assembly (Straube and Smegal (2009)

2.4 Heat, Moisture and Air Movement

In order to evaluate the performance of wall systems, it is important to understand the nature of heat, moisture and air movement within and across the wall assembly. An assembly is composed of multiple layers of different materials with different hygrothermal properties and the movement of heat, moisture and air through an assembly is a dynamic, complex, interdependent process. While hygrothermal modeling and field measurements are used to predict and evaluate the performance of assembly, an understanding of the basic mechanisms is important to understanding and interpreting the results

2.4.1 Thermal Control in Assemblies

2.4.1.1 Modes of Heat Transfer

The primary modes of heat transfer are conduction, convection and radiation.

Conduction

Conduction is the movement of heat energy via direct molecular contact. This is the predominant mechanism that moves heat through a solid material and also an important mechanism of heat energy transfer between materials that are in physical contact with each other. The flow of heat energy by conduction conforms to the fundamental equation developed by Fourier. For many practical building science applications, a one dimensional Fourier equation can be expressed as:

$$Q = A \times \frac{k}{l} \times (T_2 - T_1)$$

Where: Q = rate of heat flow (in watts (W))

A = the area (in m^2)

k = the thermal conductivity of the material (in W/m•k)

l = the length of the flow path (in m)

T_1 and T_2 are the temperatures on either side of the material (in ° K or °C)

Conduction is the primary mode of heat transfer in building enclosure assemblies. Generally, the lower the density of the material, the lower the rate of conduction through that material. Structural materials such as steel, concrete and brick are excellent conductors of heat. Even wood, which is less dense and has lower conductivity than other structural materials, has a much higher thermal conductivity than modern insulation products. Air is a poor conductor of heat which is the basis for most commercial insulation products. Products such as fibreglass and rockwool insulation are low conductors not because glass or rock are poor conductors, but because of the amount of air between the fibres. The fibres of the insulation are there to reduce convection. Expanded polystyrene (EPS) is composed of foam beads that form pockets of air within its structure. Other plastic foam insulations such as extruded polystyrene (XPS), spray polyurethane foam (SPF) and polyisocyanurate (PIC) trap pockets of inert gases within their structure. These blowing agents have a lower conductivity than air, but can leak out slowly over time to be replaced with air.

Convection

Convection is the transfer of heat energy by bulk movement of a fluid. Convection is an important mechanism of heat flow within fluids and between fluids and solid materials. Sir Isaac Newton noticed that the temperature of a heated object approaches the temperature of the air around it at an exponentially decaying rate. Using his newly developed calculus, Newton showed that the heat flow due to convection at any instant was proportional to the temperature difference at that instant. The equation he developed to express this is known as 'Newton's Law of Cooling', and is written as:

$Q = h_c * A * (T_s - T_{infinity})$

where: Q = heat flow (in watts)

h_c = convective heat transfer coefficient

A = surface area (in m^2)

T_s = surface temperature (in ° K)

$T_{infinity}$ = temperature of the air at a distance where it is not affected by the object (in °K).

For convection to occur there must be bulk movement of a fluid. This movement can occur naturally, due to temperature dependent buoyancy differences, or be driven by external forces like the wind or fans. Convection can affect heat transfer across building enclosure assemblies at several different locations. As shown in Figure 9, the exterior surface of the assembly is especially affected by wind-driven convection, also known as wind washing. The interior surface of the assembly is affected by natural convective loops, especially vertical surfaces. As shown in Figure 9, the same natural loops can also occur within the assembly at any air gaps and to a lesser extent, within low density batt insulations.

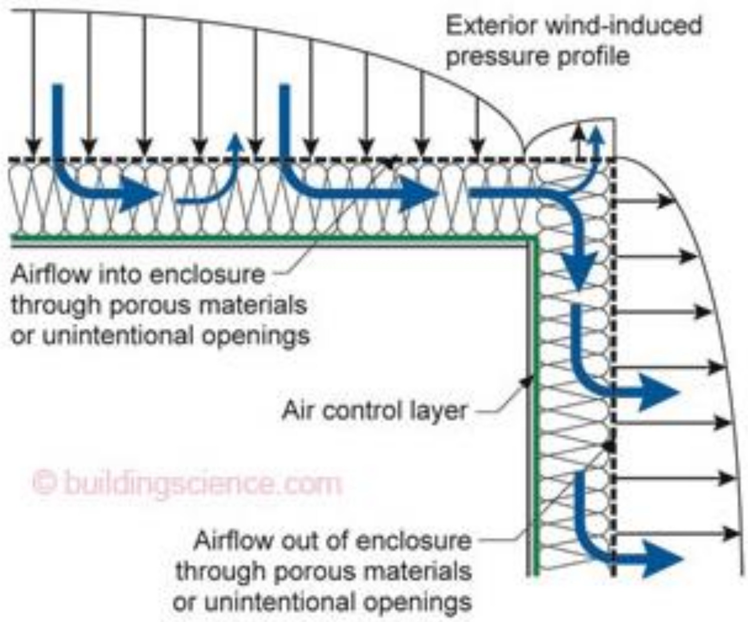

Figure 9- Wind washing effects on air-permeable insulations (Straube, 2006)

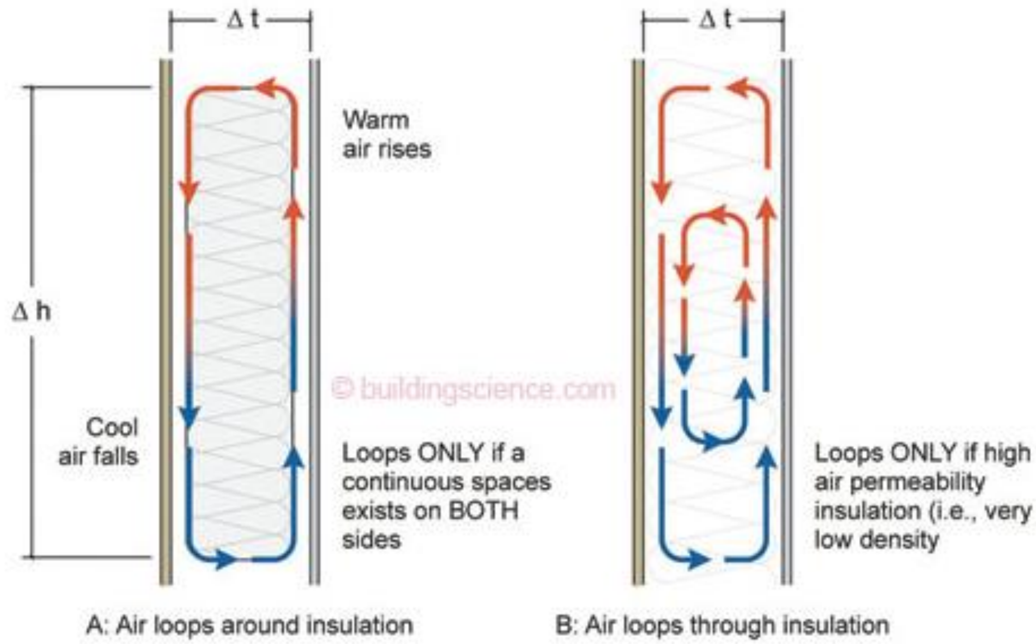

Figure 10- Convective loops around and through air-permeable insulation (Straube, 2006)

Radiation

Radiation is the emission of heat energy by electromagnetic waves through a gas or vacuum. For radiation heat transfer to occur there must be a direct line of sight between the two objects involved. All objects above absolute zero (-273 °C) emit heat energy, however it is the net difference between two radiating materials that is relevant to the rate of heat energy transfer. For the purposes of most building science applications, radiation heat transfer can be simplified using the Stefan-Boltzmann equation:

$$Q = \varepsilon \times \sigma \times A \times (T_S^4 - T_a^4)$$

Where: Q = heat flow (in watts)

A = surface area (in m^2)

T_s = the surface temperature (in °K)

T_a = outdoor temperature (ambient air temperature) (in °K)

ε = thermal emissivity of the object

σ = the Stefan-Boltzmann constant (5.67 X 10^8 W/m^2*K^4)

For most building enclosure assemblies, radiation contributes to heat flow at the exterior surface, at the interior surface and across any air gaps within the assembly. At the exterior surface, solar radiation can cause a roof or wall surface to exceed ambient air temperature, while night sky radiation losses can cause them to be colder than ambient air temperature. Radiation can affect the temperature gradient across the assembly and directly influence heat flow. On the interior surface of an assembly, cold surfaces result in net radiation from occupants to the surface, causing the occupant to feel cold, regardless of interior air temperature. Another common example of radiation affecting heat flow across an assembly is between two surfaces separated by an air gap such as between the roof and ceiling assemblies in a ventilated roof system.

2.4.1.2 The R-Value

The most common measure of the thermal resistance of a material within an assembly is the 'R-value'. The R-value is the reciprocal of 'U-Value' or conductance which is the flow of heat energy per area, for a unit difference in temperature.

In imperial, the units for U-value are: Btu/hour•ft^2•°F

Therefore the units for R-value are: hour•ft^2•°F/Btu

In metric, the units for U-value are: W/m^2•°K

Therefore the units for R-value are: m^2 •°K /W

The insulation industry has decided to report R-value over U-value as the standard measure because it is more intuitive to consumers – as the effectiveness of an insulation product increases, its R-value increases. The R-values are also useful since the R-values of the materials in an assembly can simply added together to determine the total thermal resistance.

In order to determine the R-value of a material, the U-value is first measured. The current accepted testing methods to determine the R-value of an insulation product are ASTM C-177, ASTM C-518 and ASTM C-976. In these testing procedures, heat flow is measured at a mean temperature of 75 ° F (23.9 °C). This means that insulation is usually tested with the cold side at 50°F (10°C) and the warm side at 100°F (37.8°C). The boundary temperatures used to determine a materials R-value are significant, since heat flow resistance for a given material will vary as average material temperature changes. Because of this, some insulation products will perform significantly better in service than predicted by the test, and some much worse.

2.4.1.3 Summary

The three heat flow mechanisms discussed above account for a different percentage of heat loss under different conditions. For example, radiation plays a large role in heat flow during hot sunny weather on the roof or south face of a building, but will have little influence on a cold, cloudy day or on the north face of a building. Convection plays a smaller role on still days or in a sheltered area, compared to a building in a high wind area.

The layering of materials within the assembly also affects heat loss. Low density insulation materials must be surrounded by materials that prevent air flow through them, or risk decreased performance due to convection or wind-washing. High density framing materials that pass through the insulation layer create thermal bridges which can result in local areas of high thermal conductivity and significantly reduce the overall thermal resistance of the assembly.

Due to the properties of different insulation materials, their effectiveness can vary greatly depending on the conditions they are exposed to. For example, when conduction is the primary heat flow mechanism (during a cold, still night) fiberglass insulation is more effective at preventing heat flow, than when convection and radiation are major contributors (ie. during windy or hot sunny days).

Predicting the thermal performance of a given wall assembly in a given climate is not a simple process. Sophisticated hygrothermal modeling programs are able to utilize known material properties, hourly weather files and interior condition files to predict heat and moisture flow. However, even sophisticated simulation tools require validation and calibration, as they can only simulate a limited number of mechanisms of heat and airflow and material properties are not always well known. In order to calibrate and validate such a complex model, actual field measurements are required. The tools and methods used to collect these field measurements are discussed in Appendix A.

2.4.2 Moisture Control in Assemblies

2.4.2.1 Introduction

Moisture is the cause of nearly all durability-related issues in modern buildings. The effects of moisture accumulation within a wall assembly include mould and fungal decay of wood framing, freeze-thaw deterioration of brick, stone and concrete, corrosion of metal components and staining or discolouration of building finishes.

For moisture –related problems to occur in an assembly, there must be:

1) a moisture source
2) a route for moisture to enter the assembly
3) a driving force to cause moisture movement
4) materials that are susceptible to moisture damage

(Straube and Burnett, 2005)

Unfortunately, completely eliminating all sources of moisture, creating a flawless moisture barrier or eliminating the driving forces of moisture is not practical in complex buildings constructed in the field. Using only materials that are unaffected by moisture would not be economical. The more practical approach therefore is to utilize design strategies to minimize the impact of these inevitable conditions. In order to address these issues in design, one must understand the ways in which wall assemblies get wet, store moisture and dry out.

2.4.2.2 The Wetting Process

The three main sources of moisture for above grade wall assemblies are:

1) Precipitation

2) Condensation due to air leakage
3) Vapour diffusion
4) Built-in moisture
5) Capillary uptake from ground contact

Precipitation, especially in the form of wind-driven rain is the greatest potential contributor of moisture to an above grade wall assembly. Rain deposition on the face of an exposed low-rise building can exceed 100 kg/m^2/year. Although it is relatively simple to keep this water out of the assembly along the plane face of a wall, it is much more difficult at penetrations and junctions in the wall assembly. It is at these areas, especially window and door penetrations, that moisture damage is most common.

Air leakage condensation has the next greatest potential for introducing moisture into a wall assembly. During cold weather, when framing materials are below the dew point temperature of indoor air, any exfiltration of this air through the wall assembly can result in large amounts of moisture being deposited in the assembly. Depending on the interior temperature and relative humidity and the leakage rate, this process could result in significant amounts of moisture being deposited into a wall assembly during the heating season.

Vapour diffusion outward from the interior is not a powerful wetting mechanism, however solar vapour drive from the exterior can be a major contributor of moisture to the wall assembly during hot, sunny weather. When a cladding such as brick or stone is exposed to prolonged periods of precipitation, they are able to store a significant amount of moisture. When heated by solar radiation, the resulting vapour pressure can force significant amounts of water vapour into the wall assembly, if cavity ventilation or the appropriate vapour barrier is not present. Vapour diffusion also plays a significant role in the redistribution and drying process.

Moisture that is built-in to the assembly materials can sometimes result in moisture problems. Trapping construction moisture within the wall assembly can be avoided by minimizing exposure of hygroscopic construction materials to the elements and by providing the appropriate conditions and time for adequate drying, prior to enclosing those materials within the wall assembly.

Capillary uptake moisture is not a major contributor of moisture to above grade walls. The use of capillary barriers between ground moisture and hygroscopic building materials is also a well understood method of avoiding this problem.

2.4.2.3 Moisture Storage

Since wetting and drying conditions occur at different times, often separated by days, weeks or even months, the assembly must have the ability to store moisture for extended periods of time. Once moisture enters the wall assembly, it can be stored within the assembly materials in a number of ways:

1) Trapped as liquid in poorly drained, non-porous portions of the assembly
2) Adhered to non-porous materials via surface tension as droplets
3) Adsorbed in or on the surface of hygroscopic materials

4) Absorbed and retained in the capillaries of porous materials
5) Stored as vapour in air with the assembly

The ability of the materials to safely store moisture is vital to the durability of a wall assembly. The amount of moisture that can be stored and the length of time that it can be safely stored are important factors in determining the durability of the materials that are exposed to moisture. The amount of moisture that penetrates into the wall system is a function of the wetting mechanisms described above, while the amount of time that the assembly is wet is a function of the drying mechanisms described below.

2.4.2.4 The Drying Process

The form of moisture storage within the assembly will dictate the mechanisms required to dry out the assembly. The mechanisms involved, along with the boundary conditions, assembly design and material properties will determine the rate of drying.

Moisture can leave the wall assembly by one of four processes:

1) Drainage
2) Diffusion
3) Evaporation
4) Ventilation

If a wall assembly has a free drainage path, a large proportion of the rain water that penetrates into the assembly will be quickly removed by drainage. A small percentage of that moisture however, will cling to the materials of the assembly via surface tension or trapped in depressions or the poorly drained portion of the assembly. This un-drained moisture can then be held on the surface of non-porous materials or drawn into porous materials of the assembly via capillary forces and distributed through these materials through capillary flow. Drainage is no longer an available method of removing this moisture.

Drying by vapour diffusion can occur to the interior, or to the exterior. It is driven by vapour pressure differences which typically results in drying to the exterior in the winter and to the interior in the summer. Diffusive drying is resisted by the vapour permeability of the materials in the assembly and may be eliminated as an available drying mechanism by low permeability materials.

Evaporation is the process by which moisture changes state from liquid to gas and is an essential drying mechanism for any liquid moisture not removed by drainage. Bulk water trapped in the wall, and liquid water within the capillary structure of porous materials require evaporation at the surface of the assembly, or at an air gap to be removed from the assembly.

Ventilation is the bulk movement of air through a space within the assembly. Ventilation can magnify the drying effects of evaporation by replacing air that is humid (due to evaporated moisture) with dryer outside air. Depending on the moisture content of the exterior air and the air change rate, ventilation can act as a very powerful drying mechanism for wall assemblies.

2.4.2.5 Summary

Each step in the wetting, moisture storage and drying of an assembly is dependent on many dynamic factors, including material properties (such liquid storage and vapour transport functions), moisture contents, air movement, and temperature and humidity boundary conditions. Evaluating the moisture performance of a given wall assembly in a given climate is very complex. Hygrothermal modeling programs are able to use known material properties and transient weather and interior condition files to predict performance under different conditions, but require validation and calibration. In order to validate and calibrate such complex models, actual field measurements are required. The tools and methods used to collect the field measurements for the work performed in this thesis are discussed in Appendix A.

2.4.3 Air Control in Assemblies

2.4.3.1 Introduction

In order for air to flow across a wall or ceiling/roof assembly, two factors must be present: 1) an airflow path and 2) a driving force. In modern assemblies, air flow occurs primarily at joints, holes and cracks in the assembly layers. Typical areas of concern include the wall to window interface, wall to wall and wall to ceiling joints and at mechanical penetrations. The driving force is air pressure differences across the building enclosure. The three primary causes of pressure differences are 1) wind, 2) stack effect and 3) mechanical ventilation systems. Controlling air leakage through the building enclosure has been shown to be a critical factor for energy efficiency, indoor air quality, occupant comfort and durability of residential and commercial buildings (Lstiburek, 1999).

2.4.3.2 The Effects of Air Leakage

In a heating climate, the infiltration of cold outside air and subsequent exfiltration of warm indoor air has a significant impact on heating loads. In addition to the mass flow of the warm air leaving (and cold air entering) the building, this air movement also reduces the thermal resistance of the insulation materials typically used within the building enclosure. Early air leakage studies showed that infiltration contributed between 25% and 50% of the heating load in typical residential and commercial buildings. (Nevrala and Etheridge, 1977; Caffey, 1979). Although building air tightness has been improved significantly since these early studies (Sherman and Dickerhoff, 1998), air infiltration still contributes up to 30% of total heating loads in modern buildings (Jokisalo et al, 2009). This percentage becomes higher as the thermal resistance of the enclosure increases.

In addition to thermal effects, air infiltration through the building enclosure can affect the indoor air quality and the distribution of indoor air pollutants (Lstiburek et al., 1999). Air infiltration through below grade enclosure elements could even be a route for the transport of detrimental microbes and/or harmful gases such as radon from the soil into a building's indoor space (Rantala and Leivo, 2009).

Excessive air leakage through the building enclosure can also affect occupant comfort. Typical complaints such as cold floors, localized cold spots on walls, cold draughts, large temperature differences between rooms and the inability of the heating system to maintain a comfortable temperature can often be attributed to air leakage through the building enclosure and solved with air sealing measures (Lstiburek et al., 1999).

Another important consequence of air leakage through the building enclosure is decreased durability. During cold weather, warm interior air can contain significant amounts of water vapour. As this exfiltrating air passes through the building enclosure, it can contact elements of the enclosure that are below the dew point of the air. This results in condensation and potentially the accumulation of moisture within the assembly. This process was discussed over 50 years ago by Canadian researchers (Wilson, 1961) and is known as air leakage condensation. Since many of the materials used in modern construction are more sensitive to moisture than the materials used in the past, the effects of air leakage condensation have become more troublesome, leading to mold, rot or corrosion of the materials that make up the enclosure and therefore negatively affect the durability of the building. The same effect can occur in air-conditioned building during warm weather.

2.4.3.3 Air Control Strategies

The primary plane of air flow resistance in a wall assembly is termed- the air barrier. Because it is often composed of different elements and numerous joints, the term 'air barrier system' is more appropriate. In modern wood framed construction, multiple layers within the assembly contribute to the air tightness of the assembly, however it is important to define the primary air barrier layer so that it can be detailed appropriately.

An air barrier system should meet the following requirements:

1) Continuous – around the entire building enclosure, including door and window penetrations
2) Strong- to resist wind loads and pressures, especially at joints
3) Durable- to last the lifespan of the other elements of the building enclosure
4) Stiff- so that deformations do not affect the air tightness of the system
5) Impermeable – to air flow under service conditions

In cold climes, the primary air barrier is usually located on the inside of the insulation, to minimize condensation fed by natural convection loops from the interior. Multiple air barrier layers can be used to increase assembly air tightness and minimize wind washing of low density insulations. The options for creating an air barrier are many. Some common examples of air barrier systems include sheet products such as 6 mil poly or 'smart membrane' on the interior of the framing, sealed gypsum wall board (the air-tight drywall approach), taped and sealed sheathing on the exterior of the framing members and a sealed membrane on the exterior of the sheathing.

Because the air tightness of a wall assembly is heavily dependent on both the design and the quality of the construction, it is not possible to accurately predict the air tightness of an assembly. Although some approaches are known to work better than others, any of the systems mentioned above can work if the details are correct. The only accurate way to determine the air tightness of an assembly is by measuring it. The most common method of measuring the air tightness of an assembly is by fan pressurization. This method, along with other measurement methods is described in Appendix A.

2.5 Past and Current Approaches to High-R Walls

In the pursuit of low energy buildings, researchers, designers and builders have used several approaches to reduce heat flow through walls. Each approach, along with their advantages and limitations are discussed below.

2.5.1 The Thick Wall Approach

The thick wall approach as pioneered by the Lo-Cal house, the Saskatchewan House and the Leger house relies on the traditional method of installing insulation between framing members. To allow for more insulation, the thickness of the framing is expanded. This has been accomplished using several methods:

1) The Double Wall approach - two separate frame walls supported by the floor and separated by a gap (Figure 11),

2) The Truss Wall - one interior wall supported on the floor system, which supports a second outer wall via plywood plates (Figure 12)

3) The I-Joist Wall - using deep engineered wood I- beams (more commonly used for flooring systems)

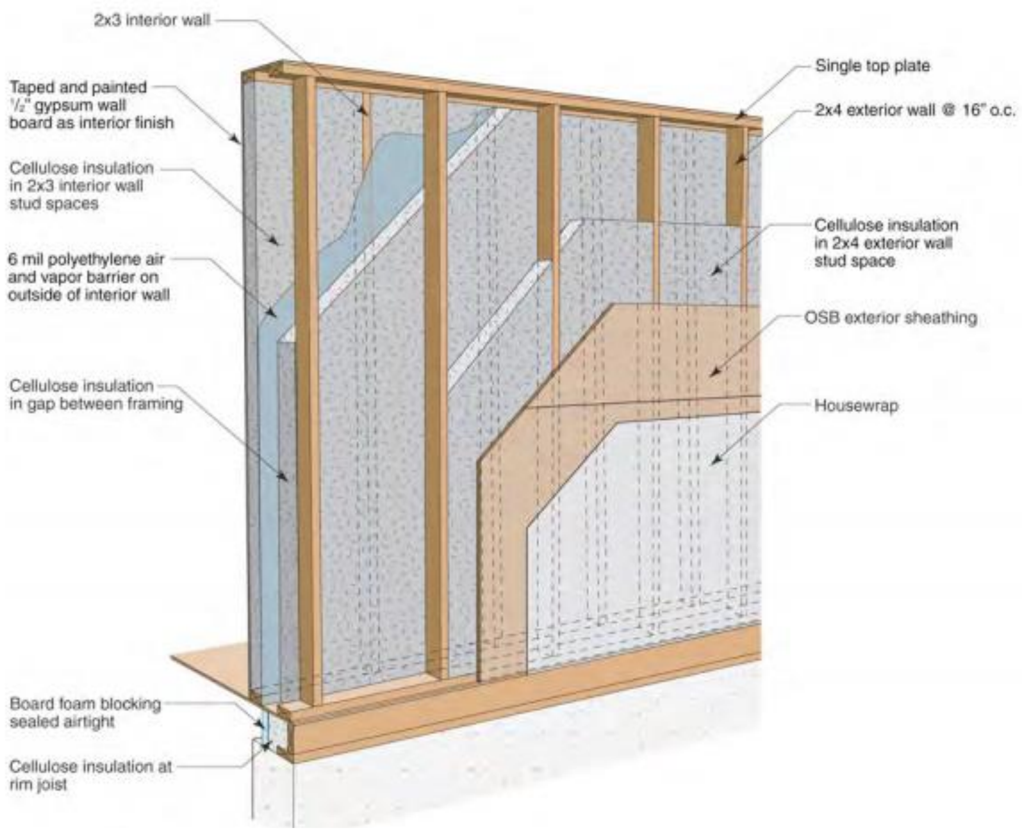

Figure 11- Double stud wall (Straube and Smegal, 2009)

The common feature of these wall systems is a deep wall cavity which is filled with insulation. The first three typically utilize dense packed cellulose, although fiberglass (popular in the 1980s) and rockwool are also options. Thermal bridging around the insulation varies between the systems, but is a factor in all of these thick wall approaches. Most of these wall systems use considerably more framing materials than a standard wall and like all thick wall assemblies, can also reduce the usable interior floor space of a home. The most critical performance concern with these thick wall systems is interstitial condensation. Because of the thermal resistance of the thick insulation layer, the outer wall sheathing will be very cold in winter and any interior air that penetrates to the sheathing will result in condensation. Field monitoring studies of double stud walls systems show peak sheathing moisture content (M.C.) levels of 20% when vapour retarding paint acts as the vapour control layer (Arena et. al, 2013) and up to 25% M.C. when normal latex paint is used (Ueno 2015). These studies allowed no intentional air flow into the walls.

With very little heat flow from the interior, drying is very slow during cold weather and the assembly must be able to safely store moisture until warmer exterior conditions are available to promote drying. Depending on the amount of moisture accumulation, the vapour permeability of the sheathing and weather resistant barrier, and the temperatures and air flow available at the exterior face of the

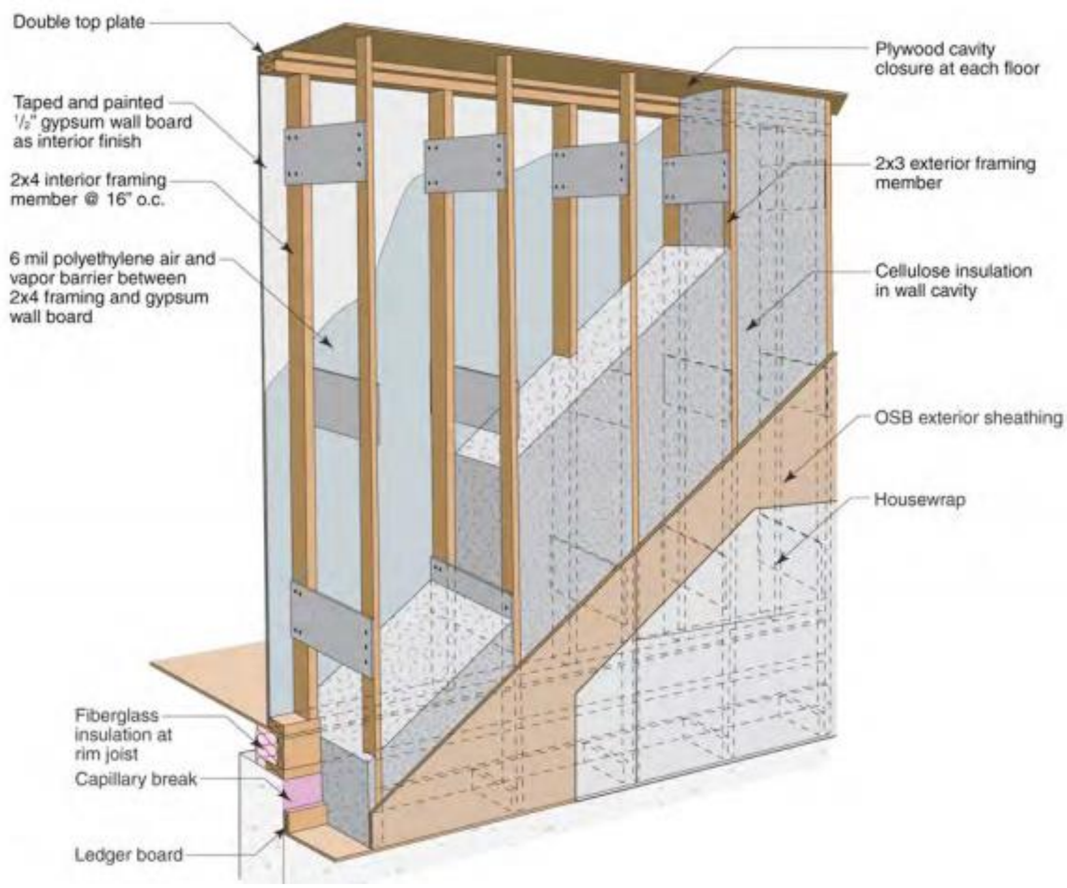

Figure 12- Truss wall system (Straube and Smegal, 2009)

sheathing, this drying process may or may not be sufficient to dry the assembly on a seasonal basis. Because of the susceptibility of thick wall designs to air leakage condensation, an interior air barrier is critical in this type of wall system. Even small discontinuities in the air barrier system can result in significant amounts of interstitial condensation during cold weather. Accumulation of condensation can lead to mould and rot, which could lead to indoor air quality issues and will also negatively affect the durability of the building. The rotting of more than 60 SIPs roof systems after only 5 years in Juneau, Alaska also shows the importance of controlling air leakage. The failure of this assembly was found to be the result of air leakage condensation at the joint at the peak of vaulted ceilings (Andrews 2001).

2.5.2 The Interior Insulation Approach

The application of insulation interior to the structural framing is usually combined with interstitial insulation, but can also be used as the primary thermal control. This strategy is popular in below-grade walls and as a retrofit in load bearing masonry or other historic buildings where the exterior cladding can not be changed. Two common examples of interior insulation strategies are:

1) Rigid Foam - foam board is applied directly to the interior structure and covered by a layer of gypsum wall board or other fire resistant finish (Figure 13)

2) Strapping - horizontal strapping is applied to the interior of the wall to create a space where batt, board or spray applied insulation can be installed (Figure 14)

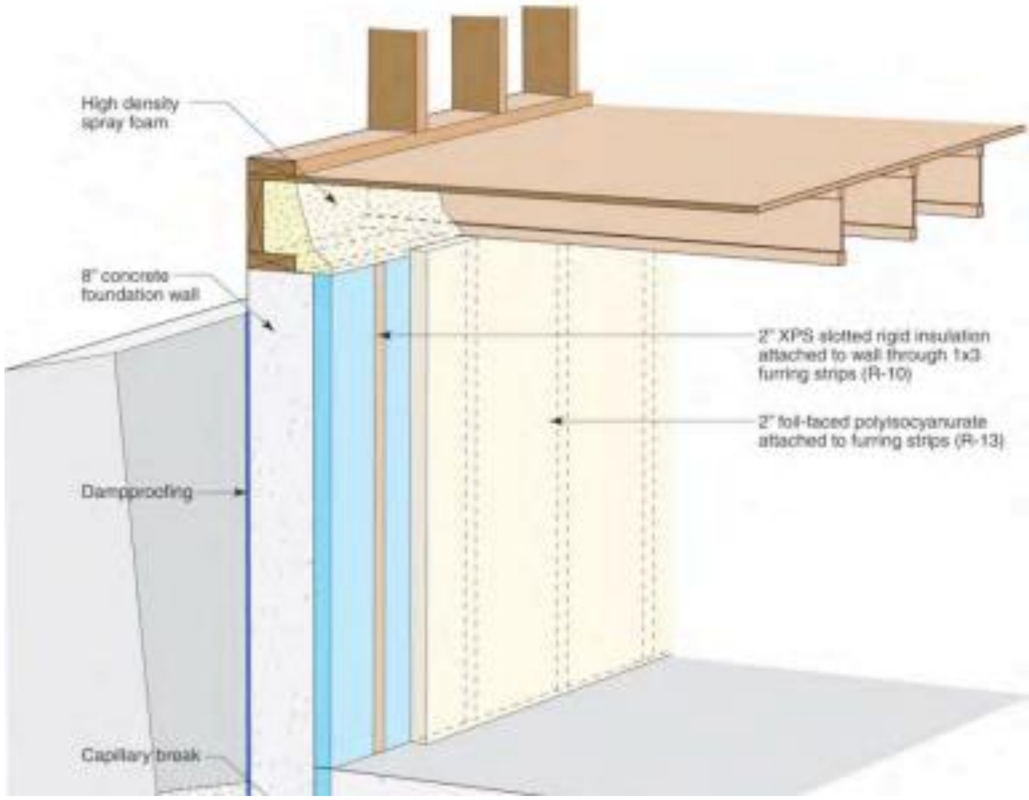

Figure 13- Foam board on interior of foundation wall (Straube and Smegal, 2009)

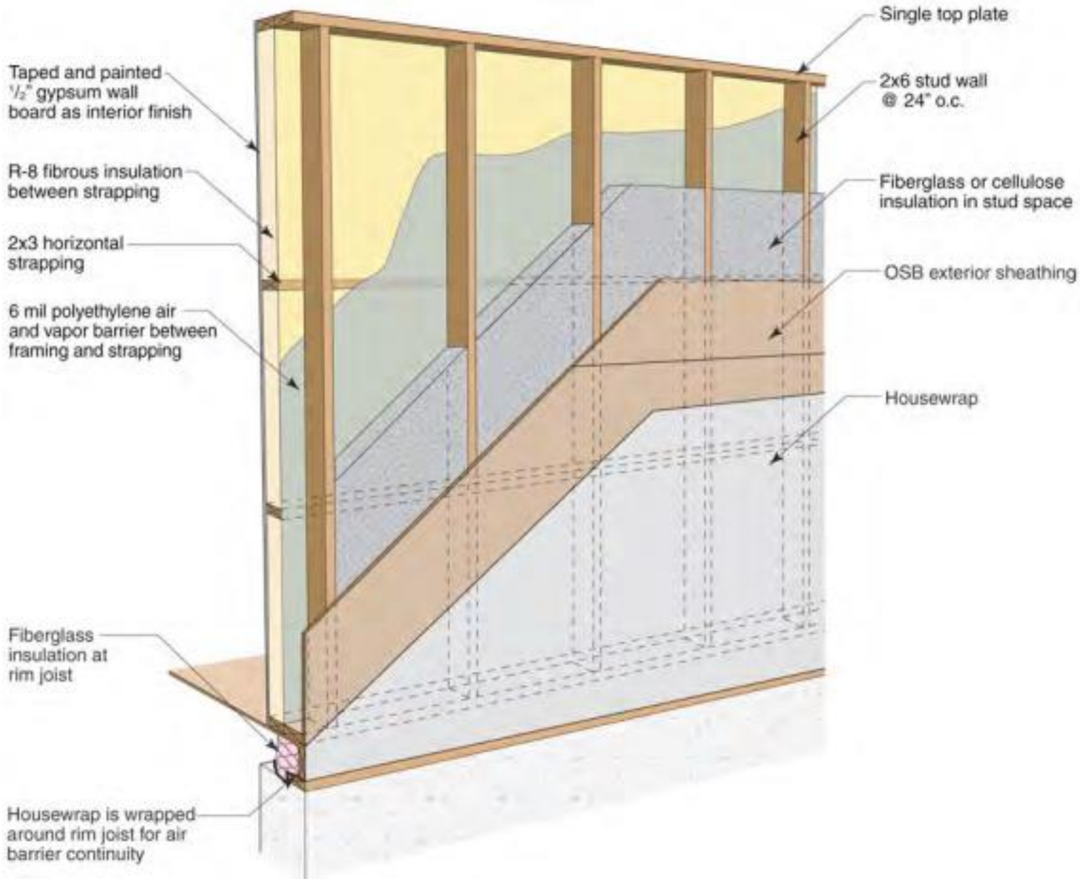

Figure 14- Wall with interior strapping

Thermal bridging is reduced in these designs because the interior insulation layer is continuous over wall studs and plates. There are still potential areas of thermal bridging at rim joists however. The main drawback in these designs, is the effect of the additional interior insulation on durability. Like the thick-wall designs described in the previous section, this strategy results in cold sheathing during winter conditions, increasing the potential for air leakage condensation. While monitoring studies of interior insulated wall systems is limited to foundation walls, it is clear that condensation risk is high when vapour and/or air flow is not well controlled at the interior face of these wall systems (Straube, 2009). Like the thick wall approach, a well detailed air barrier is critical to the durability of this type of wall system. As seen in the interior strapping example above, interior insulation is often paired with interstitial insulation in a hybrid approach – described in section 2.5.4.

2.5.3 The Exterior Insulation Approach

The benefits of the exterior insulation strategy were first documented by in the early 60s for masonry wall assemblies (Hutcheon, 1964). This approach results in higher winter temperatures of the building's structural elements. The two important benefits of this approach are to shelter the structural elements and control layers from temperature cycling and to eliminate condensation on the inner surface of the wall sheathing. Both of these benefits can result in increased durability of the wall system. Some of the more common examples of the exterior insulation approach include:

1) Insulated sheathing- A layer of rigid foam or rockwool boards is fastened to the exterior of the structural framing. Furring strips are then attached exterior to the insulation layer and fastened through the insulation to the wall framing as a means of securing the insulation and to provide attachment for the cladding system (Figure 15).
2) EIFS- A layer of rigid foam (typically expanded polystyrene) is fastened to the exterior of the structural framing. The foam is then covered with a synthetic stucco system. The stucco system is typically composed of a trowel-applied cementitous base coat with an embedded reinforcement fiberglass mesh and a finish coat composed of acrylic polymer. Early versions of this system were 'face sealed' systems which were assumed to be water-tight and made no accommodation for drainage. The result was a significant number of failures due to rain water penetration (Lstiburek, 2006). In response to this problem, drained EIF systems were developed by adding a drainage plane and gap behind the insulation level (Figure 16). The drainage plane is applied exterior to the sheathing and can be lapped building paper, trowel applied or spay-applied water barrier. A drainage gap can be created using grooved foam board, by adhering it with adhesive applied by a notched trowel or using a wrinkled house wrap.
3) Exterior Spray Foam- The application of spray polyurethane foam (SPF) to the building exterior is a common approach in commercial buildings. The major benefit of this approach is that the spray foam acts as the thermal, air, vapour and rain barrier. A major drawback of the exterior spray foam approach is that it results in a bumpy and uneven surface making cladding application challenging. The solution to this issue is to apply a cladding attachment system prior to spraying the wall and leaving a variation gap between the foam and the cladding. Some common cladding attachment systems include brick ledge and ties for masonry cladding and 'Z' brackets or the off-set wall approach (Figure 18) for lightweight cladding.

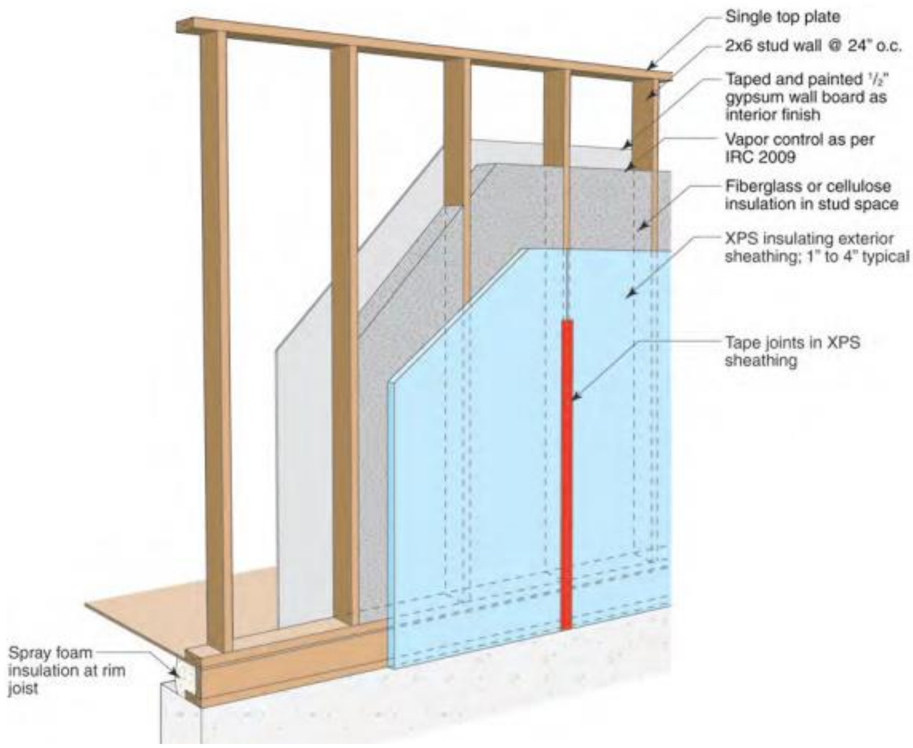

Figure 15 - Insulated sheathing wall system (Straube and Smegal, 2009)

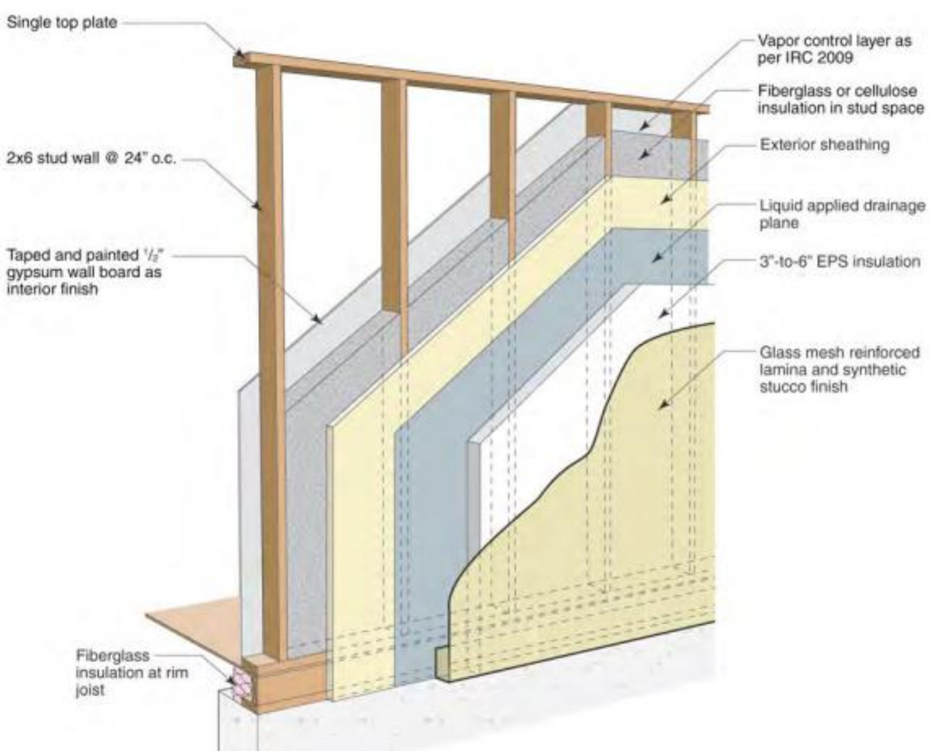

Figure 16 – EIFS Wall System (Straube and Smegal, 2009)

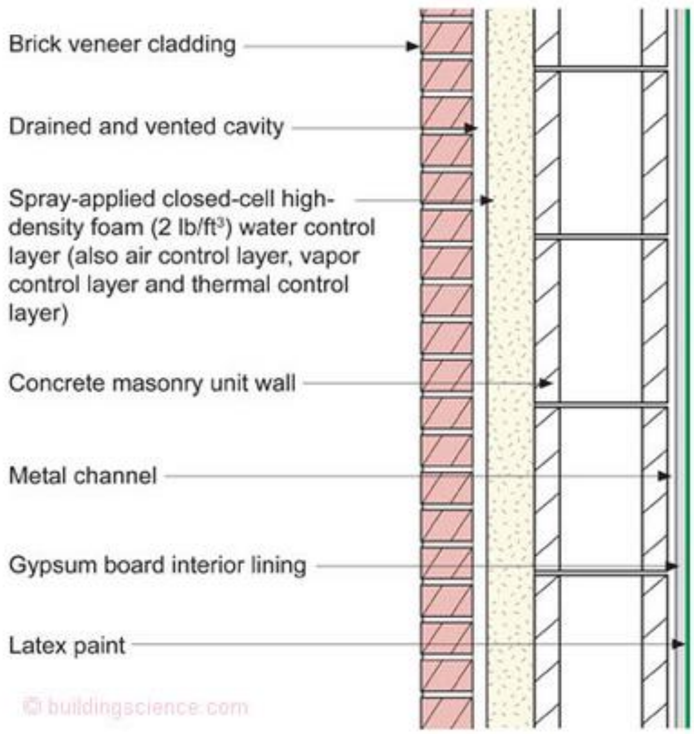

Figure 17 – Exterior Spray Foam wall system (Lstiburek, 2011)

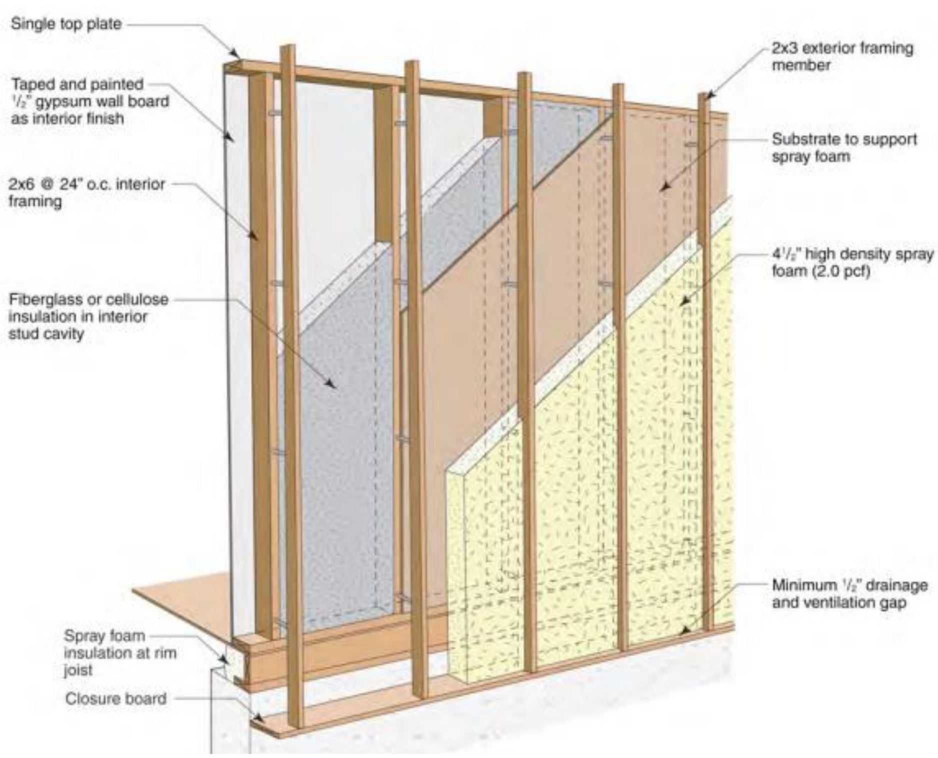

Figure 18- Off-set wall system (Straube and Smegal, 2009)

When applying this strategy in a 'super insulation' approach, a thick layer of exterior insulation is required, resulting in potential construction complications regarding the attachment of cladding and the integration of windows into the building enclosure. The cladding issue can be handled with the installation of vertical furring strips. This method has the important added benefit of creating a drainage and ventilation gap behind the cladding, although it does put some limitations on cladding choices. The window installation issue is more complicated. The window may be installed in line with the structural framing of the building (an 'innie'), or flush with the furring strips on the exterior of the wall (an 'outie'). Depending on the location of the rain barrier layer in the assembly, careful rain barrier detailing and flashings may be required to avoid water intrusion at window openings.

Another important issue with the exterior insulation approach is the potential to significantly reduce the drying potential of the wall system due to reduced heat energy flow, the potential to trap moisture behind the insulation and the potential for reduced vapour flow to the exterior. This issue gained a great deal of attention due to the massive failure of early EIFS applications. These early EIFS assemblies had no rain control layer behind the insulation and no provision for drainage. This approach was so unsuccessful that a study by the American Institute of Architects in 1995 found water intrusion in 94% of the homes inspected (Hall). Multiple class-action lawsuits resulted from this early EIFS system. While the EIFS issue was related mostly to a lack of a true rain barrier and drainage space (Keclik and Maino, 2008), decreased drying potential is a concern for all exterior insulated wall systems.

2.5.4 The Hybrid Approach

An alternative to using one of the insulation strategies described above is to combine two or more strategies in a hybrid approach. Some common hybrid approaches include:

1) Interior insulation combined with interstitial insulation (Figure 14)- The benefit of this approach compared to an interior-only strategy is that it provides more thermal resistance per unit thickness. It also provides reduced thermal bridging compared to interstitial insulation alone. The main drawbacks of this method are that it does not reduce cold-weather condensation potential by warming the sheathing and it may reduce or eliminate drying to the interior, depending on the properties of the interior insulation.
2) Exterior insulation combined with interstitial insulation (Figure 15)- The main benefit of this approach compared to an exterior-only strategy is that it provides more thermal resistance per wall thickness. It also provides reduced thermal bridging and reduced cold-weather condensation potential compared to interstitial insulation alone. If the proper ratio of interstitial to exterior insulation is used, the sheathing will remain above the dew point temperature of exfiltrating air, reducing the condensation accumulation within the wall during winter months. A dew point analysis may be required to determine the appropriate ratio for a given climate. The main drawback of this method is that it may reduce or eliminate drying to the exterior, depending on the properties of the exterior insulation.
3) Insulated concrete form (ICF) walls – ICF walls utilize insulation on both interior and exterior of a poured concrete wall. Utilizing formwork made of an insulating material (typically expanded polystyrene), the forming and insulating can be accomplished in one step. The result is a solid

concrete wall with 2-4 inches of insulation on both the interior and the exterior (Figure 19). Benefits of ICF walls include the strength and sound attenuation of a solid concrete wall and minimal thermal bridging. The high thermal mass of the walls may also provide a benefit to heat loss/gain in climates with large diurnal variations in temperature. Drawbacks include high cost and low thermal resistance per thickness. Because the concrete core has very little thermal resistance, thick layers of insulation must be applied to the interior and/or exterior to create a super-insulated wall system.

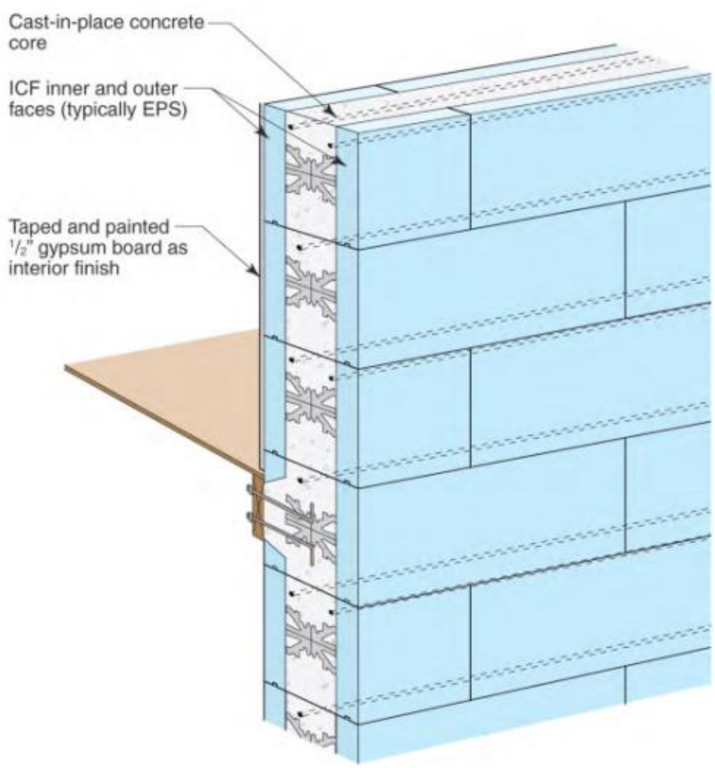

Figure 19- ICF wall system (Straube and Smegal, 2009)

3 Review of the Literature

3.1 The History of Exterior Insulation Strategies

3.1.1 Introduction

Before the time of wood framed buildings, mass wall systems of stone, sod, logs, earth, snow or other local materials were used to create shelter. These buildings were small and the wall structures were thick, had significant thermal mass and some thermal resistance. The expectations for occupant comfort were low and these types of mass wall systems provided enough shelter for survival, even in cold climates. Starting in the mid-1800s, wood framing techniques began to take over residential construction in North America. With these light framing techniques, much of the thermal mass and thermal resistance of the wall system was lost. Although some examples of seasonal exterior insulation strategies have been recorded (involving the temporary use of straw or snow piled up on the exterior walls of the building), the application of insulation to wood framed walls has primarily involved insulation within the walls, between the framing members. Despite some major limitations, this approach has been the standard practice in residential construction in North America for over 50 years.

3.1.2 National Research Council of Canada (NRC)

In 1960, the National Research Council of Canada began publishing short papers on building science topics, titled "Canadian Building Digests" (CBD). The topics discussed in this series cover nearly every aspect of design and construction in Canada. These digests include some the earliest discussions of the benefits of exterior insulation strategies.

Insulation on the exterior of the building structure was first discussed in the context of building science in CBD#16 – "Thermal insulation in dwellings" (Ball, 1961). In this article, the author describes the primary purpose for adding insulation is reducing overall heat flow, however it is also important that the thermal resistance is uniform to avoid variations in surface temperatures, as these variations can result in condensation and frost formation. This article goes on to explain that the best way to achieve a uniform thermal layer is to apply insulation to the building "in a manner similar to that of clothing on a person. In this way the insulation would be continuous over the building and its structure would be protected from the extremes of temperature both winter and summer." The issues associated with thermal bridges are further discussed in CBD #44 – "Thermal Bridges in Buildings" (Brown and Wilson, 1963). The effects of thermal bridging on thermal and moisture performance are discussed, along with several methods to reduce these effects. The use of continuous exterior insulation is presented as the "ideal solution" to the problem of thermal bridging.

In CBD #50- "Principles Applied to an Insulated Masonry Wall" (Hutcheon, 1964), a typical commercial wall assembly is described. It is composed of a structure of concrete masonry units (CMUs) and steel beams/columns, with stone cladding attached to the exterior of the CMUs with a system of ties, steel ledge supports and a full mortar bed between the stone cladding and CMUs. Insulation is applied to the interior of the CMUs with a plaster finish interior to that. The author goes on to describe the temperature profile through this wall system in winter and summer conditions (Figure 20). In this assembly, the cladding and structural components of the building, go through extreme temperature variations throughout the year. This can lead to temperature movement cracks in the CMU wall and stone cladding. These cracks can allow rain water to enter from the exterior and warm humid air to leak from the interior and condense on cold structural elements.

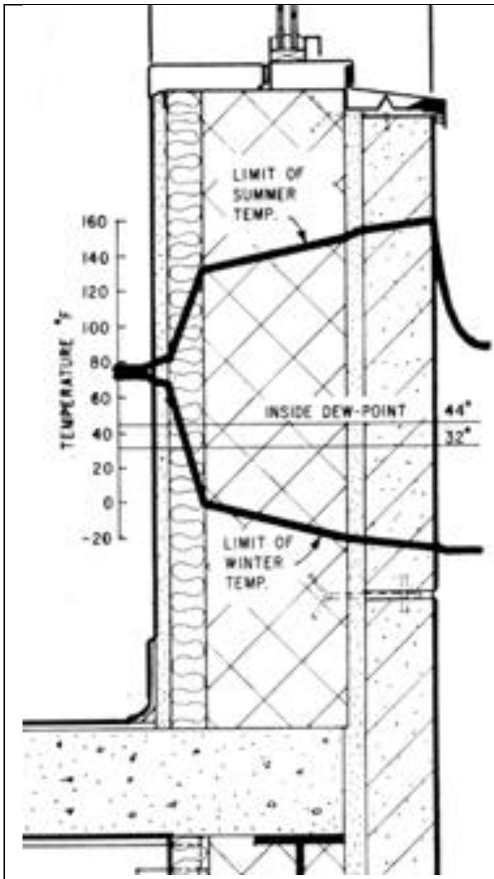

Figure 20- Temperature profile through typical CMU wall assembly (Hutcheon, 1964)

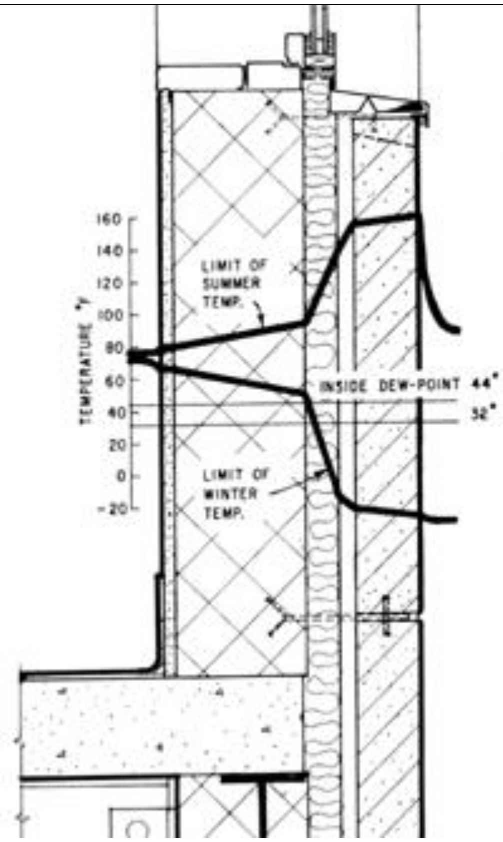

Figure 21- Temperature profile through exterior insulated CMU wall (Hutcheon, 1964)

This moisture within the wall assembly can lead to many durability issues including freeze/thaw degradation of masonry elements, corrosion of ties, ledges, beams and other steel elements and water staining of cladding and/or interior finishes. This wall assembly is also effected by thermal bridging at slabs, cross walls, steel beams and windows (which are attached to the CMUs), which will greatly reduce the effectiveness of the insulation.

The author then describes an improved wall design with insulation layer on the exterior of the CMU structural wall. Exterior to this is an air space and then the stone cladding, with open joints that allow for expansion and contraction and facilitate drainage and ventilation (Figure 21). Moving the insulation layer to the exterior of the CMUs, greatly reduces the seasonal temperature variation of the structural elements of the assembly, reducing the risk of temperature movement cracks. The exterior insulation also keeps the structural elements of the assembly above the dew point of exfilatrating air, eliminates freeze/thaw risk at the CMU wall and greatly reduces thermal bridging in the assembly.

The article concludes by mentioning that an additional benefit to the exterior-insulated design, is that it allows for continuous air and vapor control layers exterior to the structural elements of the building.

3.1.3 PERSIST

While the research and analysis of Ball (1961), Latta and Garden (1962), Brown and Wilson (1963), Hutcheon (1964), and others at the NRC represent a huge step in the development of durable, exterior insulated wall systems, the application of this knowledge by practitioners took some time. One of the first groups to put these principles into application (and document the process), was the Building Sciences branch of the Alberta Public Works Department. They began applying these principles to Alberta Government Buildings starting in the mid- 1980s (Makepeace and Dennis, 1998). The name that they gave to this design approach was the Pressure Equalized Rain Screen Insulated Structure Technique (PERSIST).

The PERSIST design approach considers a wall assembly as a series of planes, each with a specific function. These planes are arranged to maximize their effectiveness and to assure the durability of the assembly. First, the structure is designed to maintain simple, continuous planes from foundation to roof. Next, the air/vapour/rain barrier is applied in a continuous plane to the exterior of the structure. The air/vapour/rain barrier in this approach is a fully adhered bituminous membrane that is continuously supported by the structure and is flexible where movement may occur and is sealed at all penetrations. Exterior to this membrane is the insulation layer, which is continuous and fastened tightly against the air/rain/vapour barrier. Exterior to the insulation layer is the cladding layer, which includes an air gap to the insulation layer, for drainage and air movement. This layer sheds bulk water, drains any water that penetrates through the cladding and protects the structure from U.V. exposure. The cladding is attached to the structure with minimal penetration through the insulation and air/vapour/rain barrier layers.

Makepeace and Dennis (1998) used a computer simulation tool (EMPTIED) to demonstrate the potential effects that the PERSIST method would have on air leakage condensation potential. For this study, three wall systems were compared; a PERSIST wall with all insulation (RSI 10) on the exterior of the structure, a modified PERSIST wall with RSI 3.2 (R-18) on the exterior and RSI 2.1 (R-12) batt insulation added to the space between the framing members and a standard wall design with only RSI 2.1 (R-12) batt insulation between the framing members. Three interior humidity levels were studied (10%, 25% and 50%) along with 5 air leakage conditions (leakage areas of 0.0, 0.1, 1.0. 5.0 and 10.0 cm^2/m^2). The climate for Edmonton was used for the simulation. As seen in Figure 22, significant moisture accumulation was predicted for the standard wall under mid- and high RH conditions and higher air leakage. The modified PERSIST wall showed moisture accumulation only under the 50% RH condition and the higher air leakage rates, while the true PERSIST wall showed no moisture accumulation over any of these conditions.

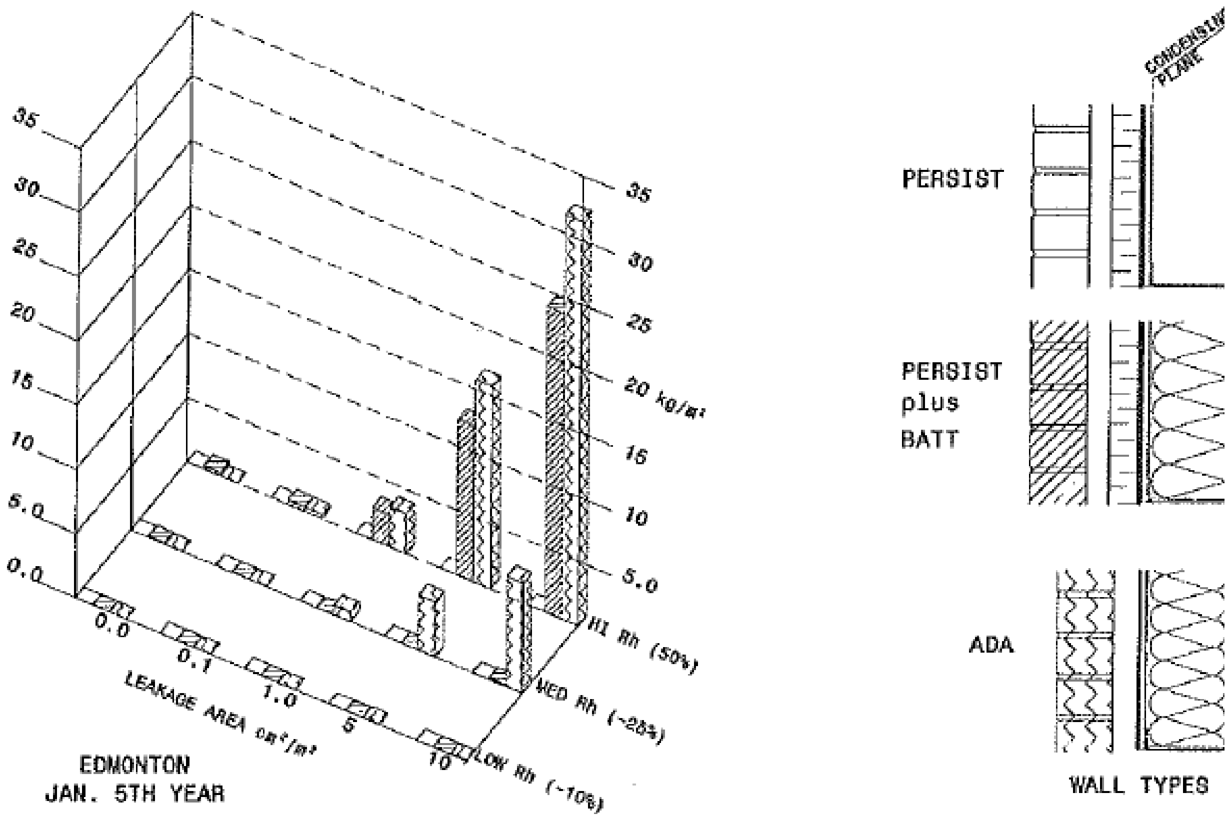

Figure 22 - Moisture accumulation results from computer simulation (Makepeace and Dennis ,1998)

The PERSIST technique was successfully applied to commercial building throughout the 1980s and 90s, however it's applicability to residential construction was not well understood. Baker and Makepeace (2000) studied this from a cost perspective. This study showed that damage due to water penetration is a serious financial issue in residential construction and can also have potential health effects. The most important benefit of applying the PERSIST method to residential construction is the reduced risk of damage due to water accumulation, however there could be other benefits including decreased heating energy requirements, comfort and health improvements and benefits for construction sequencing. Detail drawings (as seen in Figure 23 through Figure 25) were developed to demonstrate that the PERSIST concepts could be applied to residential construction and to develop cost estimates. The wall system included a standard wood stud structure with no insulation between the framing members and typical exterior sheathing. Exterior to this is a fully adhered membrane which acts as the air, vapour and water barrier. A layer of foam board insulation is then applied continuously over the structural elements of the house including the rim joist and window/door headers. Vertical strapping is used to hold the insulation tight to the membrane and to create an air gap behind the siding. Siding is attached directly to this strapping. The detail drawings for the roof were very similar to wall details with a wood stud structure with typical roof sheathing and a fully adhered membrane. Exterior to this was a layer of foam board insulation. In order to specify typical asphalt shingles, a second roof structure was built on top of the insulation layer, with vertical strapping and a second layer of roof sheathing.

Based on these details, the initial construction cost premium for a typical 1500 sq. ft. house in 1999 was estimated to be $4257, or 2.7% of the total construction cost. The authors felt that this cost premium was easily justified when considering the costs of water damage repairs and the energy benefits of the method.

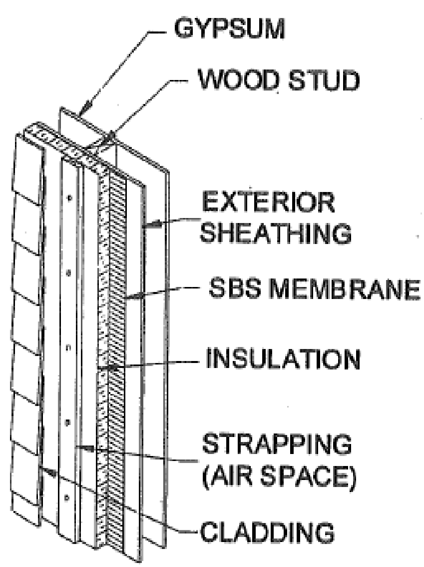

Figure 23 - Typical PERSIST residential wall section detail (Makepeace and Dennis, 1998)

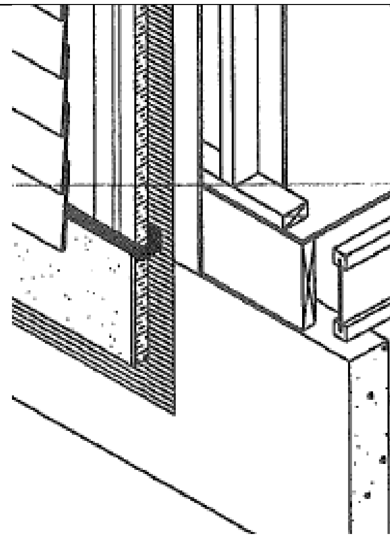

Figure 24 - PERSIST residential framing to foundation detail (Makepeace and Dennis, 1998)

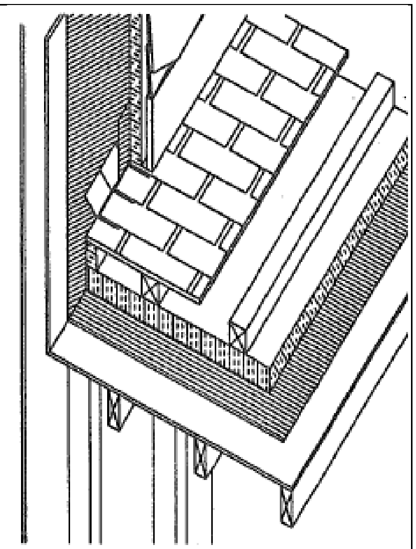

Figure 25- PERSIST residential roof and roof section detail (Makepeace and Dennis 1998)

3.1.4 The REMOTE Wall System

In 2002, researchers at the Cold Climate Housing Research Center (CCHRC) in Fairbanks, Alaska began to study the application of PERSIST techniques to residential construction (Maxwell 2005). The goal was to apply the principles behind the PERSIST method to cold climate residential construction, in a cost effective manner. The result of this study was the ‘REMOTE’ building system. REMOTE stands for Residential Exterior Membrane Outside Insulation Technique. As a cost savings measure, the system pairs the PERSIST wall with a ventilated (cold) roof design (Figure 26). The fully adhered membrane of the wall system is sealed to the ceiling plane air/vapour barrier (6 mil poly) which is behind the ceiling drywall. The other important change from the PERSIST approach is the inclusion of insulation between the framing members.

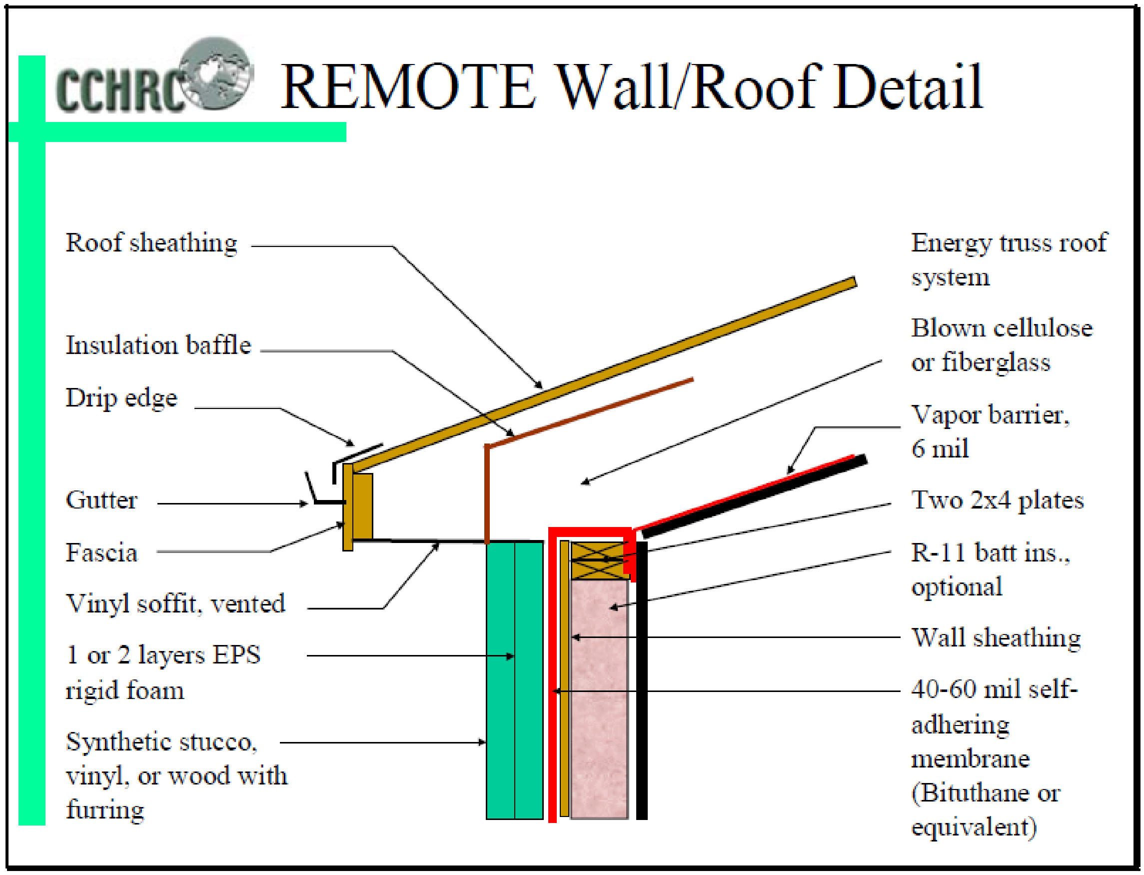

Figure 26- Typical wall/roof detail for REMOTE system (Maxwell, 2005)

In a small scale experiment, a house built with this system was compared to an identical house, built using standard construction techniques. The REMOTE test house showed a significant decrease in condensation potential compared to standard construction, however some condensation could occur under conditions of higher interior humidity (35% or higher). A direct comparison of the REMOTE house to the standard house also showed increased air tightness from 2 ACH50 in the standard house to .4 ACH50 in the REMOTE house. This improvement demonstrated the effectiveness of the externally applied fully adhered membrane as an air barrier. Construction costs were also studied. The REMOTE house cost approximately $ .85 more per square foot of heated floor space or approximately $1275 for a typical 1500 sq. ft. house in 2005. The authors also looked at this as a percentage of the wall system materials cost and found that the REMOTE wall system cost 15-23% more than the standard wall system used in Alaska at that time.

3.1.5 The Perfect Wall

The “Perfect Wall” label was first used by Lstiburek (2008). Also based on the early work done by the researchers at the NRC, the Perfect Wall concept was developed as a conceptual teaching tool. In this concept, rain control, air control and vapour control are viewed as separate functional layers. All of these functional layers are located on the outside of the building structure and the thermal control layer (insulation) is exterior to that.   A drained cladding system is used on the exterior to handle bulk water and for UV protection. Any water penetrating the cladding drains to the exterior of the building.

Several practical applications of the Perfect Wall concept are described. First, the “Institutional Wall” which is composed of a formed concrete or concrete block structural wall, with a fully adhered membrane (peel and stick, spray applied or trowel applied) on the exterior surface to act as the air barrier, vapour barrier and rain control layer. Exterior to that is the insulation layer, a drained cavity and brick veneer cladding. A second version of the Institutional Wall uses spray-applied closed cell high density foam on the exterior of the structure, which acts as the air barrier, drainage plane and insulation layer.

The second version of the perfect wall described in this report is the “Commercial Wall”. This version utilizes a steel stud wall with no insulation between framing members and a non-paper faced gypsum sheathing as the structure. A fully adhered membrane acts as the air barrier, vapour barrier and rain control layer. Exterior to that is the insulation layer, a drained cavity and brick veneer cladding. This is presented as a more affordable version of the institutional wall. This design can work in any climate, with appropriate adjustments to the thermal resistance of the insulation layer.

The third version of the perfect wall is the “Residential Wall”. This version differs from the commercial wall in that it uses a framed structural wall, with plywood or OSB sheathing. In all but the coldest climates, batt insulation can be used in between the structural members to add thermal resistance. Again, a drained cavity and cladding on the exterior are used.

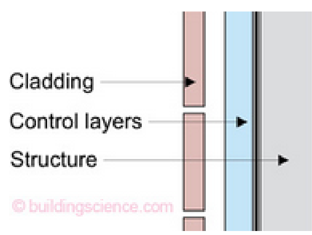

Figure 27 - The Perfect Wall concept (Lstiburek, 2005)

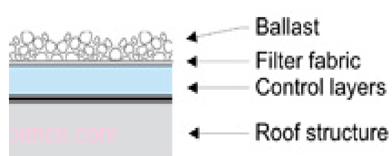

Figure 28 - The Perfect Roof concept (Lstiburek, 2005)

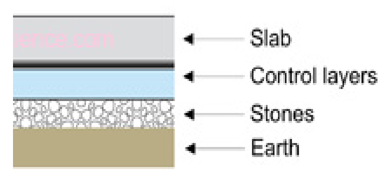

Figure 29 - The Perfect Slab concept (Lstiburek, 2005)

To show how the perfect wall concept can be applied to the entire building enclosure, the perfect roof and the perfect slab are also described.   In the Perfect Roof (Figure 28) the roofing membrane acts as the rain, air and vapour control layers and is applied directly to the roof structure. Insulation is applied exterior to this and stone ballast and a filter cloth act as the cladding, securing the insulation layer and protecting the control layers from UV and impact damage. In the Perfect Slab concept (Figure 29), the air, vapour and water control layers are directly exterior to the structural slab, with the insulation layer exterior to this and a layer of clear stone acting as the drainage layer.

3.1.6 Summary

There are several significant benefits of applying the insulation layer to the exterior of the structure. These benefits include:

1) it allows for complete continuity of the thermal layer and eliminates thermal bridging from structural elements
2) it allows for complete continuity of the air, vapour, and rain control layers on the exterior of the structure thereby protecting it, and avoiding unnecessary and large penetrations,
3) the location of the insulation layer protects the air, vapour, and rain control layers and structure from temperature swings and the resulting contraction and expansion
4) the insulation layer keeps the structure and sheathing warmer and dryer, reducing or eliminating the risk and amount of condensation on vulnerable structural elements
5) the creation of a service cavity that is completely within the thermal, air and vapour enclosure for improved continuity of these layers

There are also several significant challenges associated with exterior insulation strategies, including:

1) Increased cost due to more expensive insulation materials and non-standard construction details
2) The integration of windows and doors requires specialized detail work and more labour. Two strategies of window integration are commonly used:
    a. “Innie “ windows and doors are installed in the plane of the structural sheathing. This allows for easier integration of the windows and doors with air, vapour and water management layers (when they are applied to the exterior surface of the sheathing). Extra detail work is then required to provide a finished look and bulk water control between the window/door and the exterior face of the siding. This is often achieved with painted wood or composite trim pieces, with or without aluminum cladding.
       An additional advantage of an innie window/door is improved thermal performance due to decreased wind-washing affects and the option of continuing exterior insulation over the window frame.

    b. “Outie” windows and doors are installed in the plane of the back of the siding. For structural attachment, window/door extension bucks must be installed to the framing and the air, vapour and water management layers must be carefully extended over these bucks. This detail work requires careful planning and a significant amount of labour to assure continuity of these control layers. To provide a finished look to the interior of the window/door, extra-wide interior jambs are used with standard installation techniques. The advantages of the outie approach are mostly cosmetic, as it creates a traditional exterior appearance and deep interior sills similar to traditional structural masonry buildings.

3.2 Previous Studies of Air Leakage Condensation and Drying Potential

3.2.1 Introduction

Although limited experimental study has been performed on high-R wall systems, air leakage condensation and drying potential has been studied for more typical wall and roof systems. Understanding the methods and results along with the strengths and limitations of previous experimental studies is important in order to contribute new and useful information to this field of study. The following is a summary of previous experimental studies of air leakage condensation and drying potential.

3.2.2 Tenwold, Carll and Malinauskas, (1995) Airflows and Moisture Conditions in Walls of Manufactured Homes

This study involved field testing of wood framed walls for the purpose of measuring interstitial air flow and moisture conditions. The main goals of the research were to:

1) Quantify the air leakage characteristics of wood framed walls representative of those seen in manufactured homes
2) Identify the relationship between air flow and moisture accumulation
3) Identify the influence of wall construction details on air leakage and moisture accumulation
4) Identify the role of indoor RH on moisture accumulation within the walls

Test walls were built and installed in a natural exposure test hut in Madison, Wisconsin. Interior conditions were held at 21 ° Celsius and two humidity conditions were studied, 35% RH and 45% RH. All wall types tested were 2 X 6 wood framed walls with framing members at 16 inches on center and kraft paper-faced fiberglass batt insulation between the framing members. The interior of all test walls was covered with gypsum wall board (GWB), sealed with caulking at all framing members. A standard electrical box and electrical outlet was installed as a method of allowing air flow path through the GWB and controlling the flow path. In three of the test wall types, wafer board sheets acted as both the wall sheathing and the exterior cladding. Another wall type tested, utilized a 'foamular' weather barrier exterior to the framing and metal siding panels as the exterior cladding. A third wall type tested, utilized fibreboard sheathing and wafer board siding as the exterior cladding.

Using ventilation gaps between the cladding and the framing, the effect of wall cavity ventilation to the exterior was evaluated. Although cavity ventilation has a small drying effect on walls that that had a continuous interior air barrier at the lower interior humidity (35%), when air leakage occurred from the interior or RH levels reached 45%, there was no measurable drying effect. Cavity ventilation resulted in higher daily average pressures across the GWB, higher exfiltration air leakage rates and a reduction in the thermal resistance of the wall systems by approximately 30%. The most important variable affecting moisture accumulation within the wall cavity was interior humidity. The only walls that did not see signs of condensation under the high interior humidity condition were the walls that had fibreboard sheathing and ventilated cladding exterior to this. This was the only wall design that did not utilize a ventilated cavity approach.

The results of this study show the importance of an air barrier on both the interior and exterior of a wood framed wall when using air permeable interstitial insulation.

3.2.3 Ojanen and Kumaran (1996) Effect of Exfiltration on the Hygrothermal Behaviour of a Residential Wall Assembly

In this study, a 2 dimensional air, heat and moisture transport model known as TCCC2D was used to predict moisture accumulation in a wall due to air exfiltration. The wall chosen for the simulations was a typical wood framed wall with 2 X 4 framing members, fiberglass batt insulation between the framing members, wood sheathing on the exterior and 6 mil poly vapour barrier and gypsum board on the interior. According to these simulations, critical factors affecting moisture accumulation were:

1) Exfiltration rate- In this study, air tightness of the wall system was varied between .001 and 10 $l/s/m^2$ at 75Pa. A 50 Pa pressure was then applied to induce air leakage. The simulation results showed a direct relationship between exfiltration rate and moisture accumulation between .001 and 1 $l/s/m^2$. Above 1 $l/s/m^2$, moisture accumulation drops due to the warming effect of the exfiltrating air on the condensation surfaces.
2) Exfiltration path- several air flow paths through the wall system were tested in this study. The important finding was that the length of the air flow path within the wall cavity was directly related to the amount of moisture accumulated. The shortest paths (directly through the wall) resulted in approximately 30% of available moisture deposited, while the longest paths (1.8 m) resulted in approximately 75% of available moisture deposited.
3) Interior humidity- Two interior relative humidity levels were modeled in this study, 36% RH and 48% RH. Increasing the RH by 33% resulted in an increase in moisture accumulated of 20% at low flow rates (.1 l/s/m2 at 75 Pa) to as much as 100% at higher air flow rates (1.0 l/s/m2 at 75 Pa). These results show that the interior humidity conditions must be understood to accurately determine the tolerable leakage rate. The higher the interior RH, the tighter the wall system must be to avoid air leakage condensation issues.
4) Insulation exterior to the sheathing – Simulations were performed with and without insulation exterior to the sheathing. In the insulated case, 25 mm of rockwool board (RSI .75, R-4.2) was added to the exterior of the sheathing – representing an increase in total enclosure R-value of 30% with 23% of total insulation value being exterior to the sheathing. This change resulted in a decrease in moisture accumulation of between 20% at low air flow rates (0.1 $l/s/m^2$) and 87% at higher air flow rates (1.0 $l/s/m^2$). These

dramatic results show the importance of sheathing temperature in controlling condensation within the wall assembly.

5) Climate – The effect of climate on moisture accumulation was also found to be significant. Using the weather profiles of 9 Canadian cities, a strong relationship was found between moisture accumulation and heating degree days. A 50% increase from 2700 HDD15C (Toronto) to 4100 HDD15C (North Bay) resulted in an increase in moisture accumulation of 600%. This simulation clearly shows the importance of climate-specific design.
6) Vapour permeance of the exterior of the wall – Simulations were performed with exterior sheathing of varying vapour permeance. The study showed an inverse relationship between moisture accumulation and vapour permeance. Due to the asymptotic relationship, it would take a 25 times increase in permeance from 60 ng/m2 s Pa to 1500 ng/m2 s Pa to get a 50% reduction in moisture accumulation.

3.2.4 Janssens and Hens (2003) Interstitial Condensation Due to Air Leakage: A Sensitivity Analysis

This study involved computer modeling of air leakage condensation for a typical unvented roof system. The method consists of a repeated number of 2D steady-state heat, air and vapour transfer simulations to predict the variation in moisture performance as a result of air exfiltration. For the simulations, the numerical calculation model 2DHAV was used. This model is used to predict the variation of condensation amounts in a specific enclosure design at certain indoor conditions due to varying air leakage characteristics.

All roof systems modeled had the same geometry, structural framing (2 X 6 framing), interstitial insulation (fiberglass batts), vapour barrier (Kraft paper) and interior finish (gypsum board). Interior conditions remained constant at 20 deg. C, with a vapour pressure of 1170 Pa and an air pressure of 2.5 Pa for all simulations. Exterior conditions representing a cold week in Ukkel, Belgium (-2.5 deg. C, with a vapour pressure of 470 Pa) were used for all simulations.

The experimental variables tested were:

1) Various intended air gaps in the roofing materials
2) Various unintended air gaps in the insulation
3) Various unintended air gaps in the interior air barrier system (GWB and kraft paper)
4) Three roofing type – single layer (corrugated plates), double layer (underlayment and tiles, separated by a ventilated air gap) and three layers (like the double layer with the addition of insulated sheathing below underlayment)

The important results from this study include:

1) Air leakage can be a significant cause of moisture problems in light weight, unvented roof systems, showing the importance of a quality air barrier system.
2) The greater the thermal resistance of the interstitial insulation, the greater the effect of air leakage on condensation accumulation.
3) Increasing the thermal resistance exterior to the framing cavity significantly reduces the accumulation of air leakage condensation.
4) Increasing the ability of the roof system to dry to the exterior, using a vapour permeable underlay and a ventilated air gap significantly reduces the accumulation of air leakage condensation.

3.2.5 KALAMEES AND KURNITSKI (2010) Moisture Convection Performance of External Walls and Roofs

In this study, typical air leakage rates (obtained from field studies) were used to create a full scale laboratory study of a typical junction between a wall and an unvented roof. This joint was considered the most critical due to the stack effect in a building with balanced ventilation. Both internal and external conditions were controlled using a climate chamber. The results of the laboratory study were then used to validate a computer model which was used to perform a long-term analysis of several different assembly types under different conditions.

In all trials of the experiment, roof framing was 2 X 10 wood framing, insulation was 220 mm of mineral wool between framing members and the air/vapour barrier 'foil'. The interior air temperature was held at 22 ° C. Moisture accumulation was measured gravimetrically, using two removable sections of roof sheathing in each test sample.

The experimental variables in this study were:

1) Wall type – wood framed and autoclaved aerated concrete
2) Air barrier overlap joint treatment – completely unsealed, 10 cm left unsealed, completely sealed
3) Outdoor temperature – 0, -5 and -10 deg. C
4) Indoor 'moisture excess' – 2.5, 4 and 5 g/m3
5) Roof sheathing type – 12 mm fibreboard and 20 mm mineral wool with integrated sheathing membrane
6) Pressure difference – 10 Pa and 20 Pa

Some important results from this study were:

1) For the 12 mm fibreboard sheathing, under the low pressure (10 Pa) and partially sealed air barrier conditions (low flow rate of .18 l/s/m3), condensation accumulated when the exterior temperature was -10 deg. C.

2) For the 12 mm fibreboard sheathing, even under the high pressure (20 Pa) and unsealed air barrier conditions (high flow rate of .5 l/s/m3), no condensation occurred when the exterior temperature was 0 deg. C.
3) For the 20 mm mineral wool sheathing (with integrated membrane), no condensation accumulated under any of the temperature and pressure conditions studied. Because the resulting air flow was lower than the with the fibreboard sheathing, (due to the integrated membrane), the contribution of the added thermal resistance of the sheathing and higher vapour permeability could not be separated out.

Important results from the modeling and simulation component of this study were:

1) Air leakage rate is directly related to condensation accumulation rate.
2) Interior relative humidity is directly related to condensation accumulation rate.
3) Exterior temperature is inversely related to condensation accumulation rate.
4) In modern houses, where pressure is not directly controlled, the best way to control durability problems caused by air leakage condensation, is through building enclosure air-tightness and the use of sheathing materials with good hygrothermal characteristics (ie, high thermal resistance and high vapour permeability.
5) Hourly variation in interior and exterior relative humidity did not affect the amount of condensation formation. Utilizing an average value produced the same results.
6) Hourly variation in exterior temperature did affect the amount of condensation formed and longer term average values under predicted condensation.
7) leakage rates of 0.1–0.2 L/(s•m) at a 10 Pa pressure difference may be used as performance criteria for moisture convection in a two-story house with moisture excess and a cold outdoor climate.

3.2.6 D. DEROME (2002) Moisture Accumulation in Cellulose Insulation Caused by Air Leakage in Flat Wood Frame Roofs

This study involves a series of laboratory tests of unvented roofs using a climate chamber. Two types of cellulose insulated, unventilated flat roof assemblies were exposed to various air leakage patterns. In an attempt to simulate real world conditions, the testing was broken into 7 test periods representing the interior and exterior conditions that would occur over a 1 year period, but compressed into 185 days of testing. The conditions that were controlled were interior temperature, interior RH, interior pressure, exterior temperature, exterior RH. The moisture content of the cellulose insulation was tracked using removable samples at different points along the exfiltration path and a gravimetric weighing method.

The experimental variables were:

1) Roof assembly type – Thermos- with 200 mm of cellulose between 2 X 10 framing and Lambourd- with 200 mm between 2 X 10 framing, with an additional 150 mm above the framing
2) Exfiltration path – Long path, short path, sealed (no exfiltration, diffusion only)

Some important findings from this study include:

1) Dense packed cellulose does not prevent air flow and is not a substitute for a proper air barrier.
2) Air leakage moisture can locally affect the consistency of the cellulose, resulting in 'caking'. The effects of this caking on the thermal resistance and air permeability of cellulose is unknown.
3) In the diffusion-only roof sections, there was little difference in moisture content between the Thermos and the Lambourd roof types.
4) During the winter wetting phase, moisture content increases at the exterior side of the assembly but remains constant at the interior side. During the summer drying phase, moisture content at the interior side of the assembly increases as drying occurs to the exterior.
5) With a long leakage path, the average moisture content of the cellulose is inversely related to the volume of insulation. This shows the moisture buffering effect of the cellulose.
6) With a short leakage path, there is little difference between the 2 assemblies on local moisture content. This indicates that moisture accumulation occurs in a small fraction of the overall volume of the cellulose.

3.2.7 Desmarais et al. (2000) Mapping of Air Leakage in Exterior Wall Assemblies

The focus of this paper was to test different methods of mapping and graphically displaying air leakage flow paths and moisture accumulation patterns within typical wall assemblies. A full scale test hut was constructed inside a climate chamber. The hut was exposed to 66 days of winter conditions, followed by 47 days of spring conditions. The interior conditions were varied between 22 deg. C, 50% RH and 4 Pa pressure during winter conditions and 23 deg. C, 45% RH, 1 Pa pressure during spring conditions. The exterior temperatures were -8.5 deg. C for winter conditions and 17 deg. for spring conditions.

The experimental conditions were:

1) Wall type (typical construction, exterior insulation added and interior insulation added)
2) Air leakage path (long path, direct path and diffuse path)

Two methods were used to map air leakage patterns. The first method uses moisture content as a proxy for air leakage. The moisture content of the sheathing was mapped using a grid of removable samples which were weighed regularly to determine moisture content. Moisture pins were also used, but the moisture levels reached were beyond their range of confidence. The second method used temperature change as a proxy for air leakage. A grid of thermo couples was placed on the interior and exterior planes of the cavity insulation. From this temperature data, lines of equal temperature were plotted to demonstrate the air leakage path within the wall cavity.

Some important findings in this study were:

1) Sheathing moisture content monitoring was preferred to temperature monitoring because the moisture storage within the sheathing made the results more stable than the transient temperature data.
2) Convective loops were present within the wall cavities.

3) Maximum moisture accumulation occurs at the section of sheathing opposite the air infiltration point.
4) Moisture accumulation was highest in the wall with exterior sheathing insulation, because it resulted in sheathing temperatures above the freezing point, but below the dew point.
5) Drying was slowest in the wall with exterior sheathing because it had vapour control layers on both sides of the cavity.
6) The wall sections with no air leakage had, by far the lowest levels of moisture accumulation.

3.2.8 Summary

Based on the review of previous experimental studies of air leakage condensation, it is clear that controlling air leakage through the building enclosure is vital to building enclosure performance. In heating climates, the moisture accumulation potential of exfiltrating air far exceeds that of vapour flow through building materials and for this reason, air leakage control must be a top priority in modern buildings. These studies showed that the amount of condensation due to air leakage is directly related to air flow rate, the length of the air flow path and the interior RH, and inversely related to exterior sheathing temperature.

While drying capacity was not directly measured in these studies, two of the studies (Ojanen and Kumaran, 1996; Janssens and Hens, 2003) showed that accumulation of sheathing condensation was inversely related the vapour permeability of the materials exterior to the wood sheathing.

4 Experimental Design and Set-up

The research work reported here is part of a larger collaboration between The Natural Sciences and Research Council of Canada (NSERC), The Network of Wood-Based Building Systems (NEWBuildS), the University of Waterloo Building Engineering Group and Ryerson University's Department of Civil Engineering. The goal of the larger experimental program is to study the use of wood products in current and future building systems.

4.1 Objectives

The objective of the experimental portion of this thesis was to obtain measured data to evaluate the moisture durability performance of three different exterior insulated systems. This information can be used to confirm our understanding of the mechanisms acting in wall systems and to validate hygrothermal computer simulation models. This validation is beyond the scope of this thesis, although it is the focus of an earlier thesis project (Fox 2013).

4.2 Approach

To meet the objectives of the project, natural exposure field testing was used. Natural exposure field testing is a rigorous means to study enclosure performance as the nature, intensity, frequency, and correlation of environmental loads are by definition realistic. The exterior environmental conditions are not chosen by the experimental designers, or limited, as they are in hygrothermal modeling.

This experiment focused on the performance of the experimental walls under ideal conditions (dry start to construction, perfect air and water tightness) and then measured the consequences of the two most important mechanisms of wetting; air leakage condensation and rain penetration.

Direct and continuous measurements of temperature, heat flow, relative humidity, and moisture content were taken at various positions throughout the wall assembly during natural conditions and under imposed wetting conditions.

4.3 Scope

The scope of this experiment was limited to the physical measurements and interpretation of five pairs of the enclosure walls tested in the NSERC/NewBuilds project. The experimental study focused primarily on exterior insulated wall systems, with comparisons to the standard and the double stud walls.

4.4 Experimental Design

A range of wall systems were chosen to investigate specific aspects of the durability problem. The accumulation of air leakage condensation and the drying of accidental rain leaks were the primary areas of interest. With input from funding stakeholders and other users of the experimental results at Ryerson University, the walls and their instrumentation plan were designed. Experience from previous field studies at UW was used to guide the type and location of the instrumentation.

In all test walls, an exterior layer of polymeric house wrap (Tyvek) was used to provide the rainwater control layer (drainage plane) and secondary air barrier, a sheathing layer of OSB was used exterior to the framing, and a layer of painted Gypsum Wall Board (GWB) was applied to the interior.

A wall that represented current wall systems in Ontario housing – 2x6 with R-24 fiberglass batt insulation and OSB sheathing - was included as a Datum for comparison. This type of wall has been used for almost 30 years in Ontario and is well accepted by the industry. Such a wall system provides an effective thermal resistance of about R-15, when accounting for the thermal bridging of the framing members. A polyethylene sheet provides the air and vapor control.

The other four walls in the study represented likely methods to reach future higher R-value goals. In general, an assembly R-value of around R-30 was the target as it was felt this would meet the needs of future Canadian building code editions. In three of the walls this was accomplished by the addition of exterior insulation to the Datum wall design. Three different insulation types with a range of vapor permeance (from very low to very high) were selected. One of the walls used a thick wall approach with cellulose insulation cavity fill and framing of double 2x4.

All test walls were built, installed and instrumented with the help of Mike Fox (from Ryerson Polytechnical Institute) and other student volunteers. The test walls were inserted into the north and south sides of the University of Waterloo's natural exposure facility, the BEGHUT (see section 4.5). The north and south exposures are intended to represent the extreme temperature conditions. Solar exposure on the south results in significantly higher peak and slightly higher average annual wall temperatures, while the north has the lowest winter and annual average temperature.

The following sections describe the BEGHUT experimental facility, details of the experimental wall construction, their instrumentation, and details of the techniques used to simulate air leakage and rain wetting.

4.5 The BEGHUT

4.5.1 Description of BEGHUT

The Building Engineering Group's outdoor full-scale permanent natural exposure, test and demonstration facility is known as the BEGHUT. The facility, which is located on the University of Waterloo campus, is a square building approximately 10.5 x 10.5 m in plan and 3.0 m high floor to ceiling. The walls are oriented in the four cardinal directions. The roof is peaked to the centre with a slope of 1-in-3. A pipe mast rising from the central peak of the roof supports a weather station at 10 m above grade.

An air-to-air heat pump heating and cooling unit, and supplementary humidification units maintained the interior climate at approximately 21 ºC and 40% relative humidity during this experiment. A ceiling-mounted air distribution system is used to distribute the conditioned air evenly. Four symmetrically mounted ceiling fans are used to prevent vertical and horizontal stagnation.

The structure is of wood post-and-beam construction with a trussed roof. The foundation is a 1.2 m high, 250 mm thick, unreinforced concrete wall on a 500 mm wide, 300 mm deep strip footing. The floor consists of a 100 mm thick concrete slab-on-grade placed on a polyethylene moisture barrier and 150 mm of granular fill. The corner columns and ring beam are sheathed with plywood, insulated with 150 mm fiberglass batts, and clad with aluminum siding. The roof system is comprised of asphalt shingles, building paper, and plywood sheathing, with an additional ice and water shield extending 600 mm up from the eaves. A construction plan of the BEGHUT is provided in Figure 30.

The roof overhang (200 mm) is sized to prevent shading from the sun under most conditions. The small overhang and the drip-edge in lieu of eavestrough, provide very little direct protection from rainfall.

The post-and-beam method of framing allows for installation of seven test panels in each side (28 total) of approximately 1.2 m wide by 2.4 m in height. Twenty seven of the wall panel spaces are available for experimentation. The last space is reserved for the door, currently on the north side of the building. Figure 31 and Figure 32 show the location of each of the test panels in the BEGHUT.

The test hut is sited on relatively flat land and is fully exposed to winds from most directions. A two-story office building located approximately 30 m to the north-west and a four-story office building located about 120 m to the west provide some shelter from these directions.

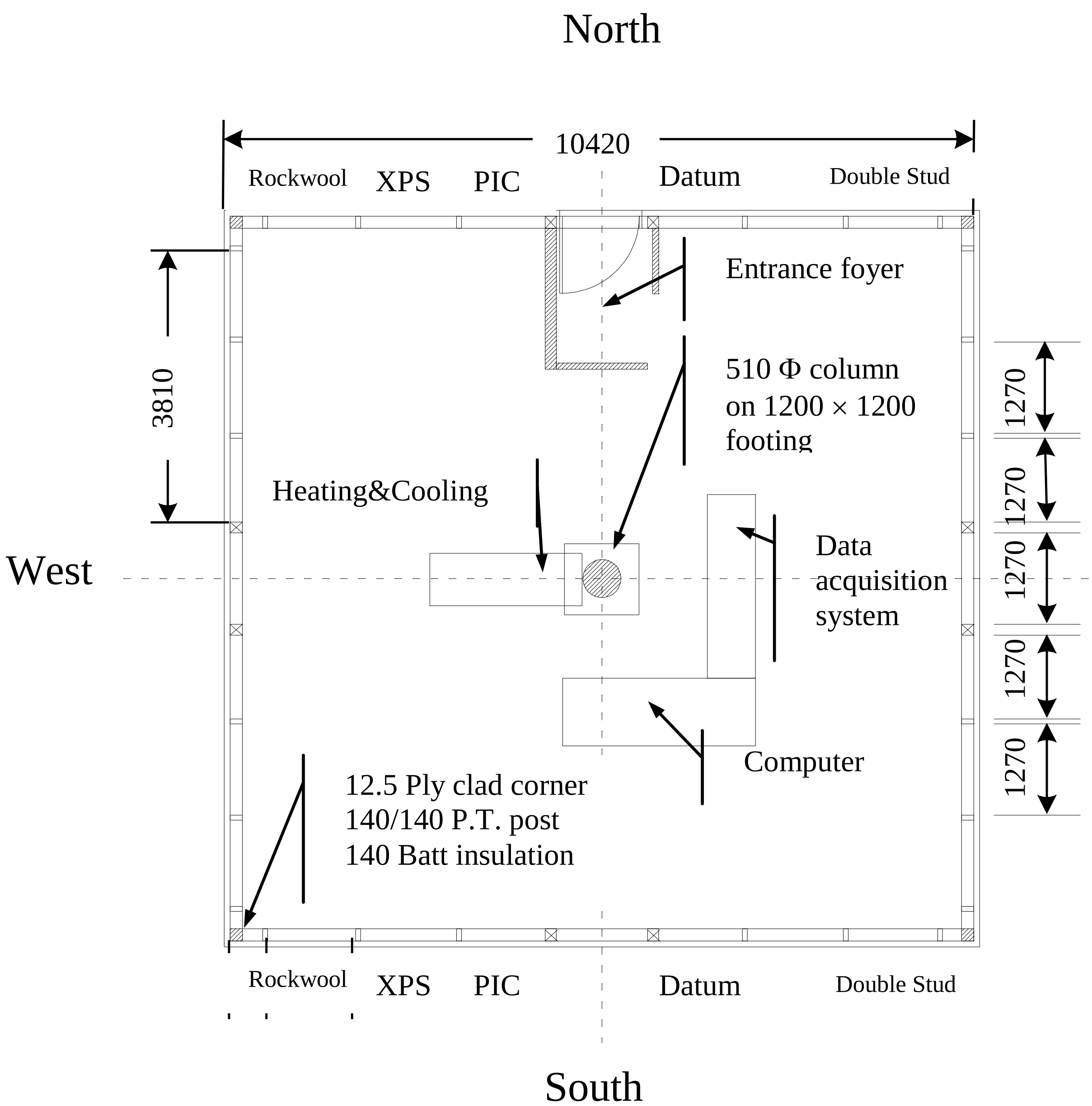

Figure 30- Construction plan of the BEGHUT and location of test walls (dimensions in mm)

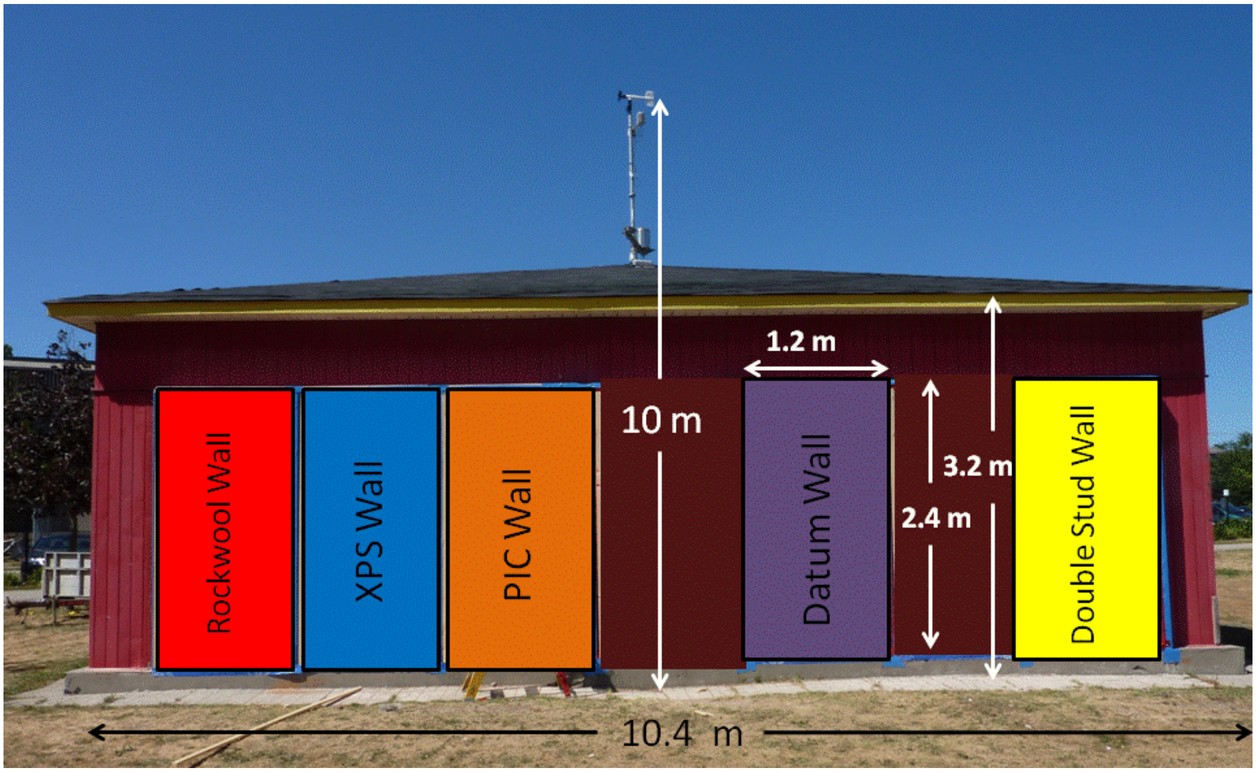

Figure 31- South elevation of BEG hut including test wall locations and dimensions

Figure 32- north elevation of BEG hut showing north test wall locations

4.5.2 BEGHUT & UW Weather Station Instrumentation

The weather station on top of the BEGHUT measures exterior temperature, exterior relative humidity, horizontal incident solar radiation, and rainfall.

A Vaisala™ HMP 35A with integral solar radiation and precipitation shield is used to measure relative humidity and temperature. To measure RH, the instrument uses a HUMICAP® sensor and a platinum Pt 100 RTD. The RH sensor has a range of 0 to 100% RH with an accuracy of approximately ±2% RH and repeatability of better than 1% RH per year. The humidity sensor produces a linearly-varying output in the range of 0 to 1 volt DC which is directly measured by the hardware and converted to RH by the software. The temperature sensor varies in resistance at about 0.38 Ohms/ºC; the voltage drop of a small current flow across this resistance is measured and converted into a temperature value by the software.

The incident horizontal solar radiation is measured by an Eppley™ pyranometer. The calibration accounts for the international standard solar spectrum and measures +/- 105 ° from vertical. This device, calibrated by the Atmospheric Environment Service, generates a small voltage signal proportional to the solar radiation.

A Rimco™ tipping bucket rain gauge is used to measure horizontal rainfall. The collector is a meteorological standard 8" diameter funnel, plated with gold to reduce surface tension effects. The bucket tips once for each 0.2 mm of rainfall. The resulting electrical pulse is measured by a dedicated counter chip. Because the gauge is mounted more than 10 meters off the ground, the catch is reduced by wind effects.

The interior environment is measured by a Vaisala™ HMP 35A RH transducer accurate to +/- 2%RH. The sensor is located near the middle of the BEGHUT at a height of 1.8 m above the floor. A 3000 Ohm YSI™ thermistor, accurate to within 0.2 ºC, measures the interior temperature. The temperature sensor is located near the RH sensor.

The UW Weather Station instrument specifications are included in Table 1. Archived data is available at http://weather.uwaterloo.ca. The exterior weather elements (temperature, relative humidity, horizontal solar radiation, and falling rain) are recorded. The weather data from the nearby Environment Canada - University of Waterloo Class A weather station substitutes weather data when not available from the BEGHUT weather station.

Table 1- UW Weather Station Instruments

Instrument	Manufacturer and Model	Units	Accuracy
Incoming Short Wave Radiation	Kipp & Zonen Model: CM11 S.N. 966046	W/m^2	+/- 10 W/m^2
Reflected Short Wave Radiation	Kipp & Zonen Model: CM11 S.N. 966038	W/m^2	+/- 10 W/m^2
Relative Humidity	Vaisala Model: HMP35C	%RH	+/- 3.0 %RH
Ambient Air Temperature	Vaisala Model: HMP35C	°C	+/- 0.4 °C
Wind Direction (top)	RM Young Model: Wind Sentry 03002-10A	0-360° (C.W.)	N.A.
Wind Speed (top)	RM Young Model: Wind Sentry 03002-10A	m/s	+/- 0.5 m/s
Tipping Bucket	Texas Electronics Model: TE252	mm	+/- 0.1 mm

4.6 Wall Panel Design and Installation

4.6.1 Common Assembly Components

The common elements in the design of all the test walls were the framing layout, the cladding, the cavity behind the cladding, the water control membrane, the structural sheathing, and the interior finish. Each of these are described below.

4.6.1.1 Framing Dimensions and Layout

Each test wall was framed with the same overall dimensions and framing layout. As shown in Figure 33, each wall was 96 inches (2438 mm) high and 48 inches (1219 mm) wide. The walls were framed with double top plates and a single bottom plate using standard 1 ½ inch (38 mm) thick framing lumber. The outside vertical members (studs) were built of 3/8 inch (9.5 mm) thick plywood to minimize thermal bridging while the two inner studs were standard 1 ½ inch (38 mm) thick framing lumber to represent standard construction. As shown in Figure 33, the center “Test Bay” was framed at 24 inches (610 mm) on-center, resulting in a cavity width of 22 ½ inches (572 mm). The center stud bay was used for all monitoring, while the outer bays acted as guard bays, providing a hygrothermal buffer zone.

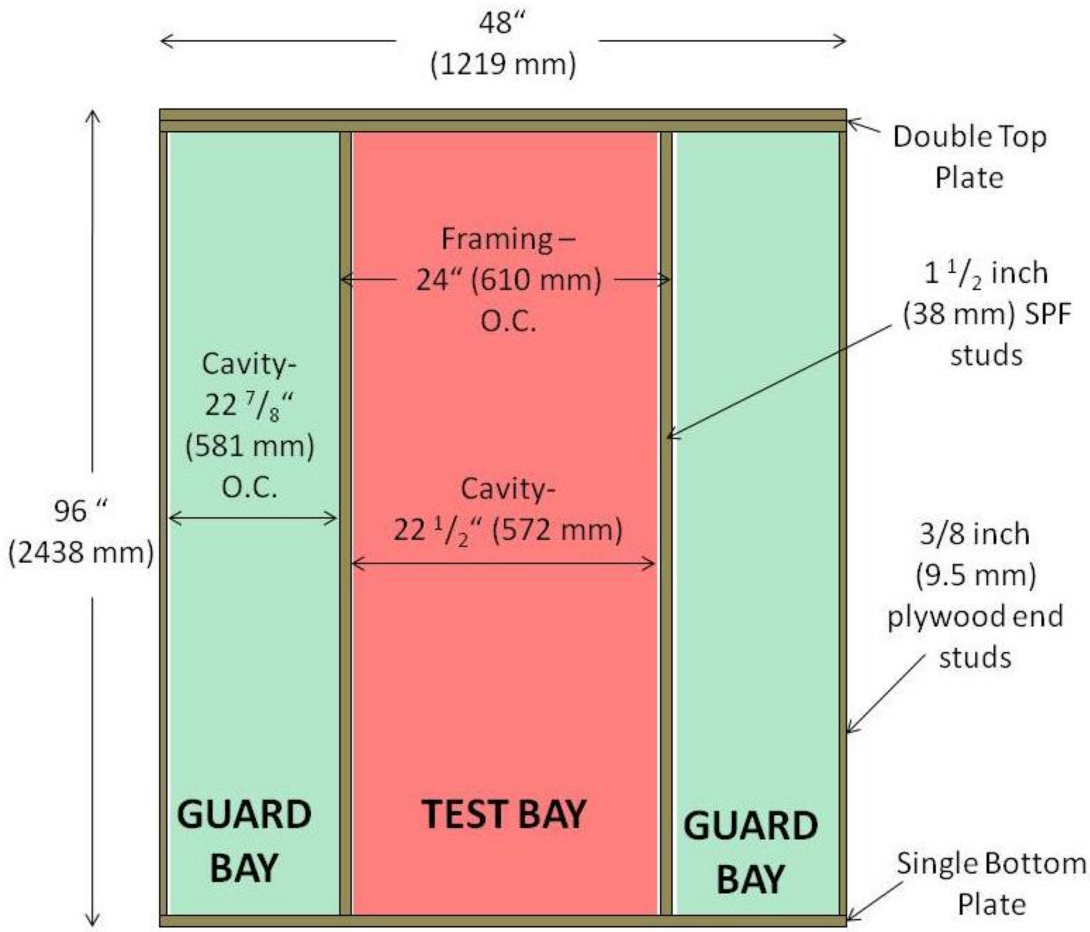

Figure 33- Framing dimensions and pattern

4.6.1.2 Cladding

A cladding of pre-painted fiber cement lap siding was applied continuously across both the North and South orientations of the test hut. Care was taken to ensure an equal number of butt joints on each test panel section. The bottom row of siding was in contact with the vapour permeable self-adhering membrane (Henry Blueskin VP) that covers the bottom edge of the insulated buck and continues to the exterior face of the foundation of the test hut, (Figure 39). The top row of siding was sealed to top edge of the insulated buck with a vapour permeable self-adhering membrane, as shown in Figure 41.

4.6.1.3 Air Gap

The cladding was installed on top of vertical pine furring strips. The furring strips were 2 ½ inches (64 mm) wide and 19 mm (3/4 inch) thick and were installed over each test wall stud, 24 inches (610 mm) O.C for the center bay, and 12 inches (305 mm) O.C. for the outside bays.

4.6.1.4 Sheathing Membrane

Tyvek-brand spun bonded polyolefin produced by Dupont was applied to all walls as a drainage plane /water control membrane. The Tyvek was stapled to the OSB sheathing and sealed to the perimeter of the OSB and to the wall buck using 60 mm wide Tuck-brand tape, produced by the Canadian Technical Tape. In this way, it was detailed as both a water control layer and as a secondary exterior air barrier. Although the walls primarily used polyethylene or drywall as the air barrier, an exterior air barrier acted as a wind washing barrier and supplemented the interior air barrier.

4.6.1.5 Sheathing

All test walls were sheathed with 7/16 inch (11 mm) thick oriented strand board (OSB). To simulate actual construction techniques, a horizontal joint approximately 1/8 inch (3.2 mm) wide was included in each test wall, 24 inches (610 mm) from the bottom. The sheathing was attached to the wall framing using 1 ½ inch (38 mm) wood screws at 16 inches (406 mm) O.C.

4.6.1.6 Interior Finish

All test walls were finished on the interior with ½ inch (12.7 mm) thick gypsum wall board (drywall) installed with 1 ¼ inch (32 mm) drywall screws at 16 inches (406 mm) O.C. and painted with 2 layers of latex paint.

4.6.1.7 End Studs

All test walls, regardless of framing thickness had end studs constructed of 3/8 inch (9.5 mm) thick plywood, attached to the OSB sheathing and drywall with sheet metal L-brackets to minimize thermal bridging and maximize space for insulation (Figure 40).

4.6.2 The Test Walls

4.6.2.1 Test Wall 1: Datum Wall

The standard base wall (Datum wall) was designed to represent the current standard practice in residential construction. As seen in Figure 34, the base wall is framed of 1 ½ X 5 ½ inch (38 mm X 140 mm) wood studs, 24 inches (610 mm) on center, with double top plates and a single bottom plate. Between framing members is R-24 (RSI- 4.2) fiberglass batt insulation. The interior air/vapour barrier is 6 mil. polyethylene sheeting.

4.6.2.2 Test Wall 2: Rock Wool (RW)

As seen in Figure 35, this wall was constructed exactly like the standard base wall, with the addition of two, 1 ½ inch (38 mm) thick layers of high density rock wool insulated sheathing (Roxul IS) exterior to the sheathing membrane. While a small number of screws were used to hold the insulation in place during the construction process, it was primarily attached by pinning it to the wall frame with furring strips. The furring strips were attached using 6 inch (152 mm) screws that passed through the insulation and into the wall framing members.

4.6.2.3 Test Wall 3: Extruded Polystyrene (XPS)

As seen in **Error! Reference source not found.**, this wall was constructed like the rock wool wall above, ut replaces the 3 inch (76 mm) thick layer of mineral wool insulation with a 2 ½ inch (63.5 mm) thick layer of XPS insulation (applied as one, 1 inch (25.4 mm) thick layer and one 1 ½ inch (38.1 mm) layer). The other difference is the elimination of the 6 mil. polyethylene interior air/vapour barrier. In this wall system, the XPS insulation will act as the vapour barrier and the drywall was detailed as an air barrier with acoustic sealant sealing the four edges of the drywall to the framing.

4.6.2.4 Test Wall 4: Polyisocyanurate (PIC)

As seen in Figure 37, this wall was constructed like the XPS wall above, but replaces the 2 ½ inch (63.5 mm) thick layer of XPS insulation with a 2 inch (50.8 mm) thick layer of foil faced PIC insulation, applied as two, one inch (25.4 mm) layers.

4.6.2.5 Test Wall 5: Double Stud

As seen in Figure 38, this wall was framed as a double stud wall. The outer wall was framed of 1 ½ X 5 ½ inch (38 mm X 140 mm) framing lumber with a double top and single bottom plate. The inner wall was framed of 1 ½ X 3 ½ inch (38 mm X 89 mm) lumber with a single top and single bottom plate. The two walls were secured together using 3/8 inch (9.5 mm) thick plywood gusset plates secured to the top and bottom plates of the walls. The result was a total wall thickness of 11 ¼ inches (286 mm). The wall cavity was filled with dense-packed cellulose insulation at a density of approximately 4 pounds per cubic foot (65 kg per cubic meter). To facilitate the installation of the cellulose, a filter fabric was applied to the interior of the wall framing, which was held in place by horizontal and vertical ½ X 2 ½ inch (16 mm X 64 mm) strapping at 24 inches (610 mm) O.C. in a grid pattern. On the interior side of this strapping, a 6 mil. polyethylene air/vapour barrier was sealed to the four perimeter edges of the wall with acoustic sealant. To control the packing density, the walls were filled 1/3 of the cavity at a time (starting at the bottom). The cellulose was weighed prior to installation of each section to ensure the proper installed density.

Datum	Fibre Cement, Tyvek, OSB, 2x6, R-22 fibreglass batt, 6 mil poly, latex paint (Base Wall)

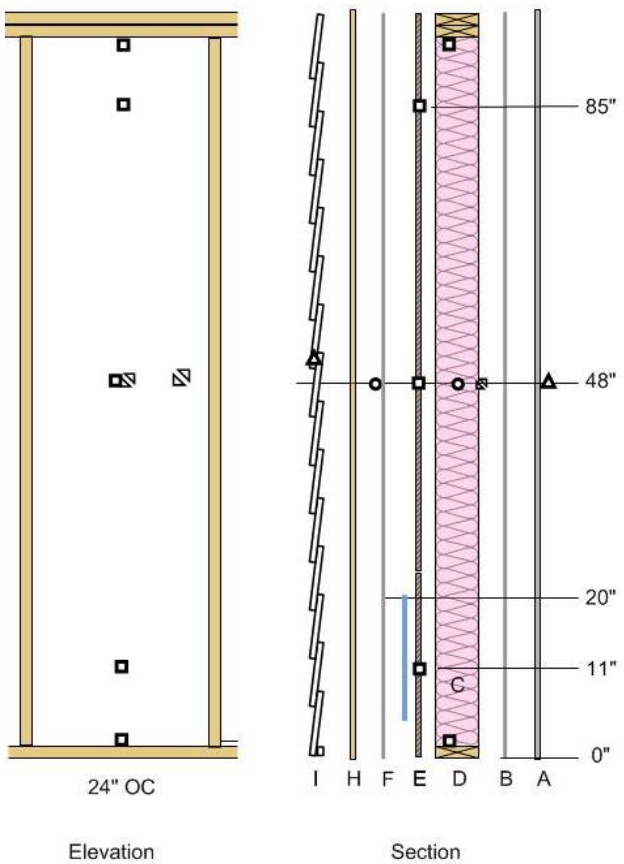

Assembly

Layer	Function	Description
A	Interior Finish	Painted gypsum board
B	Vapor Control	6 mil poly
C	Studspace	R-22 fiberglass batt
D	Framing	2x6
E	Sheathing	7/16" OSB
F	Membrane	Tyvek
G	Insulation	none
H	Drainage	1x3
I	Cladding	Cement fibre lap siding

Sensor Package

Layer	Code	Location
A	taem	Interior finish, interior face, 48"
C	r/tcnm	Studspace, interstitial, 48"
D	m/tdet	Framing, exterior edge, top plate
D	m/tdel	Framing, exterior edge, bottom plate
E	m/teiu	Sheathing, interstitial, 80"
E	m/teim	Sheathing, interstitial, 48"
E	m/teil	Sheathing, interstitial, 16"
G	r/tinm	Drainage space, interior, 48"
I	tjem	Cladding, interstitial, 48"

○ Relative Humidity and Temperature Sensor Package
□ Moisture Content Pins and Temperature Sensor Package
▲ Temperature Sensor
⧄ Heat Flux Transducer

Figure 34- Elevation and exploded vertical cross-section of the center bay of the Datum wall panel

Rockwool Fibre Cement, Rockwool, Tyvek, OSB, 2x6, R-22 fibreglass batt, 6 mil poly, latex paint

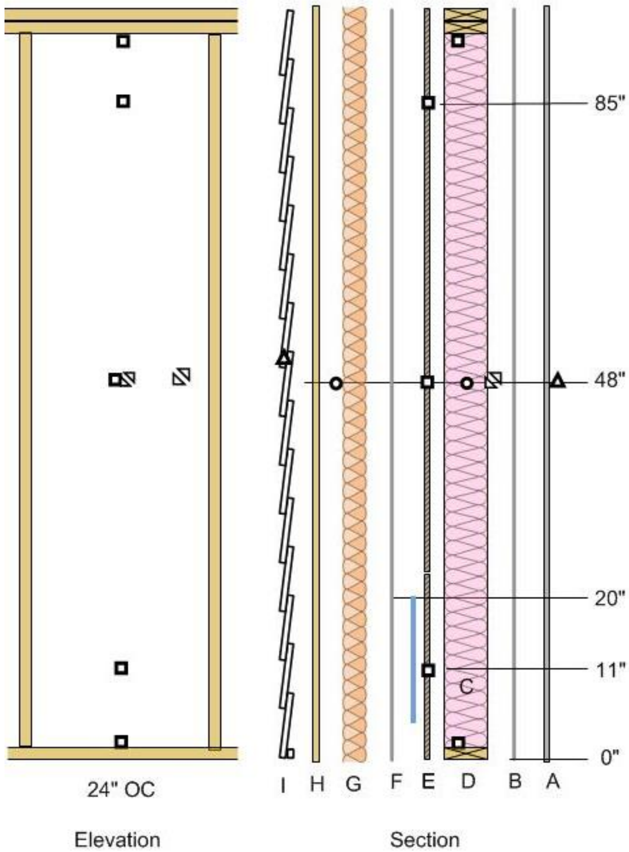

Assembly

Layer	Function	Description
A	Interior Finish	Painted gypsum board
B	Vapor Control	6 mil poly
C	Studspace	R-22 fiberglass batt
D	Framing	2x6
E	Sheathing	7/16" OSB
F	Membrane	Tyvek
G	Insulation	3" Rockwool
H	Drainage	1x3
I	Cladding	Cement fibre lap siding

Sensor Package

Layer	Code	Location
A	taem	Interior finish, interior face, 48"
C	r/tcnm	Studspace, interstitial, 48"
D	m/tdet	Framing, exterior edge, top plate
D	m/tdel	Framing, exterior edge, bottom plate
E	m/teiu	Sheathing, interstitial, 80"
E	m/teim	Sheathing, interstitial, 48"
E	m/teil	Sheathing, interstitial, 16"
G	r/tinm	Drainage space, interior, 48"
I	tjem	Cladding, interstitial, 48"

o Relative Humidity and Temperature Sensor Package
□ Moisture Content Pins and Temperature Sensor Package
▲ Temperature Sensor
⧅ Heat Flux Transducer

Figure 35- Elevation and exploded vertical cross-section of the center bay of the Rock Wool wall panel

XPS | Fibre Cement, XPS, Tyvek, OSB, 2x6, R-22 fibreglass batt, latex paint

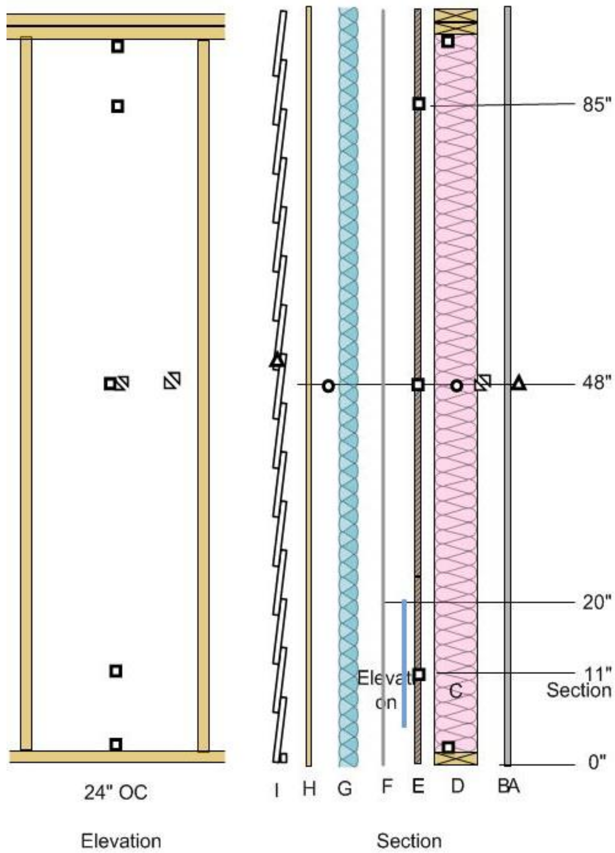

Assembly

Layer	Function	Description
A	Interior Finish	Painted gypsum board
B	Vapor Control	none
C	Studspace	R-22 fiberglass batt
D	Framing	2x6
E	Sheathing	7/16" OSB
F	Membrane	Tyvek
G	Insulation	2 1/2" XPS
H	Drainage	1x3
I	Cladding	Cement fibre lap siding

Sensor Package

Layer	Code	Location
A	taem	Interior finish, interior face, 48"
C	r/tcnm	Studspace, interstitial, 48"
D	m/tdet	Framing, exterior edge, top plate
D	m/tdel	Framing, exterior edge, bottom plate
E	m/telu	Sheathing, interstitial, 80"
E	m/teim	Sheathing, interstitial, 48"
E	m/teil	Sheathing, interstitial, 16"
G	r/tinm	Drainage space, interior, 48"
I	tjem	Cladding, interstitial, 48"

- o Relative Humidity and Temperature Sensor Package
- □ Moisture Content Pins and Temperature Sensor Package
- △ Temperature Sensor
- ⧅ Heat Flux Transducer

Figure 36- Elevation and exploded vertical cross-section of the center bay of the XPS wall panel

PIC	Fibre Cement, Poly-iso, Tyvek, OSB, 2x6, R-22 fibreglass batt, latex paint

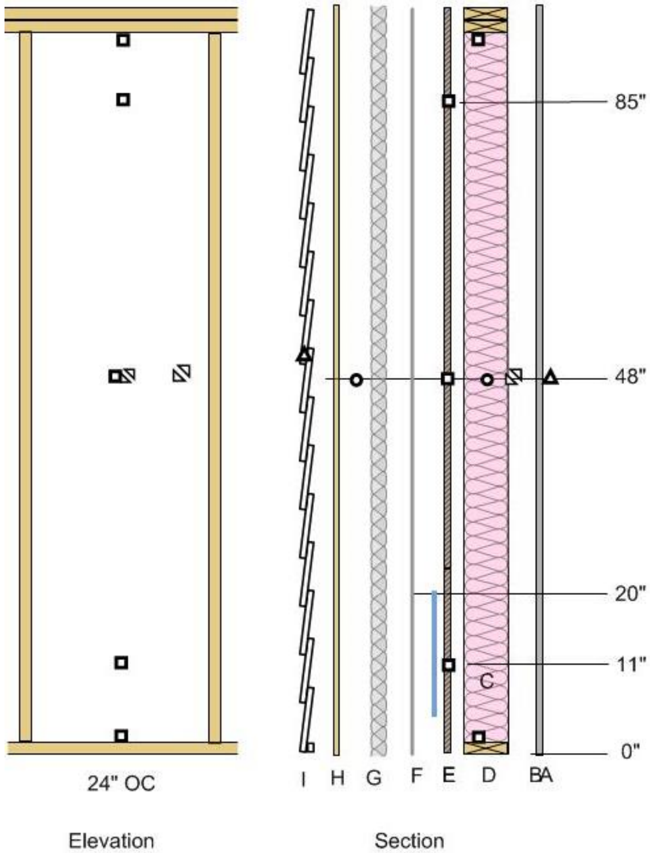

Assembly

Layer	Function	Description
A	Interior Finish	Painted gypsum board
B	Vapor Control	none
C	Studspace	R-22 fiberglass batt
D	Framing	2x6
E	Sheathing	7/16" OSB
F	Membrane	Tyvek
G	Insulation	2" Poly-iso
H	Drainage	1x3
I	Cladding	Cement fibre lap siding

Sensor Package

Layer	Code	Location
A	taem	Interior finish, interior face, 48"
C	r/tcnm	Studspace, interstitial, 48"
D	m/tdet	Framing, exterior edge, top plate
D	m/tdel	Framing, exterior edge, bottom plate
E	m/teiu	Sheathing, interstitial, 80"
E	m/teim	Sheathing, interstitial, 48"
E	m/teil	Sheathing, interstitial, 16"
G	r/tinm	Drainage space, interior, 48"
I	tjem	Cladding, interstitial, 48"

- O Relative Humidity and Temperature Sensor Package
- ◘ Moisture Content Pins and Temperature Sensor Package
- ▲ Temperature Sensor
- ⧅ Heat Flux Transducer

Figure 37- Elevation and exploded vertical cross-section of the center bay of the PIC wall panel

Wall 7	Fibre Cement, Tyvek, OSB, Double-stud, Dense-pack cellulose, latex paint

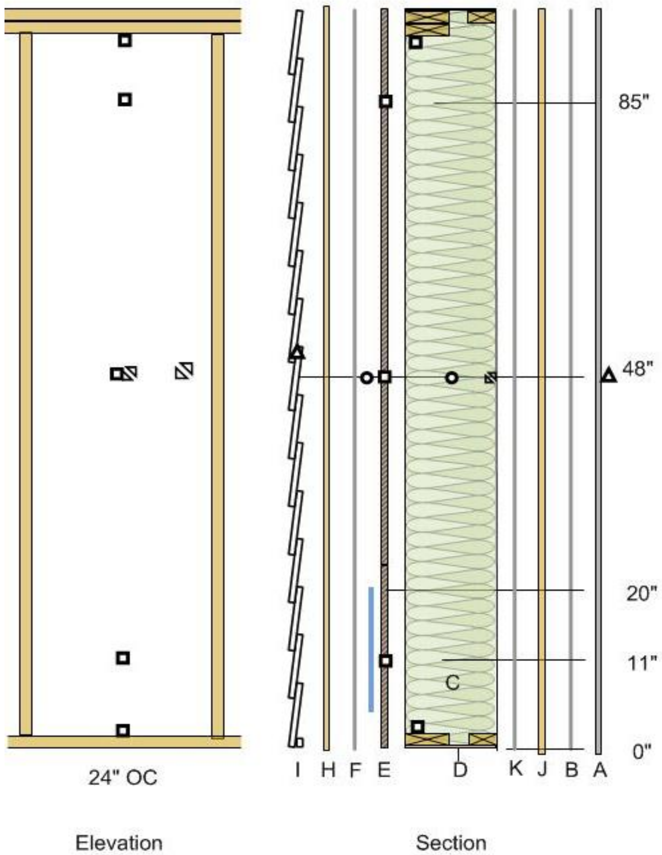

Assembly

Layer	Function	Description
A	Interior Finish	Painted gypsum board
B	Vapor Control	6 mil poly
C	Studspace	R-22 fiberglass batt
D	Framing	11 ¼ double stud
E	Sheathing	7/16" OSB
F	Membrane	Tyvek
G	Insulation	none
H	Drainage	1x3
I	Cladding	Cement fibre lap siding
J	Strapping	1x3
K	Filter fabric	landscaping fabric

Sensor Package

Layer	Code	Location
A	taem	Interior finish, interior face, 48"
C	r/tcnm	Studspace, interstitial, 48"
D	m/tdet	Framing, exterior edge, top plate
D	m/tdel	Framing, exterior edge, bottom plate
E	m/teiu	Sheathing, interstitial, 80"
E	m/teim	Sheathing, interstitial, 48"
E	m/teil	Sheathing, interstitial, 16"
G	r/tinm	Drainage space, interior, 48"
I	tjem	Cladding, interstitial, 48"

○ Relative Humidity and Temperature Sensor Package
□ Moisture Content Pins and Temperature Sensor Package
△ Temperature Sensor
⧄ Heat Flux Transducer

Figure 38- Elevation and exploded vertical cross-section of the center bay of the double stud wall panel

4.6.3 Insulated Wall Bucks

In order to hygrothermally isolate the test walls from the test hut and from each other, a specially designed air and vapor resistant, insulated buck was installed to surround each test panel. As shown in Figure 39 the bottom of the buck sits directly on the test hut's 8 inch (200 mm) high concrete foundation wall and is constructed of 1 ½ inch (38 mm) thick XPS insulation and ½ inch (12.7 mm) thick plywood, covered with a self-adhering membrane. The sides of the buck (the 'jamb') are shown in Figure 40. For the test walls that are directly adjacent to each other, the sides of the buck are constructed of 12 inch (305 mm) deep I-joists, with the web area filled in with ½ inch (12.7mm) thick XPS insulation on both sides and self-adhering membrane covering the exterior wood flange. Where the test walls are adjacent to the support posts, the sides of the bucks are constructed like the bottom of the buck, with 1 ½ inch (38 mm) thick XPS insulation and ½ inch (12.7 mm) thick plywood covered with a self-adhering membrane. As shown in Figure 41, the top of the buck is constructed with ½ inch (12.7 mm) thick plywood, cantilevered outward from the support beam with self-adhering membrane on the bottom and 1 ½ inch (38 mm) thick XPS insulation on the top side. Another layer of self-adhering membrane was applied to the top surface of the XPS.

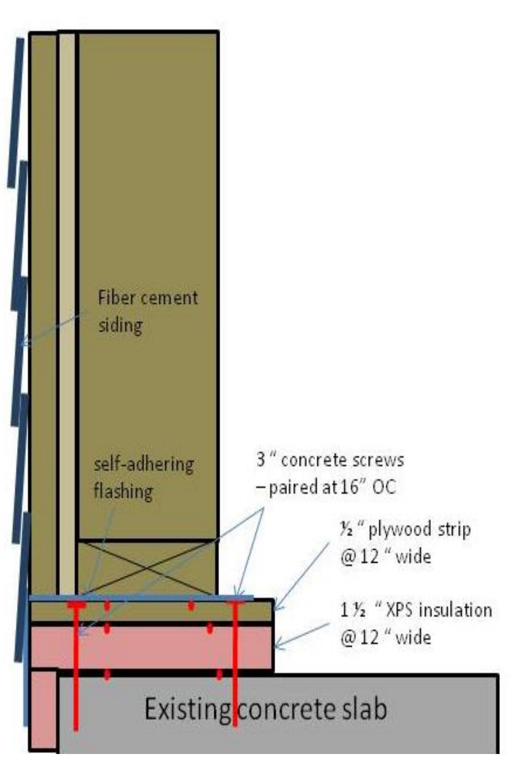

Figure 39- Bottom Buck detail

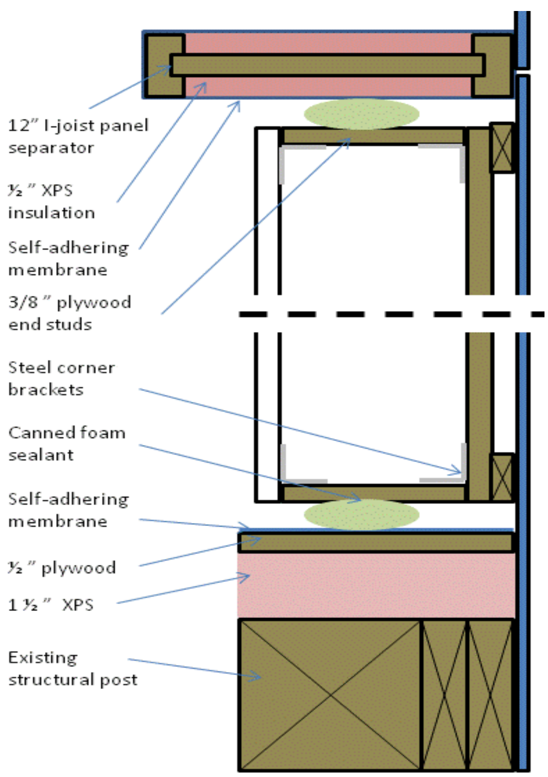

Figure 40- Side Buck Detail

4.6.4 Head Flashing

To control water intrusion at the junctions between the test walls and the test hut, a continuous head flashing was applied to the north and south sides of the test hut. As shown in Figure 41, this assembly was constructed of a sloped layer of ½ inch (12.7 mm) thick plywood with 1 ½ X 1 ½ inch (38mm X 38 mm) lumber attached to the underside of the outer edge. This was the covered with a continuous bent aluminum flashing that was layered under the siding above and includes an angled drip edge.

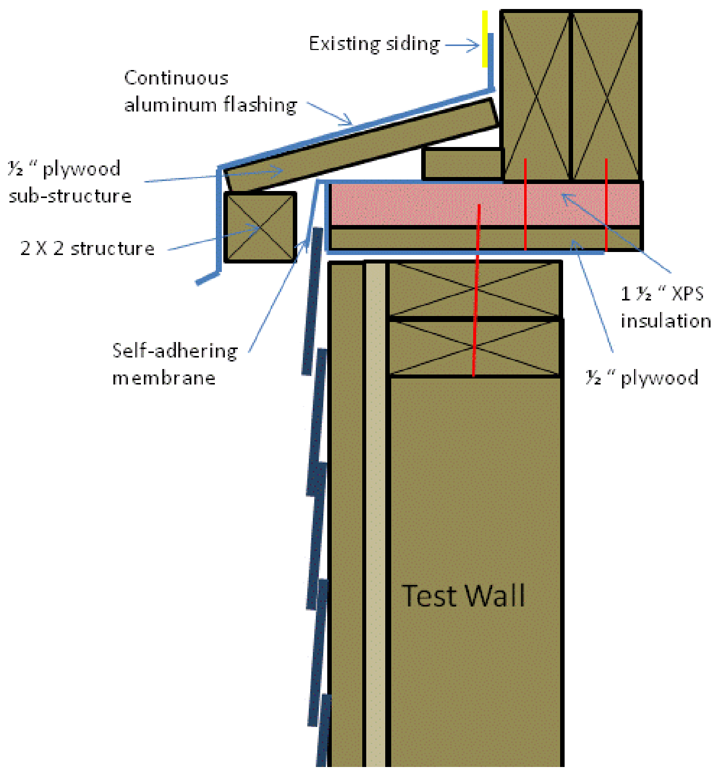

Figure 41- head buck and flashing detail

4.7 Instrumentation

4.7.1 Sensors Locations

4.7.1.1 Moisture Content/Temperature Sensors

The moisture content/temperature (MC/T) sensor is composed of 2 moisture pins and a thermistor temperature sensor. As shown in Figure 34 to Figure 38, each test wall was fitted with five MC/T sensors: at the top and bottom plates and at three positions in the OSB sheathing. All MC/T sensors were installed along the center line of the test panels, within the test bay.

Figure 42 shows the positioning of the MC/T sensors for the bottom half of the wall (the top half was symmetrical). For the top and bottom plates, the MC/T sensors were installed 3/8 inch (10 mm) from the inner face of the OSB sheathing. The upper and lower sheathing sensors were installed 11 ¼ inches (286 mm) from the top and bottom plates respectively, while the middle sheathing sensor was installed half way up the wall (46 ½ inches (1181 mm) up from the bottom plate). As shown in Figure 43, the moisture pins were installed 1 inch (25.4 mm) apart, with the temperature sensor 1 inch (25.4 mm) from the right side pin. All moisture pins and temperature sensors were installed 7/32 inch (5.5 mm) below the inner surface. This distance represents half of the thickness of the OSB sheathing. In the cellulose walls only, the moisture pins were covered with vinyl tubing filled with silicone to protect the pins from corrosion and cellulose conductivity.

The sensor wires were routed horizontally from the sensor through the wall panel studs and into the space between the wall panel and the buck, where they turn to the interior of the BEGHUT. All penetrations were then sealed with caulking. This approach was taken to minimize the impact on air and heat flow within and through the test bay.

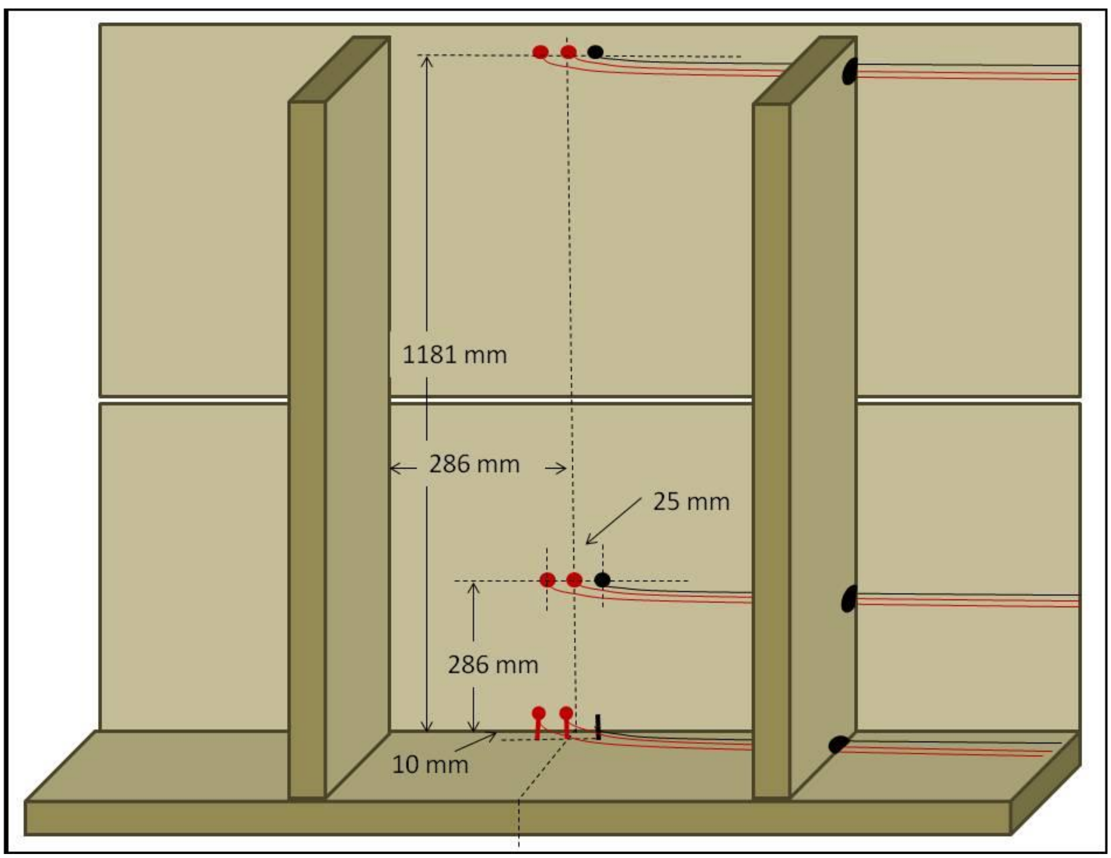

Figure 42- Position of moisture pins in bottom half of wall assembly (top half is symmetrical)

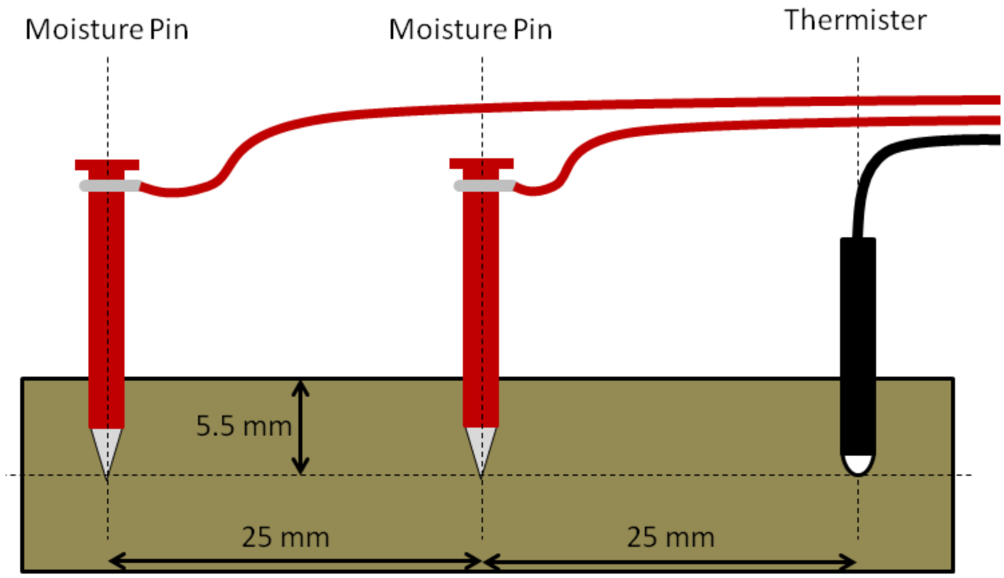

Figure 43- Cross sectional detail of moisture pin installation

4.7.1.2 Temperature/Relative Humidity Sensors

Also shown in Figure 34 through Figure 38, two relative humidity/temperature (RH/T) sensors were installed in each test wall. One RH/T sensor was installed within the insulation at the center point of the test wall: 46 ½ inches (1181 mm) up from the bottom plate, 11 ¼ inches (286 mm) from the inner studs and mid-way through the depth of cavity. The second RH/T sensor was installed in the air gap behind the siding. It was secured to the outer face of the sheathing membrane, half way up and half way across the test walls. Sensor wires were routed horizontally into the space between the wall panel and the buck, where they turned to the interior of the BEGHUT. All penetrations were sealed with caulking or spray foam.

4.7.1.3 Temperature-Only Sensors

Also shown in Figure 34 through Figure 38, two thermistor temperature sensors were used to monitor temperature at two other positions in the assembly. One thermistor was applied to the interior surface of the gypsum wall board and another was installed between overlapping layers of siding. Both were installed at the horizontal and vertical center point of the wall. The siding sensor wires were routed horizontally into the space between the wall panel and the buck, where they turned to the interior of the BEGHUT. All penetrations were sealed with caulking or spray foam.

4.7.1.4 Heat Flux Sensors

For the Datum wall and the PIC wall, heat flux transducers were used to measure heat flow. For each of these walls, two heat flux sensors were installed half-way up the wall, on the exterior face of the gypsum wall board. One sensor was installed at the center line of the test cavity and the other was installed over the left side framing stud. A dado was cut into the wood framing member to accommodate for the thickness of the sensor. Sensor wires were routed horizontally through the wall panel studs and into the space between the wall panel and the buck, where they turned to the interior of the BEGHUT. All penetrations were sealed with caulking or spray foam.

4.7.2 Detailed Sensor Description

As described in the section above, all of the test panels were instrumented to measure temperature, relative humidity and moisture content at various points in the panel assemblies. The following section provides detailed descriptions of the sensors used in the instrumentation of the wall panels. Measurement theory and techniques are described in more detail in Appendix A.

4.7.2.1 Temperature Sensors

All of the temperature sensors are precision thermistors (produced by Fenwal) with a 10 000 Ohm @ 25° Celsius and an interchangeability of better than 0.2 ºC. The thermistors and their soldered connection to the instrumentation wiring were coated with an electrically insulating and waterproof liquid plastic. The resistance vs. temperature correlation curve data was input into a spreadsheet and the following relation was determined and applied.

$$T = -0.101R^3 + 4.346R^2 - 77.18R + 446.05$$

Where: T is temperature in ^{o}C and R is electrical resistance in Ohms.

4.7.2.2 Relative Humidity Sensors

To measure relative humidity, Honeywell (model HIH-3610-004) RH sensors were used. These small (4 x 6 x 10 mm) sensors have NIST-traceable calibrations and an accuracy of better than 2% RH. The sensors were sealed in specially fabricated protective spun bonded polyolefin packaging along with the thermistors used for temperature readings.

4.7.2.3 Wood Moisture Content

Moisture-content sensors were installed in the wood framing and the OSB sheathing. The moisture-content sensor for the wood framing consists of two stainless steel nails that were driven into the wood framing, 25 mm (1 inch) apart. For the pins in the OSB sheathing, small (1.6 mm diameter) holes were pre-drilled into the sheathing to aid in the positioning of these pins. Accompanying each set of moisture pins, is a thermistor temperature sensor, set to the same depth as the pins. A pre-drilled hole of 3 mm in diameter was used to position the thermistor into the sheathing and wood members. Silicone sealant was used to secure the sensor in place.

The moisture content is measured by passing a 12-volt direct current between the pins. The voltage is applied for about 1 second to allow the readings to stabilize. The resistance values are recorded and software then calculates the moisture content and corrects for temperature and wood species. This is described in more detail in Appendix A.

Measurement of moisture content is not as representative as the measurement of temperature and relative humidity. The recorded moisture content does not necessarily represent the average moisture content of the wood stud or OSB sheet into which the pins are inserted. Moisture gradients, through the thickness and across the length and width of the material are present as a result of drying/wetting of the material and the environmental conditions that promote it, as well as variations in material properties. The actual accuracy of the resistance based meters used in wood is estimated as ±2% within the range of 6 to 25%; however, a considerable loss in accuracy can be expected outside this range. Above fiber saturation (25 to 30%), these sensors will generally return lower values than actually exist, whereas below 6%, the resistance becomes so high it cannot be properly measured.

4.7.2.4 Heat Flux Sensors

For the Datum and PIC walls on the south face, heat flow sensors were installed to measure the heat flow through the middle of the center cavity and the framing members adjacent to the center cavity. The heat flux sensors used were Model F-010-4 from Concept Engineering. They have a heat flux range of zero to 9.5 kW/m^2, a temperature range of -50 deg. C to +150 °C, and accuracy of +- 5% with a linearity of +- 2%. Each sensor is individually calibrated and is supplied with a sensitivity constant.

4.7.3 Inter-Wall Wetting Mechanisms

Two systems were designed to allow wetting of the wall during service – an exterior wetting mat installed between the OSB sheathing and the Tyvek sheathing membrane, and an interior air injection system. These systems were designed to produce large moisture movements in the test wall and replicate rain leaks and air leakage condensation respectively.

4.7.3.1 Wetting Mats

The wetting mats were applied to the exterior surface of the OSB sheathing board, interior to the Tyvek sheathing membrane, as shown in Figure 44 . This system is used to represent a leakage of rain water through the cladding and sheathing membrane.

The moisture is applied at a macro level via flexible plastic tubing with carefully punctured exit holes. The exit holes release water between a folded sheet of plastic mesh reinforced paper towel (Figure 45). The tube and paper towel are stapled to the OSB. The tubing was secured horizontally across the exterior of the sheathing and brought to the interior of the BEGHUT in the gap between the test wall panels and the insulated bucks.

The water is injected using a syringe, into the exposed end of the tube and the tube is subsequently emptied by forcing air through the tubing after each water injection. The tendency of the injected water is to spread out (by capillary flow) across the paper towel with some gravity effect drawing water downward. The tubes apply the water near the top of the sheets, allow the water to spread out and downward, covering the entire sheet.

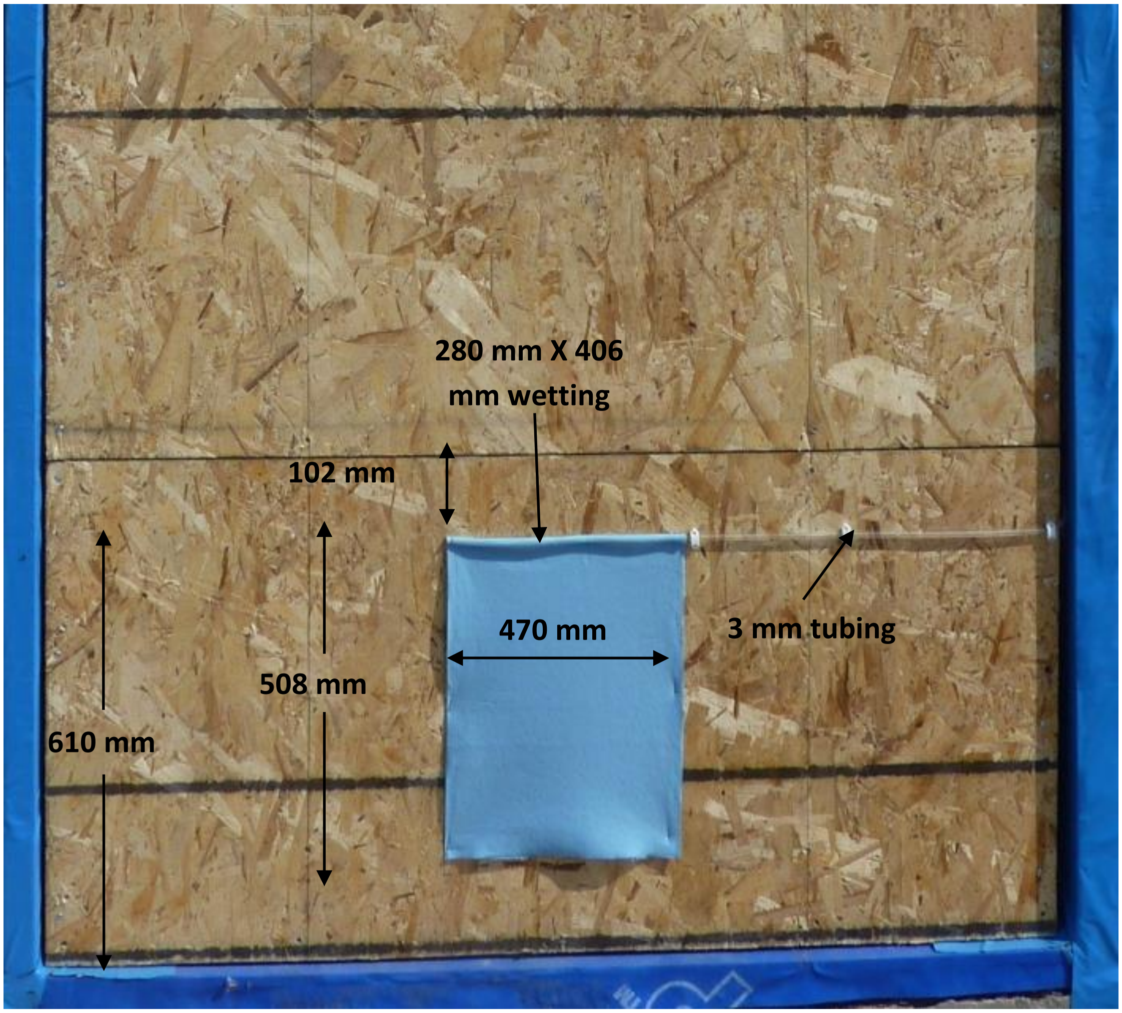

Figure 44- positioning of wetting mat on exterior face of OSB sheathing

4.7.3.2 Air Injection System

An air injection system was designed to pump interior air (21 deg. C, 40% RH) into the center test bay of each test wall. This system is used to represent an interior air leak, from a point source such as an electrical outlet box. The injection of interior air acts as a potential wetting system during the coldest months of the year as air leakage condensation will occur within the wall assembly at any surface that the air flows past that is below the dew point of the air being injected.

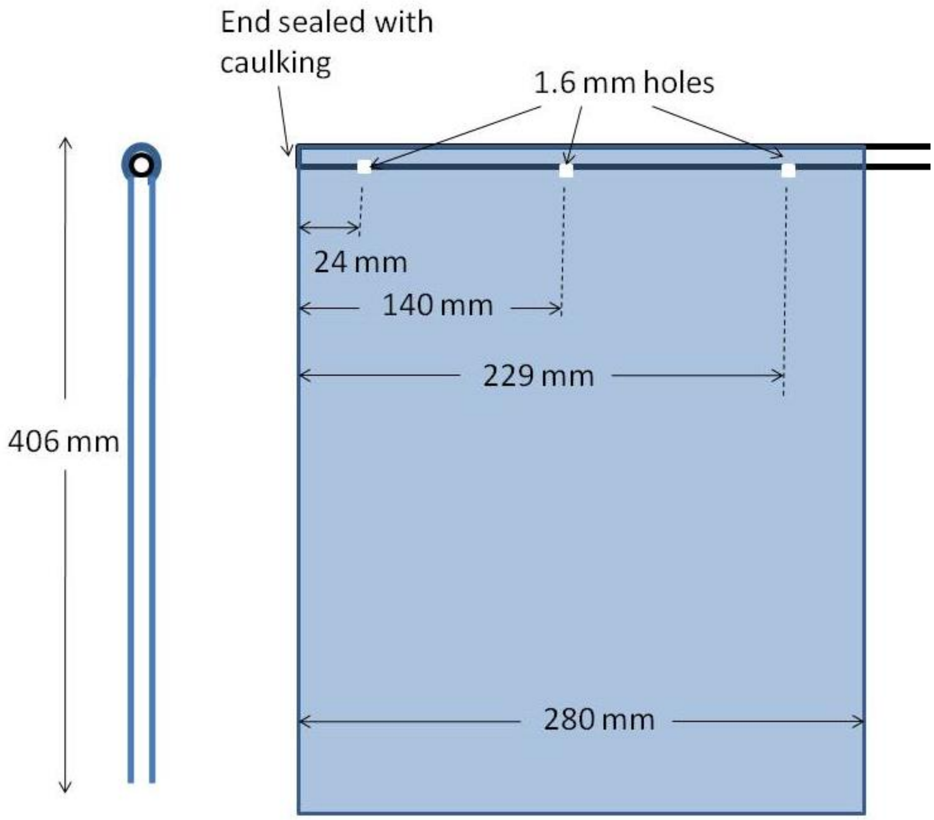

Figure 45- Detail drawing of wetting mat system

As shown in Figure 47, the system is composed of a high pressure blower motor and fan, attached to a distribution system of ¾ inch (19 mm) diameter polyethylene pipe. A ball valve is used to divert excessive flow from the piping and across the blower motor to reduce its operating temperature. Manifolds are used to distribute air to each wall and air flow rotameters with integral needle valves (Omega Model FL 2008) are used to measure and control the flow entering each test wall panel.

The air is introduced to the center of the test bay, at a height of 12 inches (305 mm) from the bottom of the wall through a 1 ½ ” diameter plumbing cleanout. An air relief path was provided at the top plates to direct air back into the interior of the BEGHUT. This relief path was deemed necessary as the exterior sheathing membrane acted as a reasonably effective air barrier in these test walls. As shown in Figure 46, the relief hole was created by drilling a horizontal 1 inch (25 mm) diameter hole almost all the way through the top plates, at the centerline of the wall panel. A second, vertical 1 inch (25 mm) diameter hole was drilled through the lower top plate to intersect the first hole near the plane of the interior face of the OSB sheathing. The opening of both the inlet and outlet was sealed airtight until the air injection system was operated.

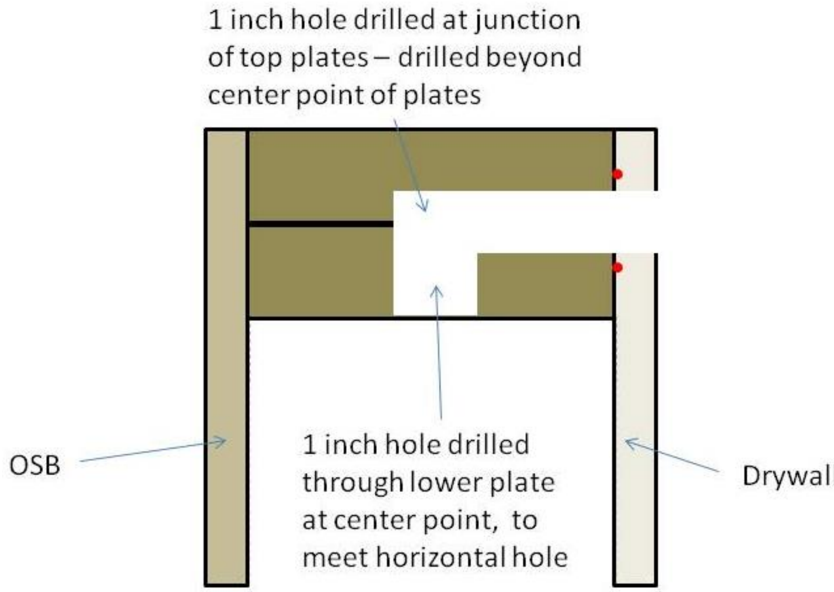

Figure 46- Cross section air relief port at top of test walls

A flow rate of .24 l/s (30 CFH) was chosen based on air leakage rates expected in new residential construction during winter conditions. This is an approximation of the in-service leakage of a house with a pressurized air leakage rate of 0.2 cfm/ft^2 (1.02 l/s/m^2) at 50 Pa in a cold climate. This is the maximum acceptable air leakage limit for the Energy Star for New Homes program. The methods and assumptions used to determine this air leakage rate are described in Appendix C.

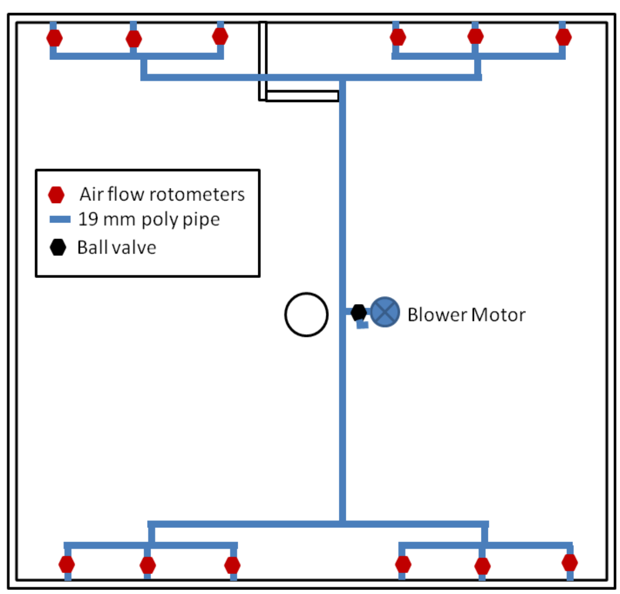

Figure 47- Plan view of BEGHUT with schematic of air injection system

4.7.4 Boundary Conditions

4.7.4.1 Interior

Interior conditions were maintained near 21 °C and 40% relative humidity (RH) for the duration of the experiment. The temperature conditions were maintained with a thermostatically-controlled, ducted air-source heat pump system. Four ceiling fans were used to minimize vertical stratification. Humidification was provided by a controlled heated bucket humidifier and summer-time dehumidification was provided by the cooling (air conditioning) mode of the air source heat pump, but was not specifically controlled. Interior temperature and relative humidity conditions were monitored by two temperature/RH sensors approximately 8 feet from the floor and recorded with the data acquisition system.

4.7.4.2 Exterior

Exterior conditions were natural atmospheric conditions. The exterior weather elements (temperature, relative humidity, solar radiation, and falling rain) were also recorded with the data acquisition system. The weather data from the nearby Environment Canada - University of Waterloo Class A weather station is also used for reference and to fill in any missing data.

4.7.5 Data Acquisition

The data acquisition (DAQ) system was comprised of a Campbell Scientific CR 1000 analog to digital converter and data logger with 4 Campbell Scientific multiplexers (Model AM 16/32). Schematic diagrams of the system can be seen in Appendix D. All channels were scanned every fifteen minutes and the data is averaged and saved at 60 minute intervals.

5 Results

The test walls were installed July 2012, and trimmed and finished in August, 2012. Wiring of the sensors was completed in September, 2012. Preliminary data collection began in October 2012. The data was reviewed for data quality by inspection and some sensors were found to be mislabeled, and others non-responsive. These sensors were fixed or replaced and full data collection began in November, 2012

In Phase 1 of testing, the walls were left to perform as-built from November 2012 through February 19th, 2013. Phase 2 involved air injection wetting, which was performed from February 19th through March 22nd, 2013. Phase 3 was a drying phase, during which the test walls were allowed to dry to equilibrium moisture content under as-built conditions. Phase 4 was the wetting mat wetting phase, which lasted from June 3rd through July 5th, 2013. The final phase of testing was a drying phase, where the walls were again allowed to dry down under as-built conditions.

The monitoring of 210 sensors over the period from November1st, 2012 to July 5th, 2013 generated about 1.285 million data points. The data was downloaded periodically from the data logger, and entered in a number of spreadsheets for analysis.

5.1 Thermal Performance

5.1.1 Sheathing Temperature

Sheathing temperature can be used as a simple measure of wall assembly durability. High temperatures can accelerate the breakdown of organic materials, while extreme temperature cycling of the sheathing and sheathing membrane can cause movement, stress and fatigue that impact the long-term durability of the materials that form these layers and the fasteners and sealants used to secure them. More importantly, during winter conditions, cold sheathing can result in condensation of water vapor transported by vapour flow and/or air exfiltration. This condensation within the wall assembly can accumulate and lead to mould and rot within the assembly.

5.1.1.1 Hot Weather Performance

Figure 48 shows the temperature of the upper sheathing position during the hottest week of the year. The south facing walls were used as the most extreme hot condition. The three walls with exterior insulation remained significantly cooler during the day and warmer at night than the standard wall over this time.

To highlight the performance differences between the test walls during hot weather, these results are summarized numerically in Table 2 below.

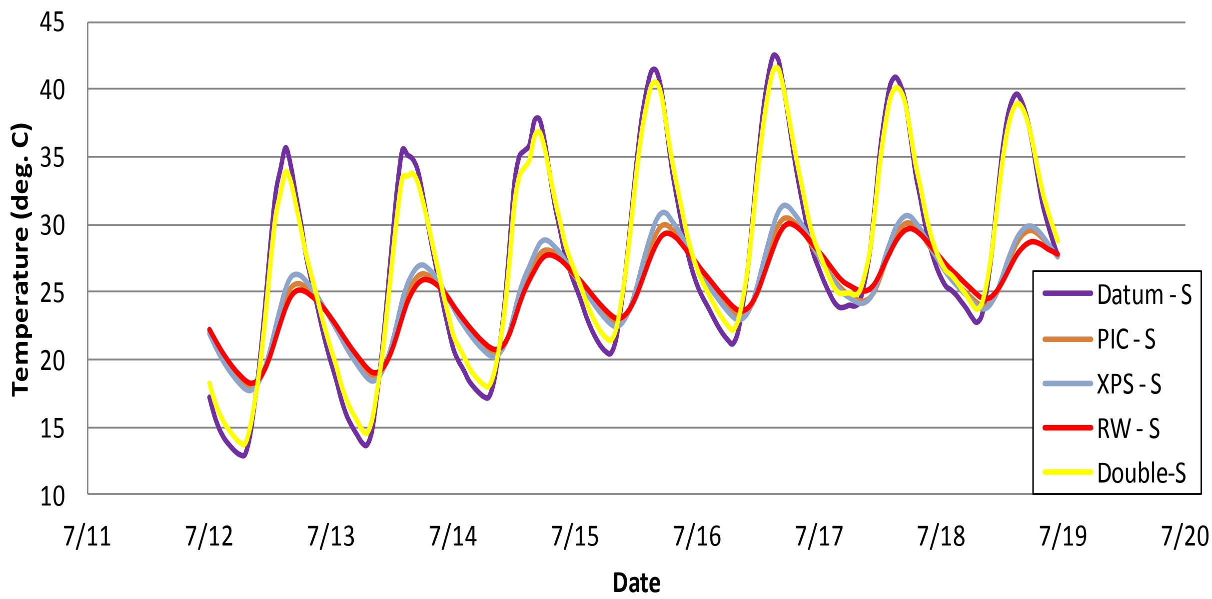

Figure 48- upper sheathing temperatures for a hot week - south elevation

Table 2- South elevation upper sheathing temperature summary (in °C)– during hottest week of the year

Hottest Week of the Year					
Walls	**Datum - S**	**PIC - S**	**XPS - S**	**RW - S**	**Double - S**
Average	27.4	24.9	25.0	24.9	27.5
Max.	42.5	30.5	31.4	30.1	41.5
St. Dev.	7.7	3.1	3.4	3.0	7.1

Based on the lower peak and average sheathing temperature values, and the reduced variation (standard deviation) in temperature, the exterior insulated walls show better potential durability than the Datum and Double Stud wall systems during hot weather. The thermal mass of the cellulose insulation in the Double stud wall is likely responsible for the slightly lower peak temperature and standard deviation relative to the less well insulated Datum wall. The PIC and RW walls performed slightly better than the XPS walls under these hot conditions, indicating a small thermal performance advantage during hot conditions for these two insulation types.

5.1.1.2 Cold Weather Performance

As seen in Figure 49, the three exterior insulated walls had significantly warmer sheathing temperatures during the coldest week of the winter than the Datum and Double stud walls. During this cold week, no induced air leakage or wetting mat injections were used. The north facing walls were used as the most extreme cold condition. Clearly, the three walls with exterior insulation remained significantly warmer than the datum and double stud walls over this time.

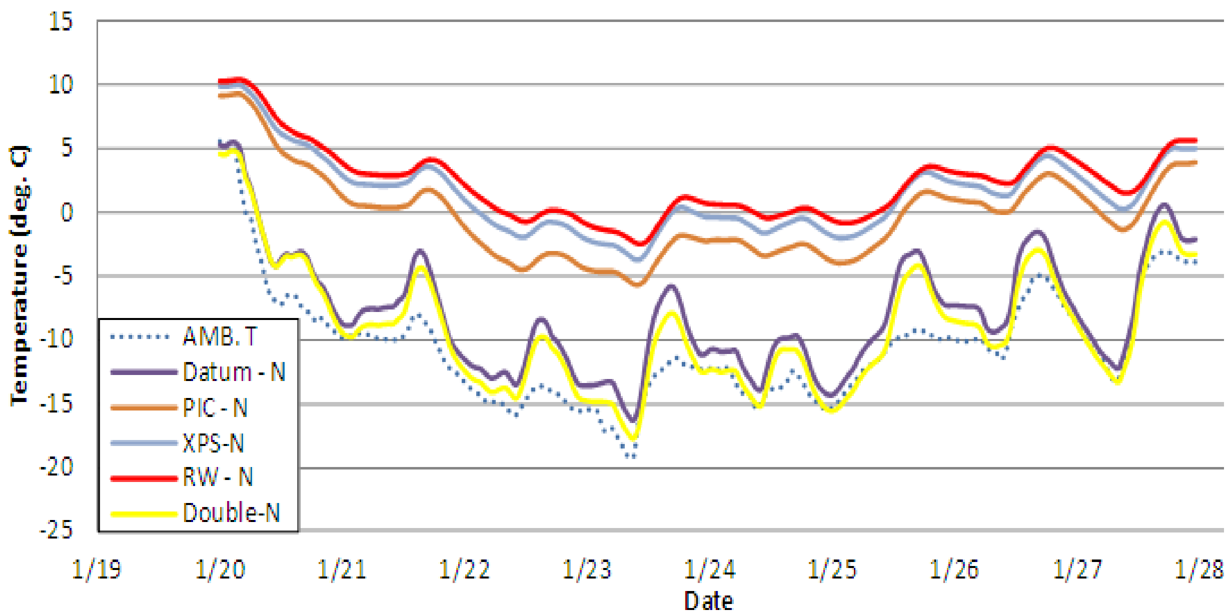

Figure 49- upper sheathing temperatures for a cold week - north elevation

To highlight the performance differences between the test walls during cold weather, these results are summarized numerically in Table 3 below.

Table 3- North elevation upper sheathing temperature summary (in °C)– coldest week of the year

Coldest Week of the Year					
Wall	**Datum - N**	**PIC - N**	**XPS-N**	**RW - N**	**Double - N**
Average	-7.7	-0.1	1.6	2.5	-8.9
Min.	-16.3	-5.6	-3.7	-2.5	-17.7
St. Dev.	5.0	3.6	3.2	3.1	5.1

As expected, the results showed that the exterior insulated walls have warmer sheathing temperatures and therefore a lower risk of condensation than the Datum or the Double stud walls. Compared to the Datum wall, the Double stud wall had slightly lower sheathing temperature based on its high thermal resistance. The exterior insulated walls performed slightly better than predicted. Based only on average temperatures and the nominal ratio of interior to exterior insulation (2 to 1) the average sheathing temperature was expected to be -0.2 °C. This discrepancy is likely due to the thermal effects of air films, air gaps and the temperature dependence of insulation materials and will be further discussed in Section 6.1.1. Based on the average and minimum sheathing temperatures, the Roxul insulation held a slight advantage in thermal performance over the XPS wall which performed better than the PIC walls under these cold conditions. Further comparisons of the thermal performance of the three exterior insulations is presented in section 6.1- Thermal Performance.

5.2 Moisture Performance

5.2.1 Condensation Potential

Although sheathing temperature is often used as a proxy for condensation potential, a more comprehensive method of predicting condensation is through vapour pressure analysis. This analysis technique takes into account not only sheathing temperature, but also the vapour flow control features of a wall system, to give a more complete indication of condensation potential. Because of the interior vapour barrier (6 mil. poly) of Datum, the Double stud and the RW walls, they are more sensitive to the exterior vapour pressure. In contrast, the XPS and PIC walls utilize the exterior insulation layer as the primary vapor control layer resulting in the wall cavity being more sensitive to the interior vapor pressure

Using the hourly temperature and relative humidity data from the center of the framing cavity, the hourly vapour pressure within the framing cavity was determined by calculating the saturation vapour pressure (based on cavity temperature) and multiplying by the measured relative humidity using the equation:

$P_w = P_{ws} * RH$

$P_w = (611.2 * e^{((17.67 * Tcavity)/(Tcavity +243.5))})*(RH)$

Where: P_w = partial water vapour pressure (in Pa)
P_{ws} = saturation vapour pressure (in Pa)
T_{cavity} = temperature (in ° C) at the center of the wall cavity
R.H. = the relative humidity at the center of the wall cavity

(ASHRAE, 2009)

Due to the high vapour permeability of the insulation in the cavity, the vapour pressure of the air was considered constant across the cavity. The hourly saturation vapour pressure was then calculated at the interior surface of the sheathing, using the sheathing temperature data. Using these two values, the hourly relative humidity (RH) at the interior surface of the sheathing was calculated using the equation:

$RH = (P_{w, cavity}/P_{ws, sheathing})*100$

Whenever the RH was at 100% or above, condensation is expected. To compare the performance of different walls, each hour at 100% humidity or above was counted as 1 hour of condensation.

5.2.1.1 Air Sealed Condition

To determine condensation potential in the air sealed (as-built) condition, the data prior to the start of the air leakage testing was evaluated. This included data from October 4th 2012, through February 9th, 2013 (3307 hours). The average exterior temperature over this period was -1.4 °C. Figure 50 shows the percentage of total of hours of potential condensation for all three sheathing positions. With no intentional air leakage, no condensation is expected for the Datum wall, the XPS wall or the RW wall.

The PIC wall showed a small potential for condensation with 3 hours (.03% of total hours) on the south elevation and 23 hours (.2% of total hours) on the north, while the double stud wall showed a large potential for condensation with 2403 hours (24% of total hours) on the north elevation and 2639 hours (26% of total hours) on the south.

Since only the double stud wall showed significant periods of condensation potential under the test conditions, it was not possible to evaluate the relative performance of the other test walls using condensation hours. One method to accomplish this is to compare the predicted sheathing RH values. The average and peak sheathing RH of the three measurement locations for each test wall can be seen in Figure 51. The height of the column indicates the peak sheathing RH reached during the collection

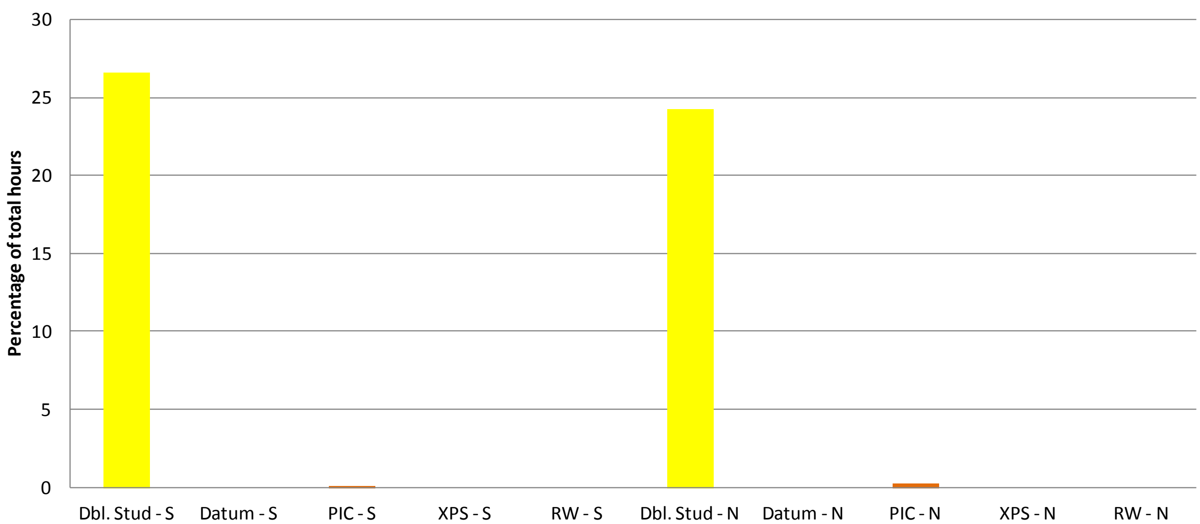

Figure 50- percentage of total hours with potential for condensation – air-sealed condition

period, while the black line on the column indicates the average sheathing RH. While RH values greater than 100% are not possible in reality, the value indicates the amount of moisture available for condensation on the sheathing.

The double stud wall had by far the highest levels of sheathing RH, with a peak of 275% and an average of 92% on the south side and a peak of 183%, and an average of 90% on the north. These extreme RH levels are a result two unfavorable conditions 1) high levels of built-in moisture within the hygroscopic cellulose insulation and 2) cold sheathing temperatures. The extreme temperature gradient across the cellulose layer results in a vapour pressure gradient across the cellulose causing a concentration of built-in moisture at the cold exterior sheathing.

Of the remaining walls, the PIC and XPS walls had the highest RH values with peaks at or near 100%. Although the sheathing temperatures were higher than the Datum wall, so were the interstitial moisture levels. Because these two walls do not have a 6 mil polyethylene sheet as an interior vapour barrier, they are more closely coupled with the interior RH levels resulting in higher sheathing RH levels and greater condensation potential in the air-sealed condition.

The Datum wall has significantly lower peak and slightly lower average RH values than the PIC and XPS walls. This is a result of the 6 mil polyethylene vapour barrier which prevents vapour flow from the interior. Without access to interior moisture, the sheathing RH remains low despite its low temperature.

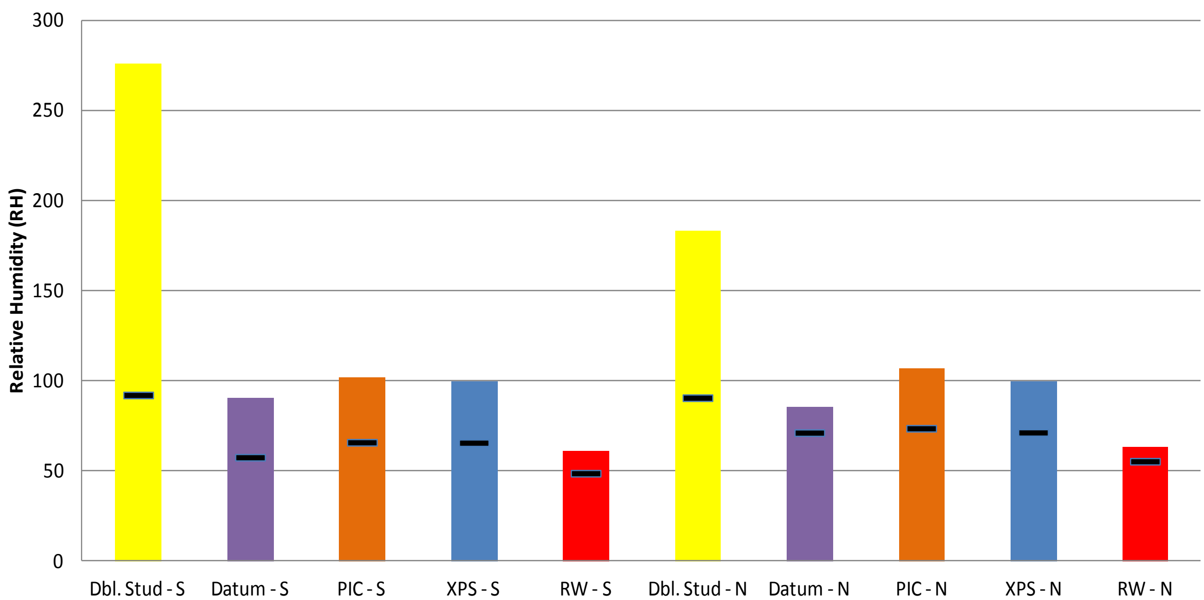

Figure 51 – Peak and average RH of the sheathing - air sealed condition

The Rockwool wall showed much lower peak and average RH values than the other walls tested. This is a result of two favorable conditions: warmer sheathing temperatures and a polyethylene vapour barrier preventing vapour flow from the interior.

The testing confirmed that the OSB temperature was very low and showed that the RH was surprisingly high, likely because of the hygroscopic nature of the cellulose insulation. Hence, the Double Stud wall had an elevated risk of condensation during cold weather and thus the wall has a higher risk of sheathing moisture damage even with no sources of rain leakage or other exterior wetting. The Datum wall has cold sheathing which showed no hours of condensation. The sheathing was warmer in the PIC and XPS walls, but the higher RH because of lack of a low-perm vapor barrier increased the risk of condensation. However, almost no hours of condensation were measured. The Rockwool wall had two favorable conditions: warm sheathing and low interstitial moisture levels (because of its high vapor permeance and the presence of an interior vapor barrier) which resulted in the lowest condensation potential.

5.2.1.2 Air Leakage Condition

The air leakage phase of testing occurred from February, 19th 2013 to March 22nd, 2013 (a total of 2215 hours). The average exterior temperature over this period was -2.4 °C. During air leakage, there were periods where the RH at the interior surface of the sheathing exceeded 100% for all test wall assemblies.

As shown in Figure 52, the Double stud wall had by far the greatest number of condensation hours. The sum of the three measured locations totaled approximately 1738 hours (26% of total hours) of condensation on the south elevation and approximately 2542 hours (38 % of total hours) on the north. These extreme levels of predicted condensation were a result of cold sheathing temperatures, built-in moisture within the cellulose plus the constant supply of moisture from the interior air. Due to the hygroscopic nature of the insulation, large amounts of moisture can be stored within cellulose and become concentrated at the cold sheathing.

The Datum wall had the next highest condensation potential with a total of 506 hours (7.6 % of total hours) of condensation on the south elevation and 385 hours (5.8 % of total hours) on the north. Like the Double stud wall, this high level of condensation potential is a result of cold sheathing temperatures in combination with a constant supply of moisture from the interior air. Because the Datum wall does not have the moisture storage capacity of the Double stud wall, interstitial moisture levels were not as high, resulting fewer condensation hours.

The PIC wall has a total of 61 hours (0.9 % of total hours) on the south elevation and 144 hours (2.2 % of total hours) on the north. The XPS wall had a total of 27 (0.4 % of total hours) hours of condensation on the south and 0 hours on the north. The rockwool walls had 0 hours of condensation on the south and 63 hours (0.9 % of total hours) on the north.

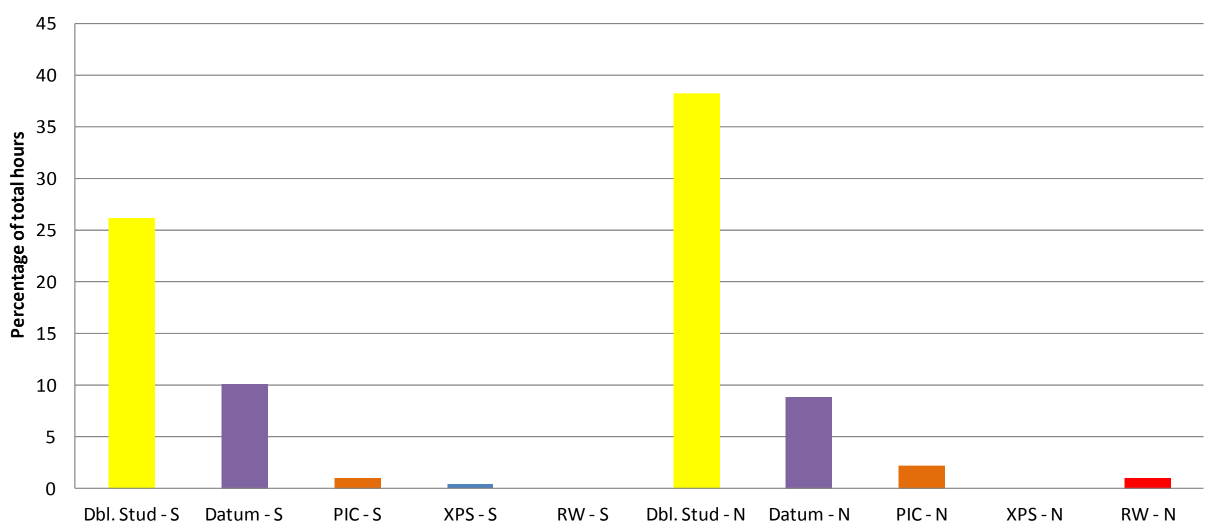

Figure 52- Percentage of total hours with potential for condensation - air leakage phase

Based on the vapour pressure analysis above, the three exterior insulated walls have a much lower condensation potential than the Datum and Double stud wall assemblies. With no intentional air leakage, only the Double stud wall shows condensation potential under the conditions of this study. This is likely a result of the built-in moisture content of the cellulose combined with cold sheathing temperatures. Under the air leakage condition, both the Double Stud and the Datum walls showed a high potential for sheathing condensation as the warm, humid interior was able to condense against the cold sheathing. The exterior insulated walls all showed low condensation potential during the air leakage condition.

5.2.2 Moisture Content Measurements

While the vapour pressure analysis is a proxy for the amount of sheathing condensation, moisture content (M.C.) sensors provide a direct measurement of moisture accumulation at the OSB sheathing and wood framing members. This moisture includes the built-in moisture, the absorption of condensation or bulk water, as well as the adsorption of moisture in the air and redistribution of moisture from surrounding materials. It is also important to consider that measured moisture content is the net effect of both wetting and drying mechanisms. Moisture content is reported as a percentage of moisture, by mass. A detailed discussion of resistance-based moisture content measurements can be found in

Appendix A: Measuring Heat, Moisture and Air Movement in Assemblies.

Hourly M.C. measurements were taken from October 2012 through August 2013 for all 5 positions. The lower OSB moisture content measurements (north elevation) are shown in Figure 53 as an example. As indicated on this graph, during Phase 1 of testing, the walls were left to perform as-built from October 2012 through February 19th, 2013. Phase 2 involved air injection wetting, which was performed from February 19th through March 22nd, 2013. Phase 3 was a drying phase, during which the test walls were allowed to dry to equilibrium M.C. under as built conditions. Phase 4 was the wetting mat wetting phase. From June 3rd through June 8th, 300 ml of water was injected into the wetting mats on the exterior of the OSB sheathing. From June 26th through July 5th, another 420 ml of water was injected into the wetting mats on the exterior of the OSB sheathing. The final phase of testing was a drying phase, where the walls were again allowed to dry down, under as-built conditions.

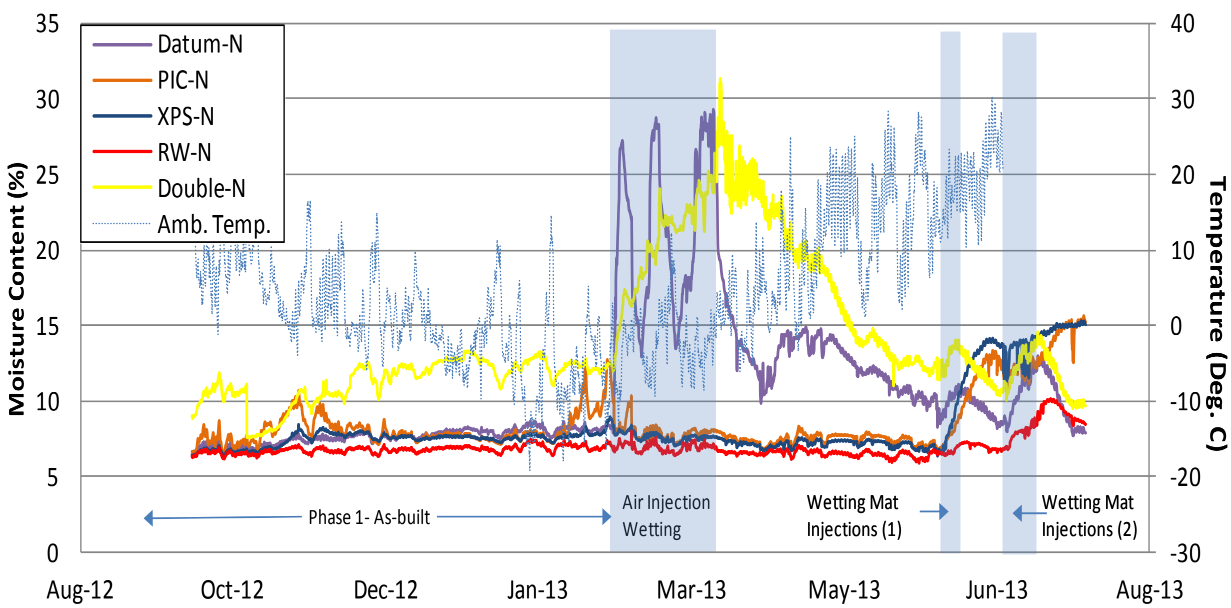

Figure 53 – Sheathing moisture content of all north walls over the entire test period

5.2.2.1 Condensation: As-Built Condition

Moisture content plots for each measurement location under as-built conditions are shown in Figure 54 through Figure 63. Under the as-built conditions (Phase 1), the OSB sheathing moisture content remained primarily between 6 and 8 percent for the Datum wall and the exterior insulated walls, with a few brief peaks of 10 to 12 % for the PIC wall during extended wet weather. As predicted by the vapour pressure analysis, the OSB moisture content for the Double stud wall was significantly higher than the other test walls, reaching as high at 16%.

Under as-built conditions, the moisture content for the top and bottom plates remained between 10 and 13 percent for the Datum and exterior insulated walls. The PIC walls showed plate M.C.s that were 1-2% higher than the others, but were still considered dry (less than 15%). The Double stud walls however showed significantly higher moisture content levels for the top and bottom plates, reaching as high as 25% for the upper plate on the south face. Both the north and the south side Double stud walls show a trend of increased moisture content with higher position in the wall, demonstrating the buoyancy of the water vapour within the interstitial air. The exception to this trend was at the bottom plate on the north side, which had a higher moisture content than any of the sheathing positions. This trend indicates an accumulation of moisture draining down from the sheathing condensation above.

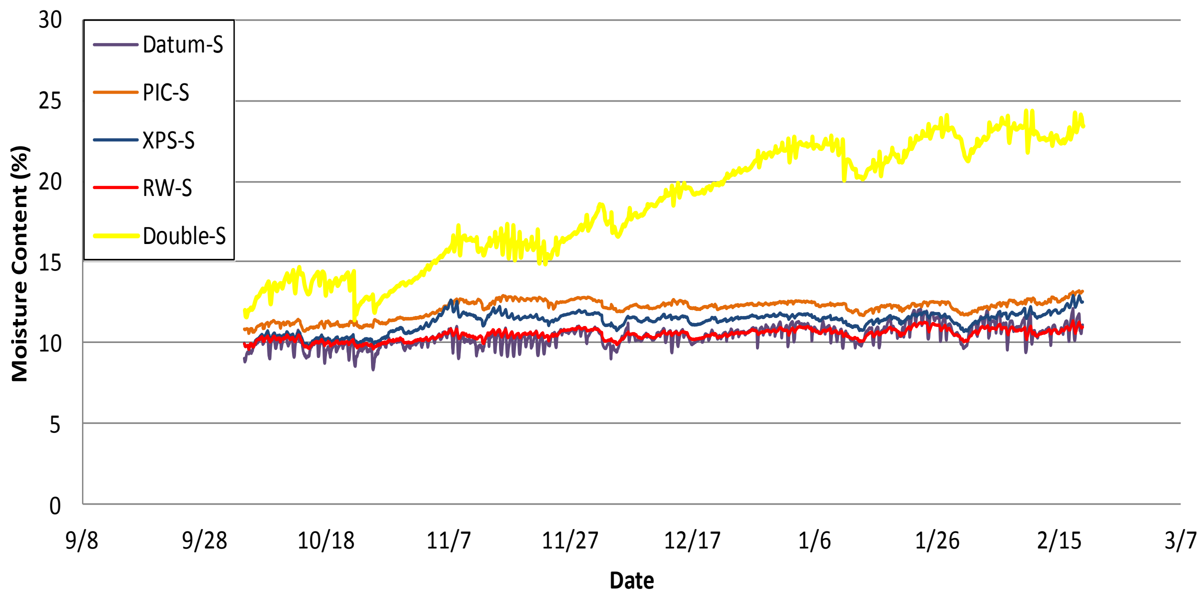

Figure 54- Moisture content at top plates during as-built phase – south elevation

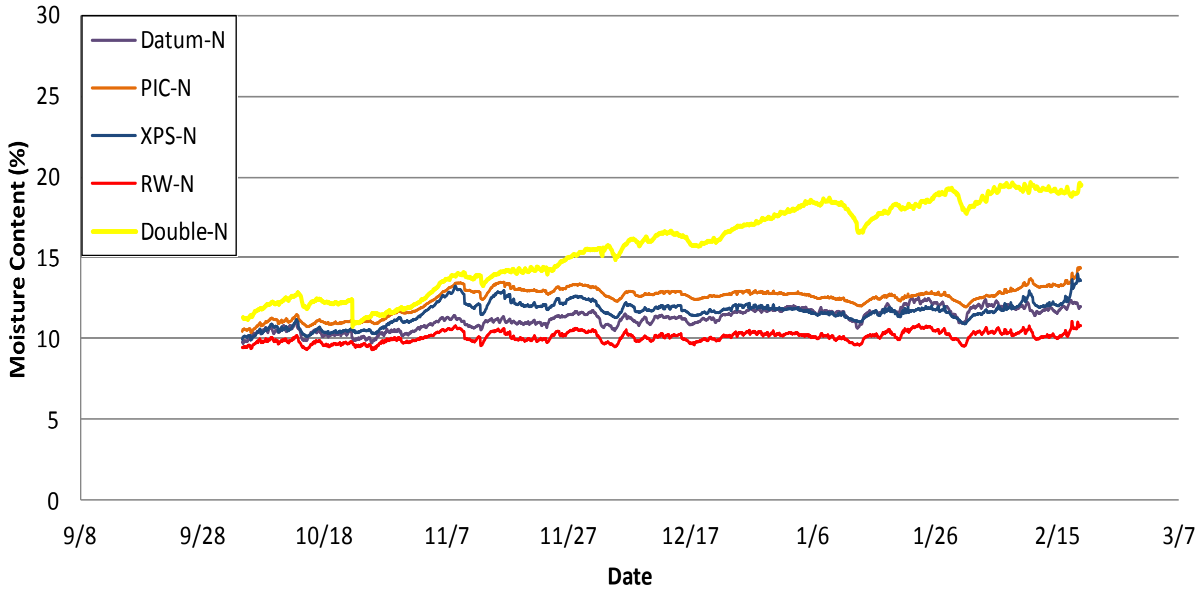

Figure 55- Moisture content at top plates during as-built phase – north elevation

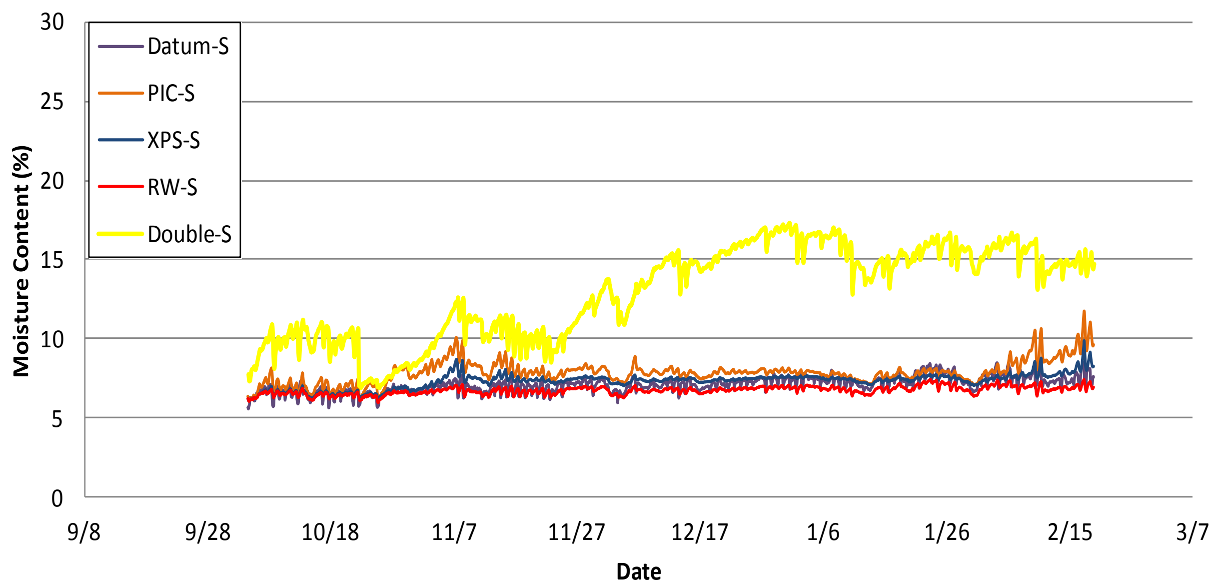

Figure 56- Moisture content at upper sheathing during as-built phase – south elevation

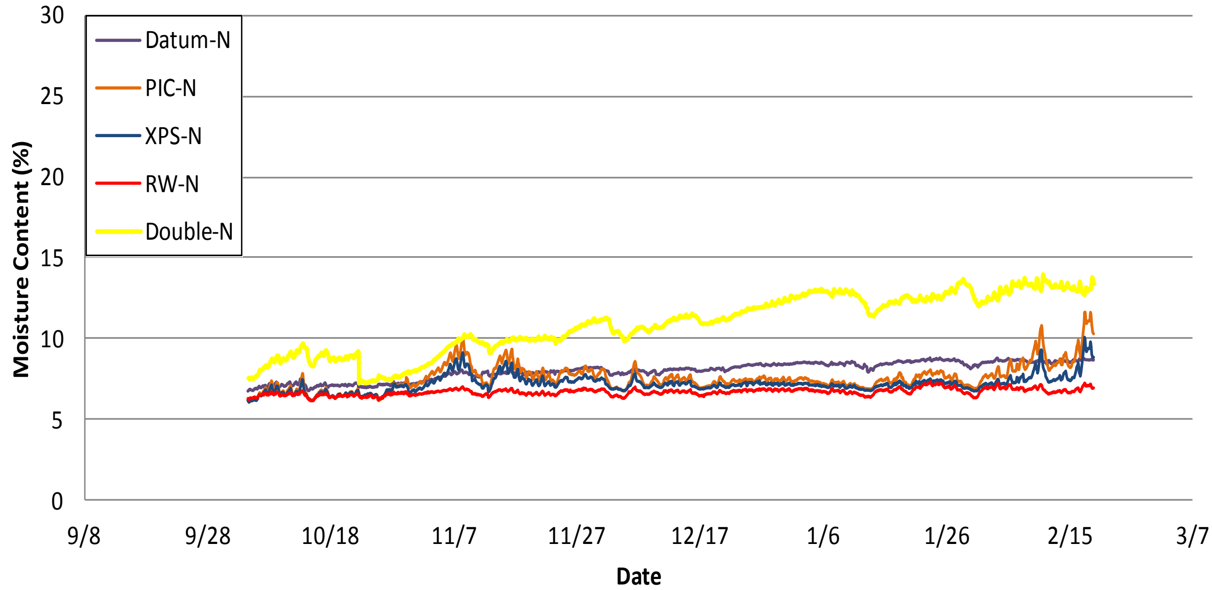

Figure 57- Moisture content at upper sheathing during as-built phase – north elevation

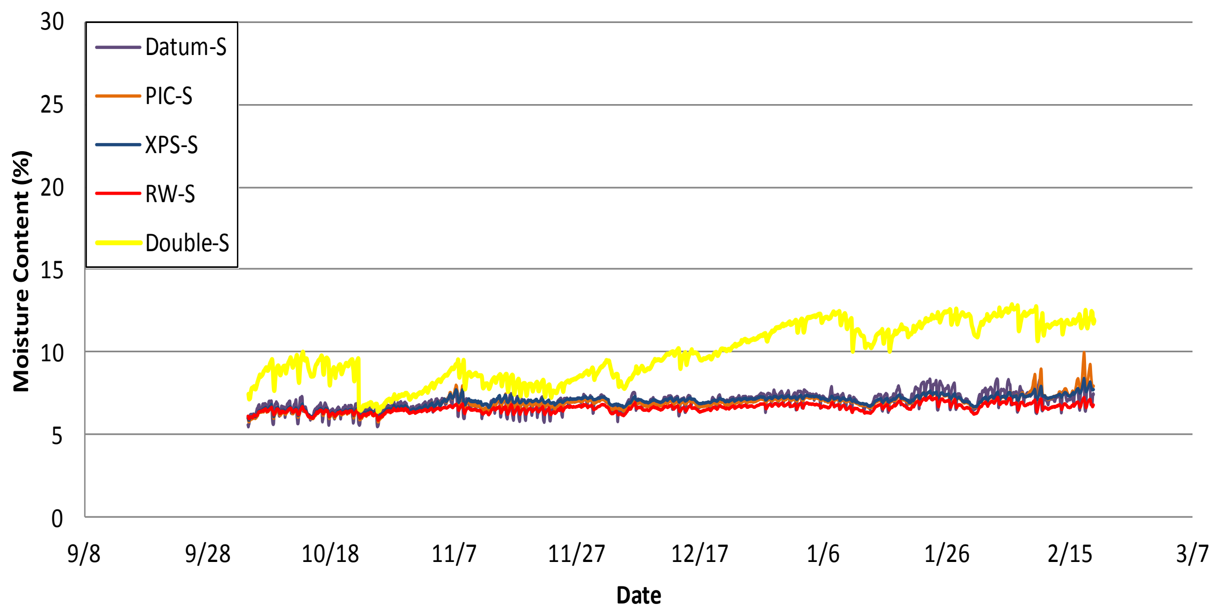

Figure 58- Moisture content at middle sheathing during as-built phase – south elevation

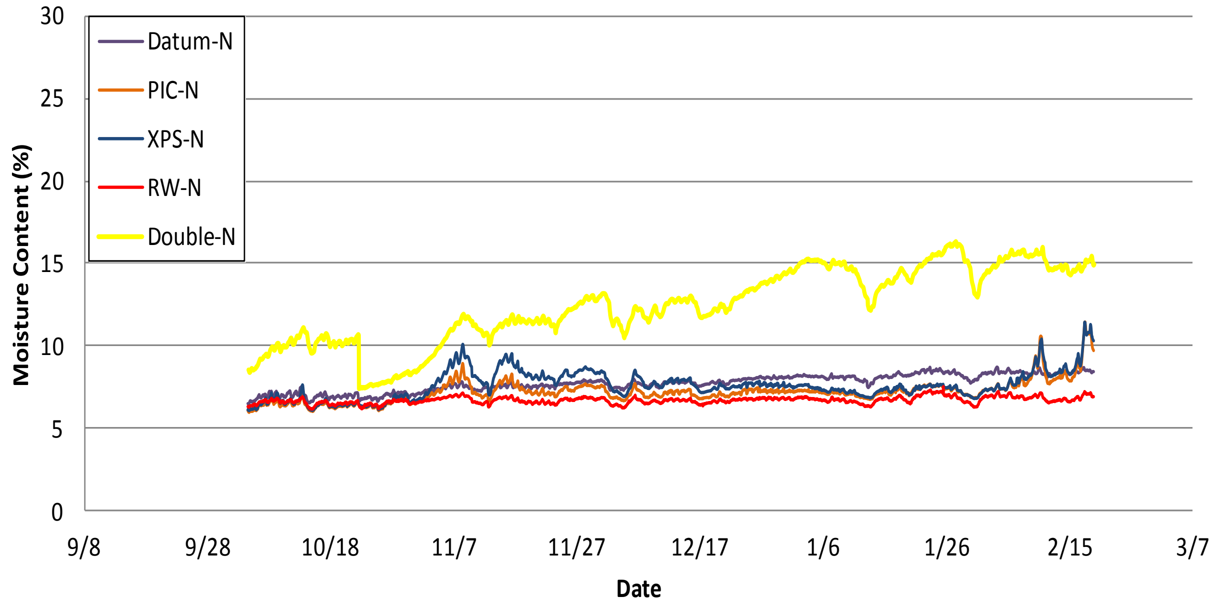

Figure 59- Moisture content at middle sheathing during as-built phase – north elevation

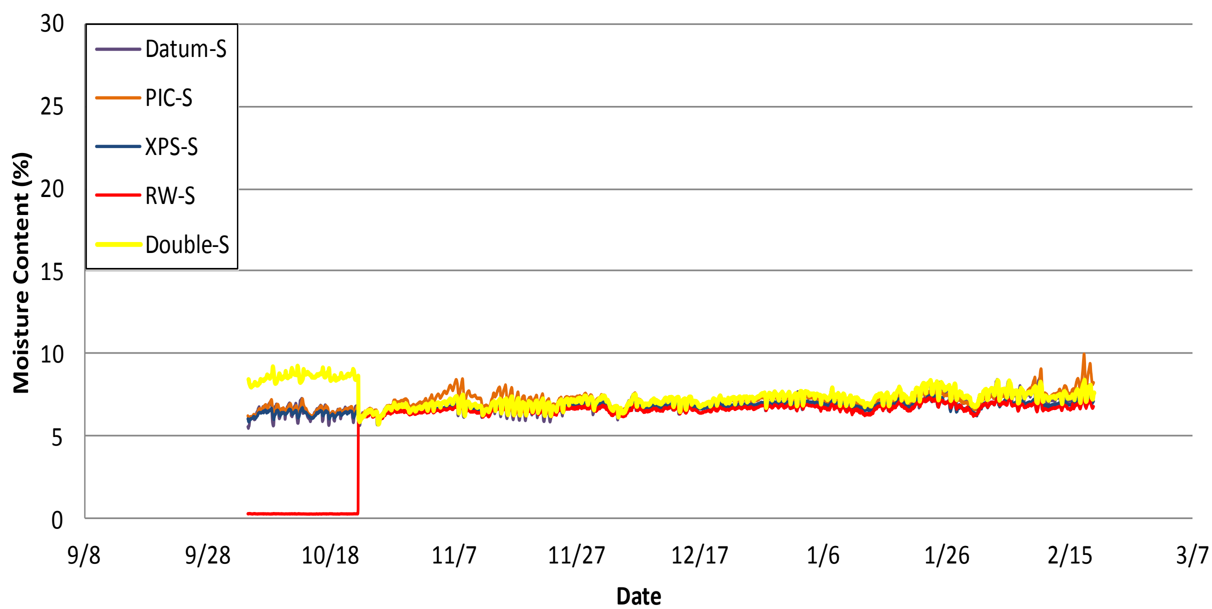

Figure 60- Moisture content at lower sheathing during as-built phase – south elevation

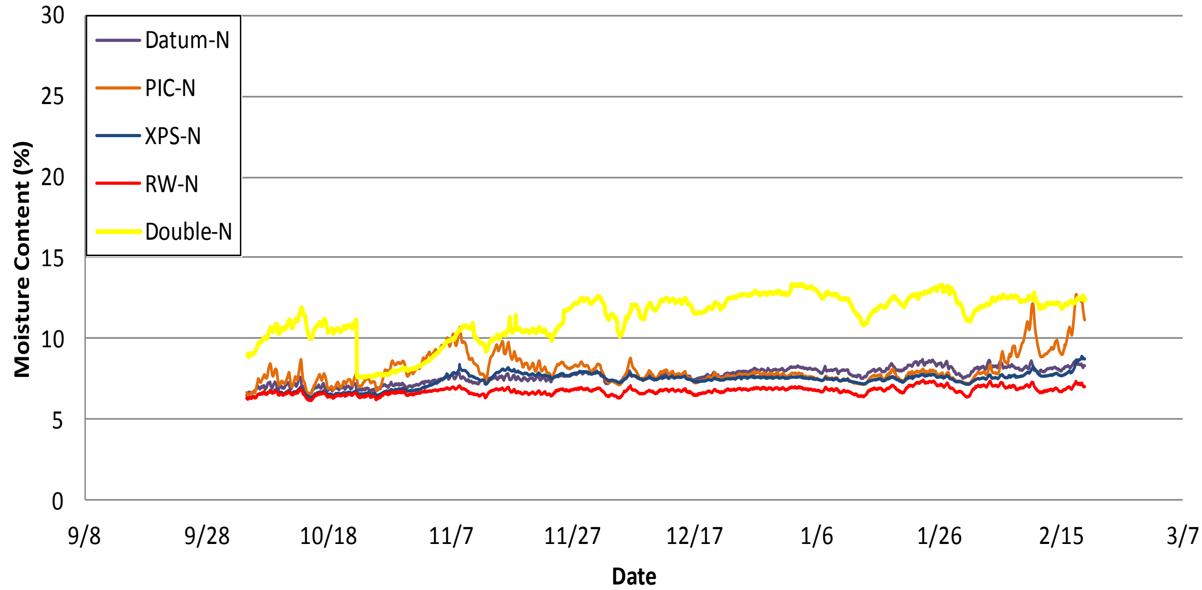

Figure 61- Moisture content at lower sheathing during as-built phase – north elevation

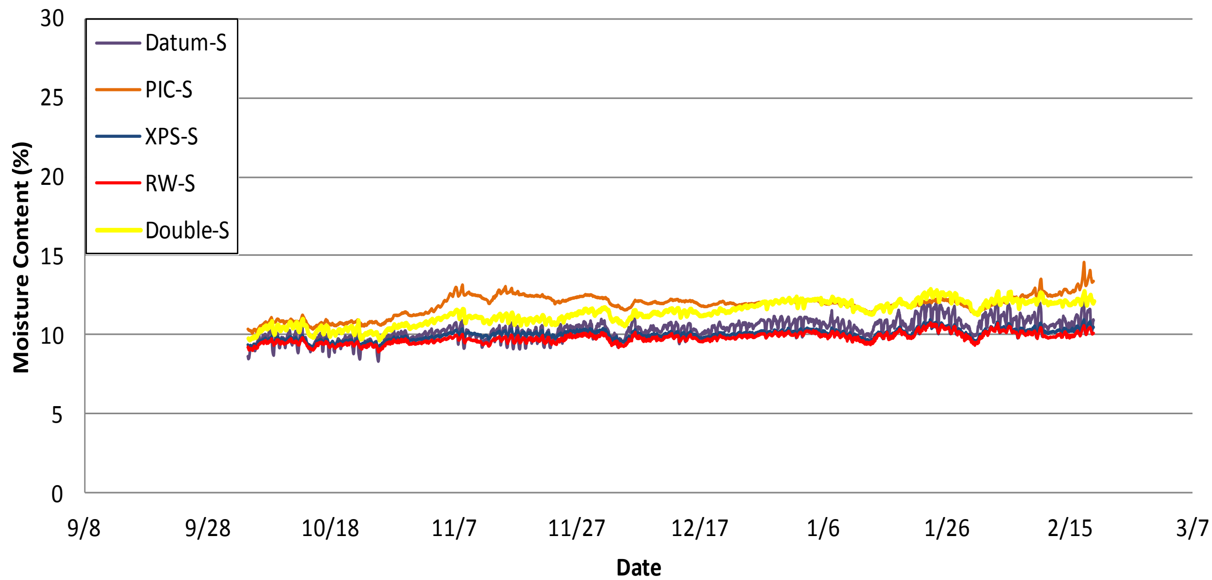

Figure 62- Moisture content at bottom plate during as-built phase – south elevation

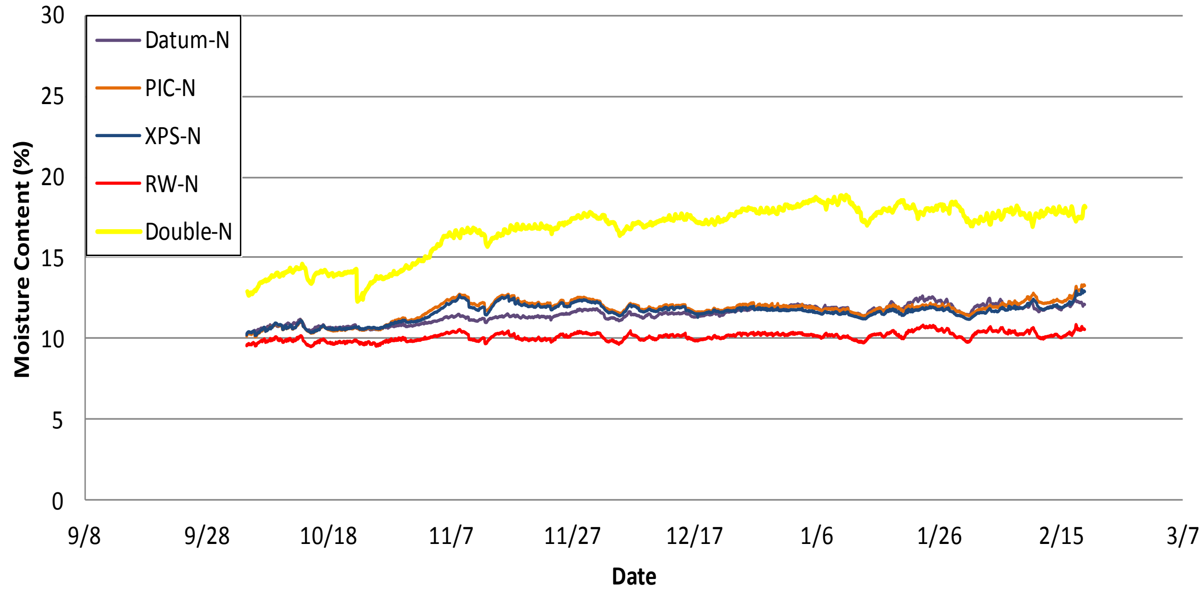

Figure 63- Moisture content at bottom plate during as-built phase – north elevation

5.2.2.2 Simulated Air Leakage Condensation

Figure 64 through Figure 73 are plots of moisture content during phase 2 (air injection wetting) and phase 3 (the subsequent drying phase) of testing. The air injection phase had little effect on the moisture content of any of the walls at the top plate or upper sheathing positions. On the lower half of the walls however, the air injection resulted in significant increases in moisture content in the Double Stud and Datum walls.

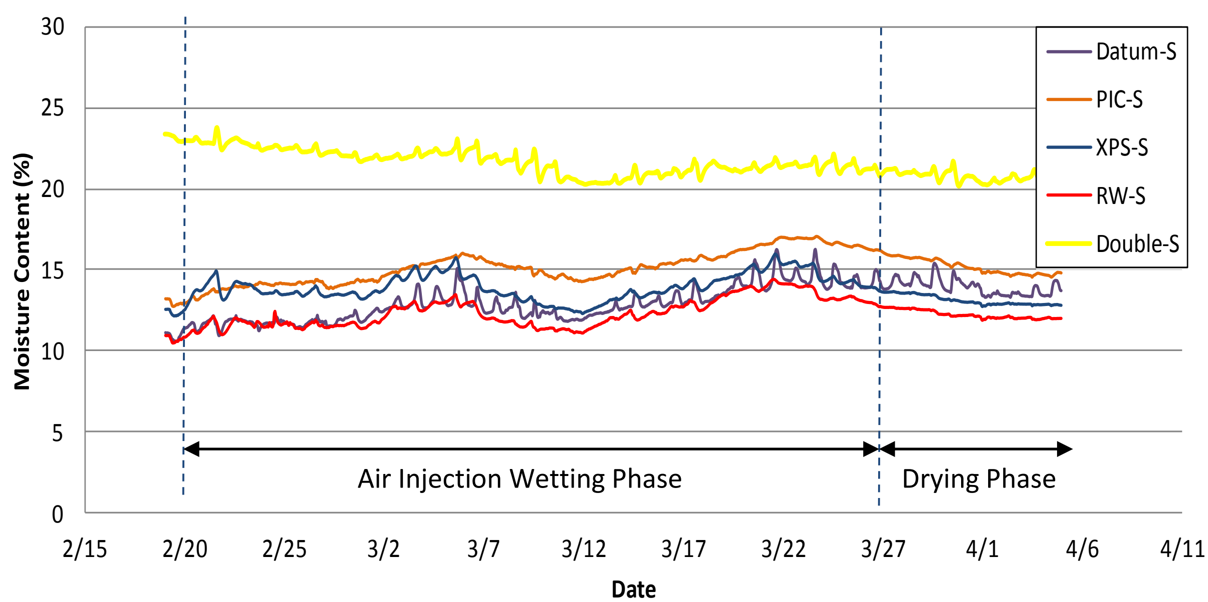

Figure 64-Moisture content at top plate during air injection wetting and drying phases – north elevation

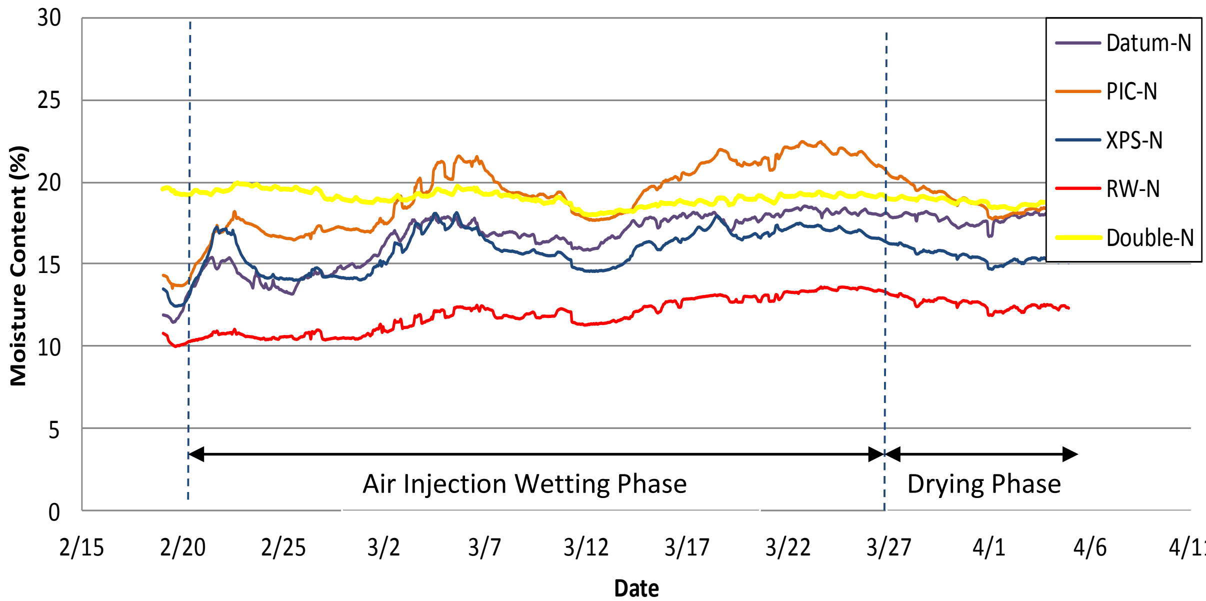

Figure 65- Moisture content at top plate during air injection wetting and drying phases – south elevation

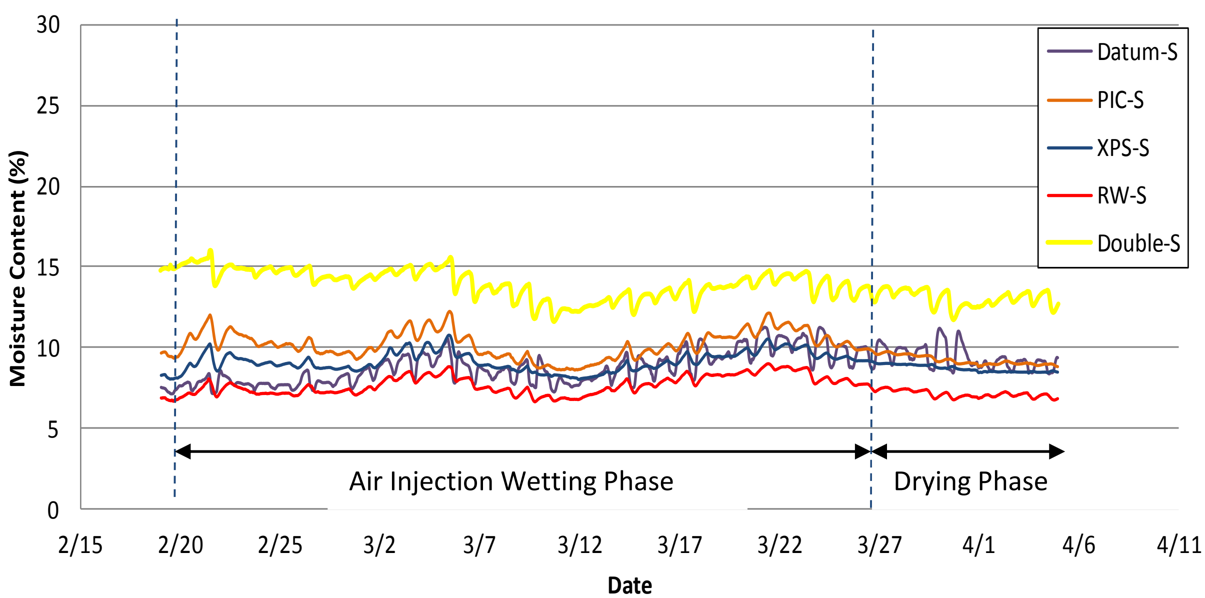

Figure 66-Moisture content at upper sheathing during air injection wetting and drying phases – north elevation

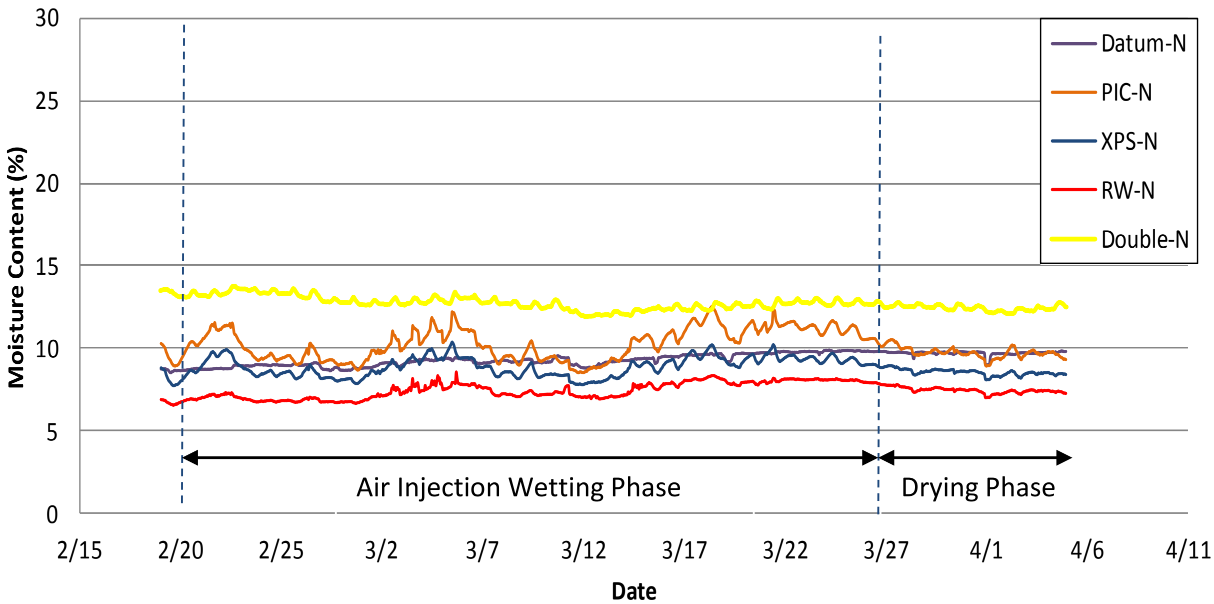

Figure 67-Moisture content at upper sheathing during air injection wetting and drying phases – south elevation

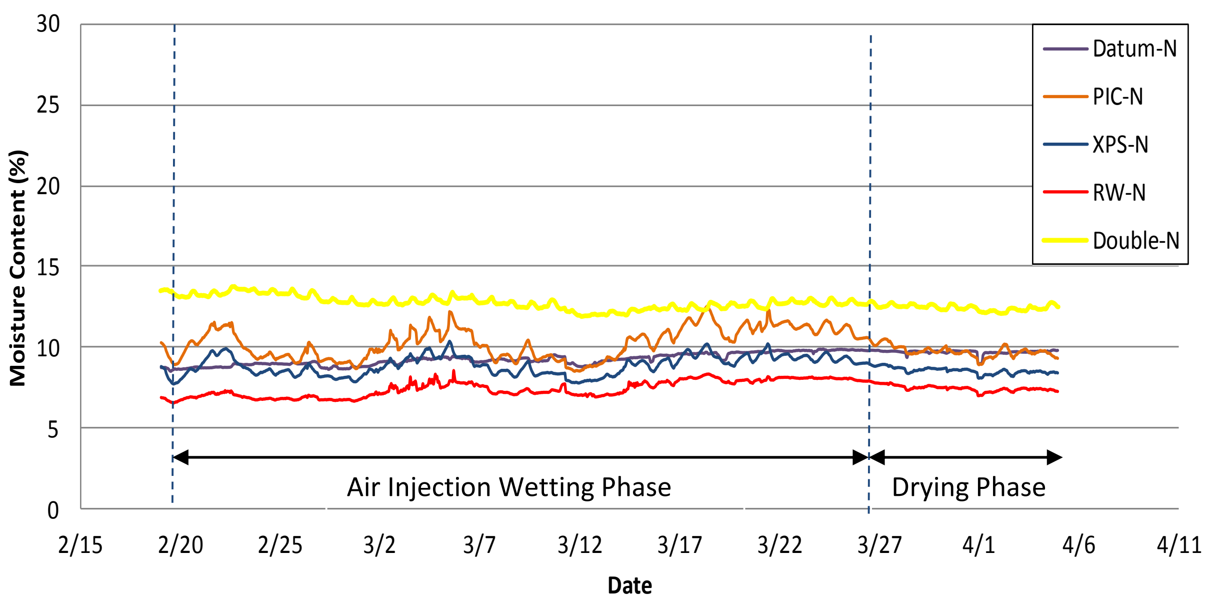

Figure 68- Moisture content at middle sheathing during air injection wetting and drying phases – north elevation

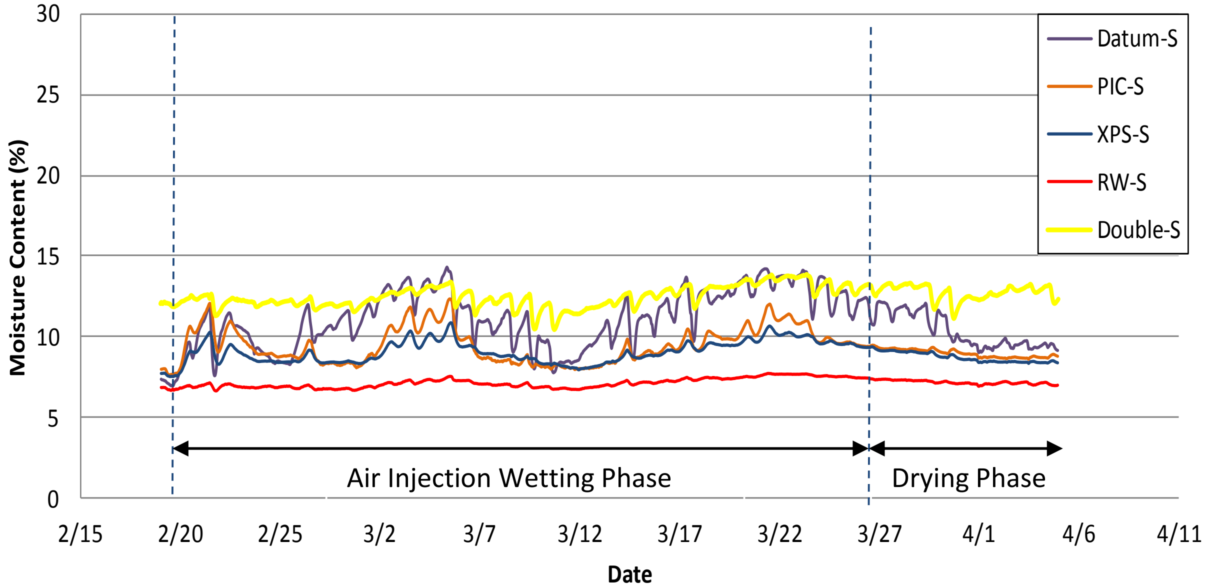

Figure 69- Moisture content at middle sheathing during air injection wetting and drying phases – south elevation

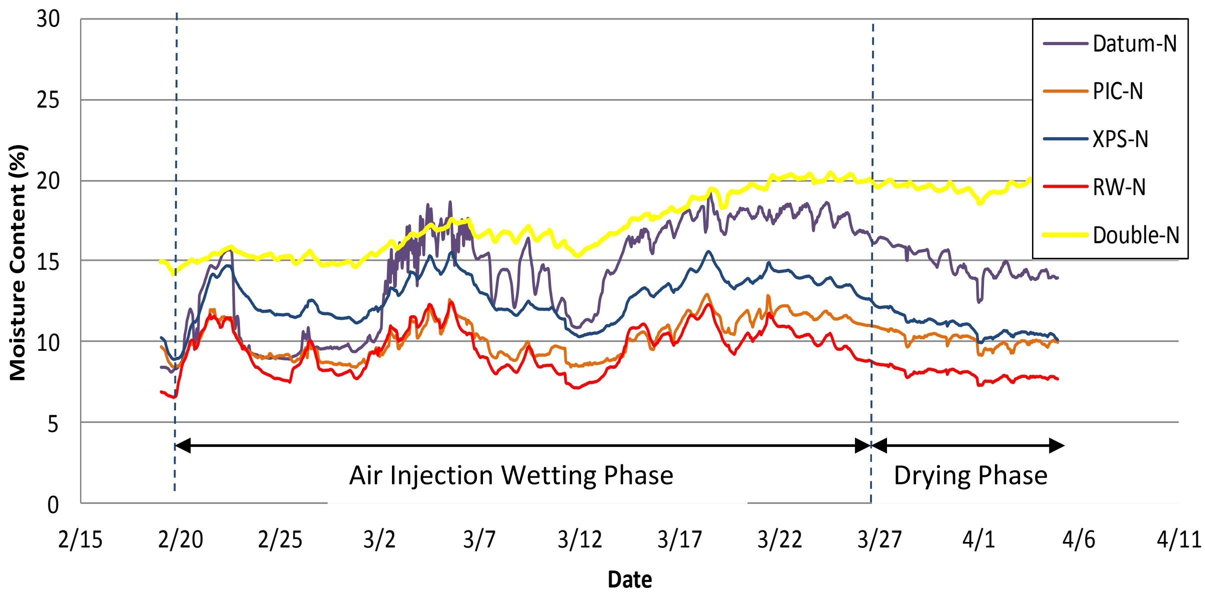

Figure 70- Moisture content at lower sheathing during air injection wetting and drying phases – north elevation

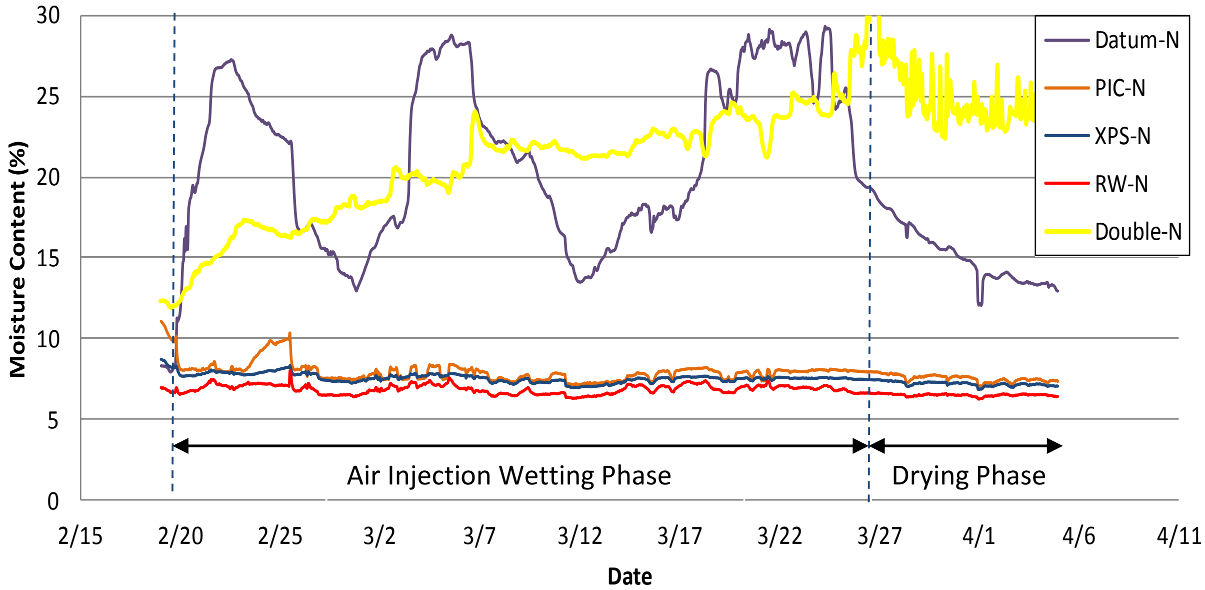

Figure 71-Moisture content at lower sheathing during air injection wetting and drying phases – south elevation

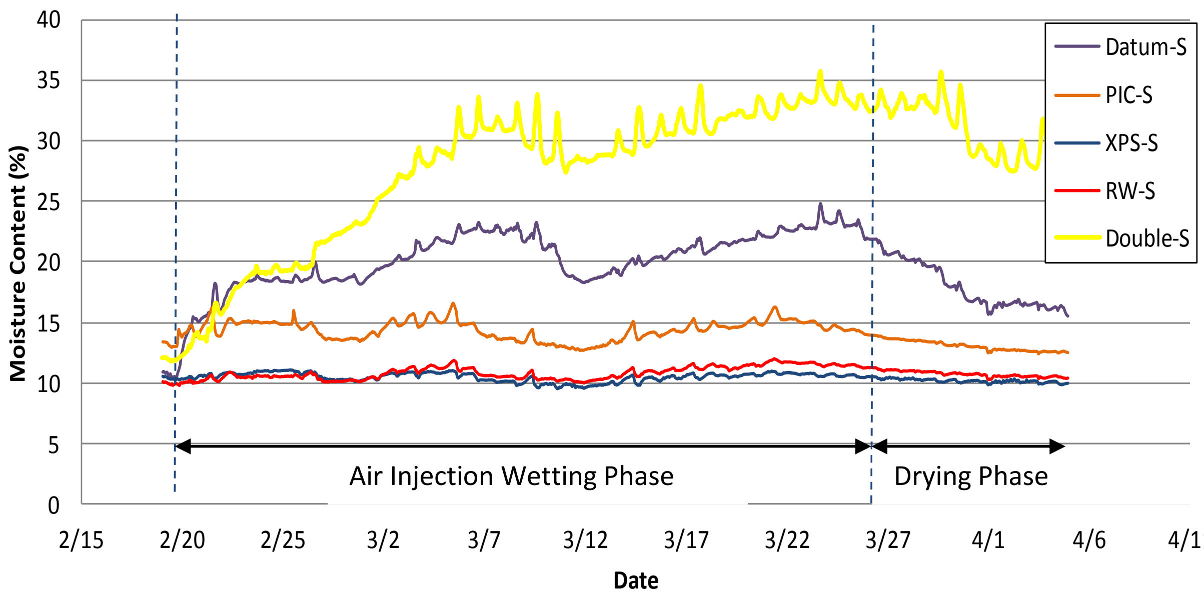

Figure 72-Moisture content at bottom plate during air injection wetting and drying phases – north elevation

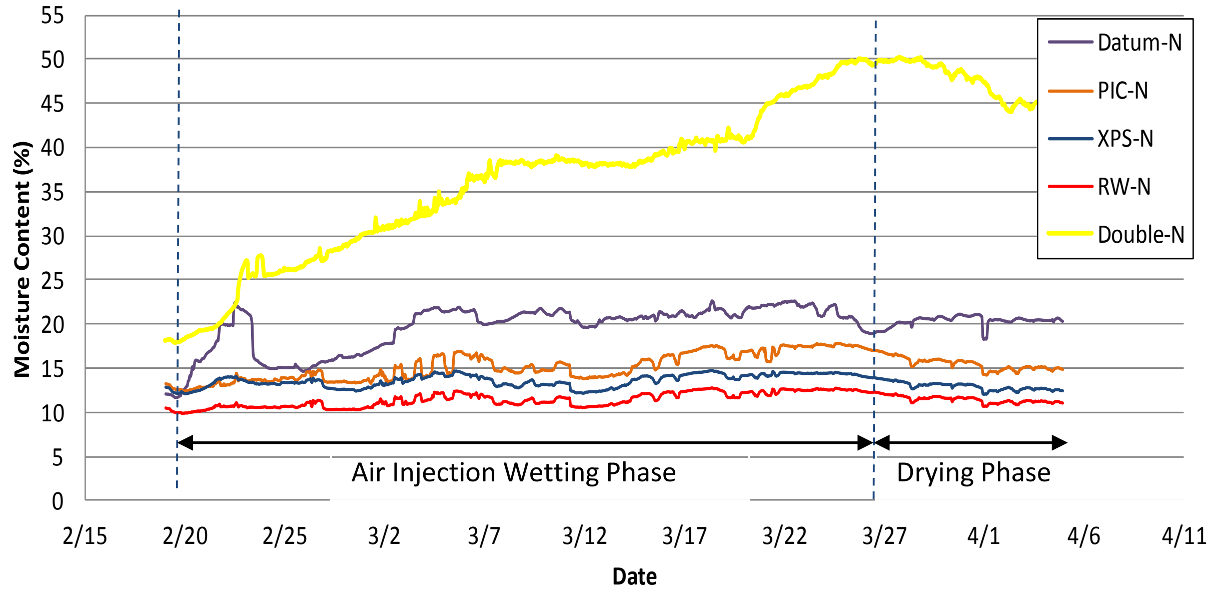

Figure 73-Moisture content at bottom plate during air injection wetting and drying phases – south elevation

To quantify the effect of air injection wetting on each wall, at each measurement site, the average M.C. during phase 1 was compared to the average M.C. during the final week of the air injection wetting phase. These changes are summarized in Figure 74 and Figure 75 below.

Both the sheathing and plate moisture content readings show that all three exterior insulated walls were effective at resisting the accumulation of sheathing condensation under both the air sealed condition and the air leakage condition. OSB moisture contents remained mostly below 15% for all exterior insulated walls, at all positions. The only occurrences of moisture content exceeding 15% were for the north elevation PIC wall, with the top plate reaching 22% M.C. and the bottom plate reaching 17% M.C. during the air leakage condition.

As predicted by the vapour pressure analysis, the warmer sheathing temperatures of the exterior insulated walls reduced air leakage condensation significantly compared to the Datum and Double Stud walls. The Rockwool wall performed slightly better than the PIC and XPS wall. This is likely a combination of the high vapour permeability of the rockwool allowing drying to the exterior and the effective vapour barrier in that assembly preventing vapour flow from the interior.

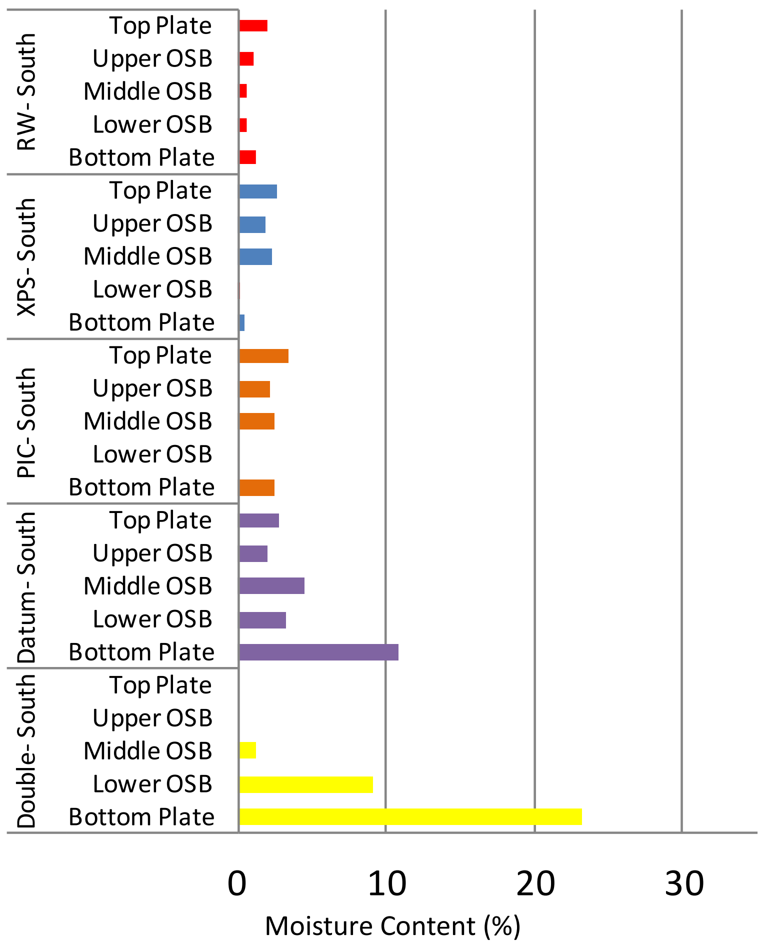

Figure 74- Change in moisture content due to air injection wetting - south elevation

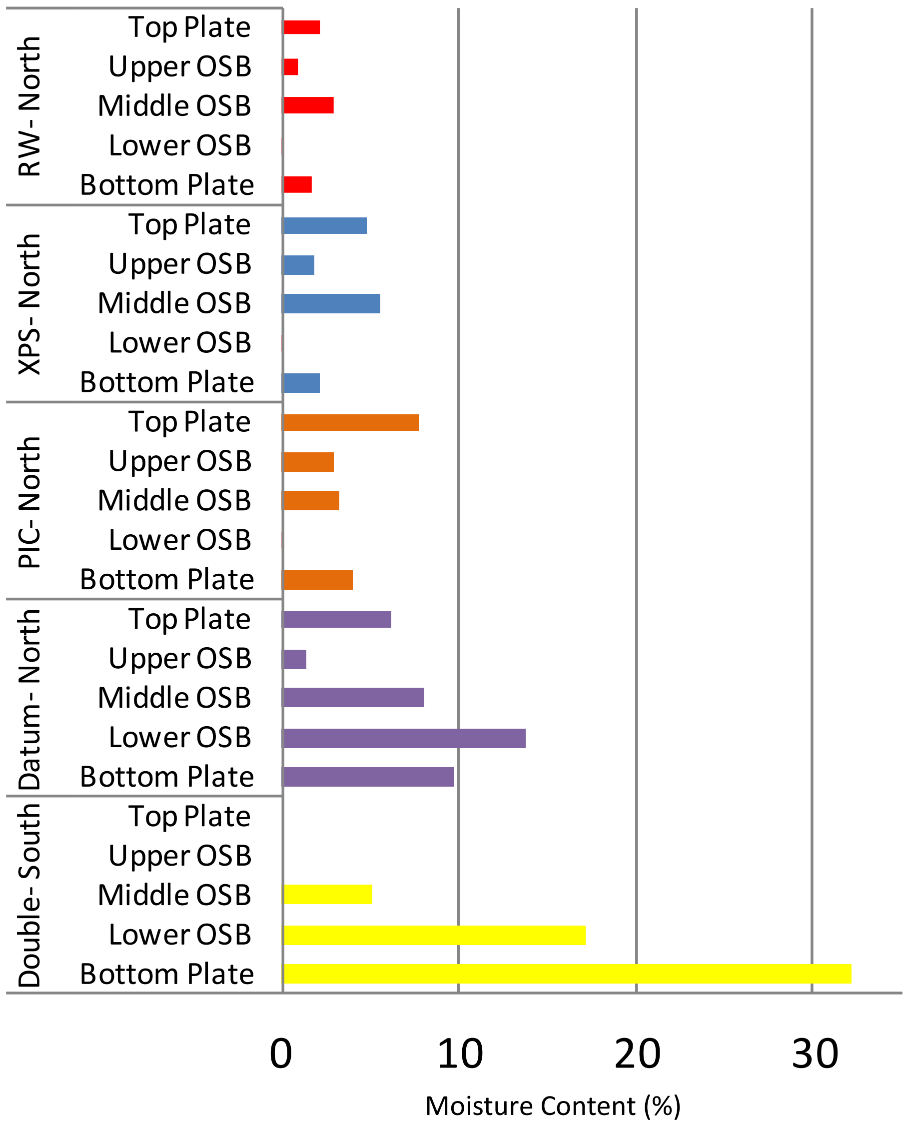

Figure 75- Change in moisture content due to air injection wetting- north elevation

The Datum wall remained dry during the air sealed condition, with moisture content remaining below 10%. During the air leakage condition however, the Datum wall experienced significant moisture accumulation with the lower OSB position approaching 30% on the north elevation. These results indicate the sensitivity of this type of wall system to air leakage condensation in even moderately cold climates.

The moisture content of the Double Stud walls was significantly higher than the other test walls during the air sealed condition, with the top plate on the south side approaching 25% M.C., and the bottom plate on the north side approaching 20%. These measurements confirm the results of the vapour pressure analysis and demonstrate the migration of moisture within the cellulose to the sheathing during cold weather (ie, ping-pong moisture), and indicate that this wall system is sensitive to built-in moisture. During the air leakage condition, the moisture content of the Double Stud walls were generally higher than the other test walls with extremes of 30% at the north lower sheathing position and 50% at the north bottom plate. These results indicate significant sheathing condensation and drainage of liquid water towards the bottom of the wall and demonstrate the sensitivity of this wall system to air leakage condensation.

As the air injection phase increased the OSB and wood moisture content of most walls, the Datum Walls dried much more rapidly than the Double stud walls. This can be most easily seen in the plots of the lower sheathing and bottom plate positions in Figure 70 through Figure 73. This difference is likely due to the large amount of moisture being stored in the hygroscopic cellulose insulation in the Double Stud walls and possibly by the lower sheathing temperature of the Double Stud walls. This confirms the results of the vapour pressure analysis, which shows a significantly higher number of condensation hours for the Double Stud walls (because of the colder sheathing) than the Datum walls during the air leakage condition. This stored moisture requires longer to dry to the exterior and extends the period of increased sheathing M.C. compared to the Datum wall.

For the three exterior insulated walls, the air injection procedure did not produce a sufficient increase in moisture content to allow for a definitive assessment of drying capacity.

5.2.3 Rain Leaks and Drying Capability

The wetting mat procedure was used to apply a controlled amount of water directly to the exterior surface of the OSB sheathing, simulating a rain water leak at the corner of a window or other area of water concentration.

The primary method of quantifying drying capability was to track the change in sheathing moisture content (M.C.) during and following the wetting mat water application. The lower sheathing position was the focus of the assessment since it was within the field of the wetting mat. Plots of the lower sheathing M.C. during and following the wetting mat water application for the north and south elevations can be seen in Figure 76 and Figure 77 respectively.

These plots show that the different wall assemblies reached different peak M.C.s at different times, and required different times to return to dry conditions. Three metrics were chosen to compare the drying capacity of the test walls 1) slope of the M.C. vs. time plot during drying, 2) time to dry 3) integration of the time/M.C. plot.

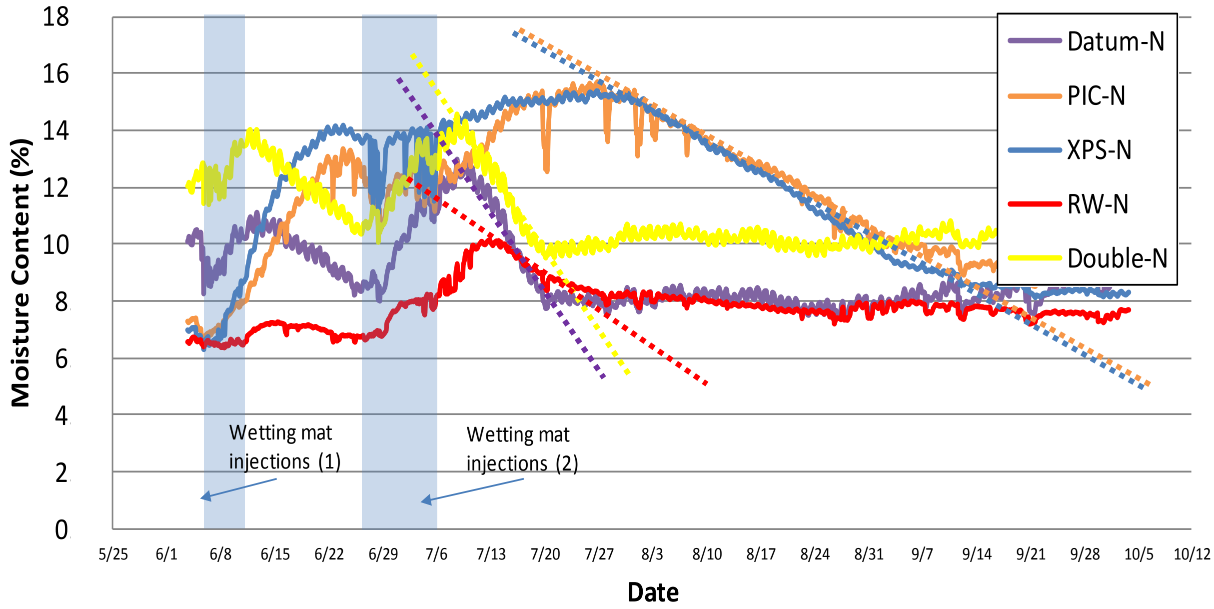

Figure 76- Moisture content at lower sheathing position for north elevation walls

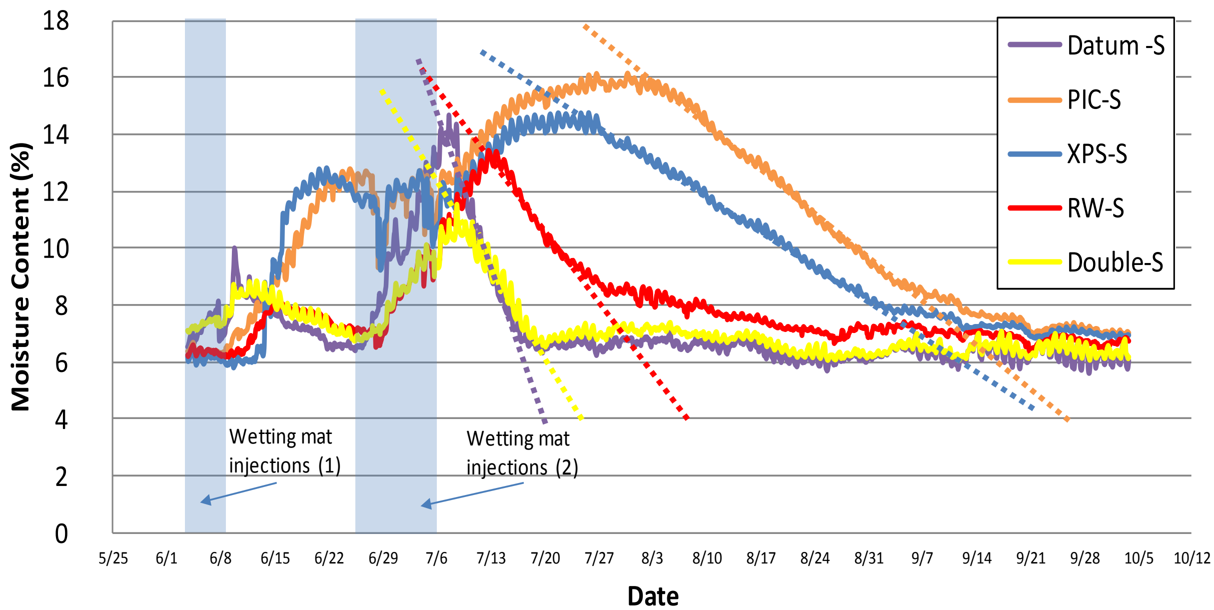

Figure 77- Moisture content at lower sheathing position for south elevation walls

5.2.3.1 Slope of the M.C. vs. Time Plot

The dotted lines in Figure 76 and Figure 77 show the slope of the M.C. vs. time plot during the drying phase that followed the rain wetting phase.

The Datum and Double Stud walls had the steepest slope with drying rates of - .36 to - .45 percent per day. The high drying rate compared to the exterior insulated walls was due to the warmer sheathing temperatures and the ability of these walls to dry to the exterior due to low vapour resistance exterior to the sheathing (i.e., just the Tyvek) and the ready availability of energy during the summer drying months.

The Rockwool wall on the south side had a slightly lower drying rate than the Datum and Double Stud walls at - .32 percent per day. The drying rate is similar due to the low vapour resistance of the rockwool allowing rapid drying to the exterior, but slightly lower due to the lower sheathing temperatures. On the north side, the Rockwool wall had a much lower slope likely due to the fact that this wall never did reach a high enough peak sheathing moisture content to provide meaningful results (10% MC would be considered dry by most).

The PIC and XPS walls consistently exhibited the lowest drying rates of all of the walls tested. These walls showed slopes between - .16 and - .23 percent per day. This low drying rate is a result of the high vapour resistance of the exterior insulation and the lower sheathing temperatures, both factors which limited drying to the exterior. Drying to the interior was possible because of the lack of a vapor barrier but did not provide sufficient flow to reach the faster drying rates exhibited by the Datum wall.

5.2.3.2 Time to Dry

On the south elevation walls, time to dry was measured from the end of the wetting process (July 6th, 2013) until the sheathing M.C. fell below 8%. On the north elevation, the PIC, XPS and Double stud walls did not return to 8% M.C. For the PIC and XPS walls, 9% was used as the definition of dry, while 10% was used for the Double Stud wall.

The results of this analysis are shown in Figure 78. The Datum wall, the Double stud wall and the RW wall returned to dry quite quickly. These three walls required 232, 238 and 343 hours on the south side and 295, 339 and 367 hours on the north side respectively. The PIC and XPS walls required a significantly longer time to dry. The PIC wall required 1639 and 1650 hours, while the XPS wall required 1399 and 1635 hours on the south and north elevations respectively.

Clearly, the largest factor affecting time to dry is the vapour resistance of the assembly layers exterior to the sheathing. The two walls with high vapour resistance insulation exterior to the sheathing (PIC and XPS) required approximately 6 times the amount of time to dry down after wetting compared to the other test walls.

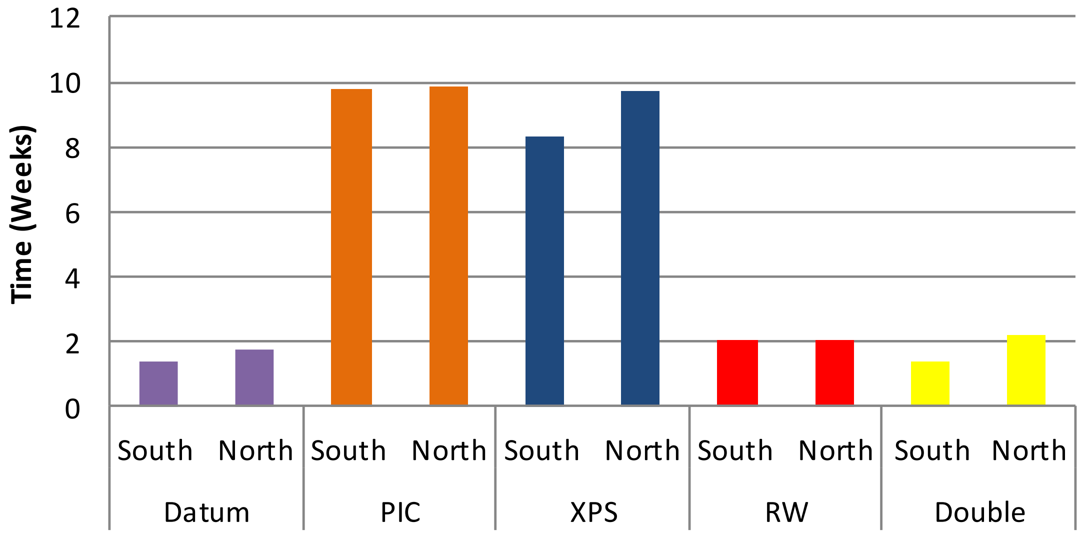

Figure 78- Time required to return to dry condition after wetting mat phase

5.2.3.3 Integration of M.C. Plot

A third metric was developed as a more complete measure of drying capacity, accounting for both the peak moisture content reached and the time required for drying. The area under the M.C./Time curve was calculated from the beginning of the wetting mat wetting phase (June 3rd) through the end of September. In order to measure the change in M.C. due to the wetting and drying processes, the plots were first normalized by subtracting the starting M.C. The result is a metric that is the inverse of drying capacity; the lower the value, the higher the drying capacity.

As shown in Figure 79 below, the results of this analysis show that the Datum wall has the highest drying capacity with between 2200 and 2600 M.C.-hours for south and north elevation walls respectively. The Double stud and Rockwool walls had approximately double the moisture-content hours of the Datum wall with 3987 and 5182 M.C.-hours respectively on the south side and 3524 and 3502 M.C.-hours on the north side respectively. This is likely due to the hygroscopic nature of the cellulose insulation in the Double stud wall and the cooler summer-time sheathing temperatures the RW wall. The PIC and XPS exterior insulated walls had approximately 6 times the number of M.C.-hours of the Datum wall, with 13811 and 11721 M.C. hours on the south side respectively and 12597 and 13952 M.C. hours on the north side respectively, due to the high vapour resistance of the foam insulation boards.

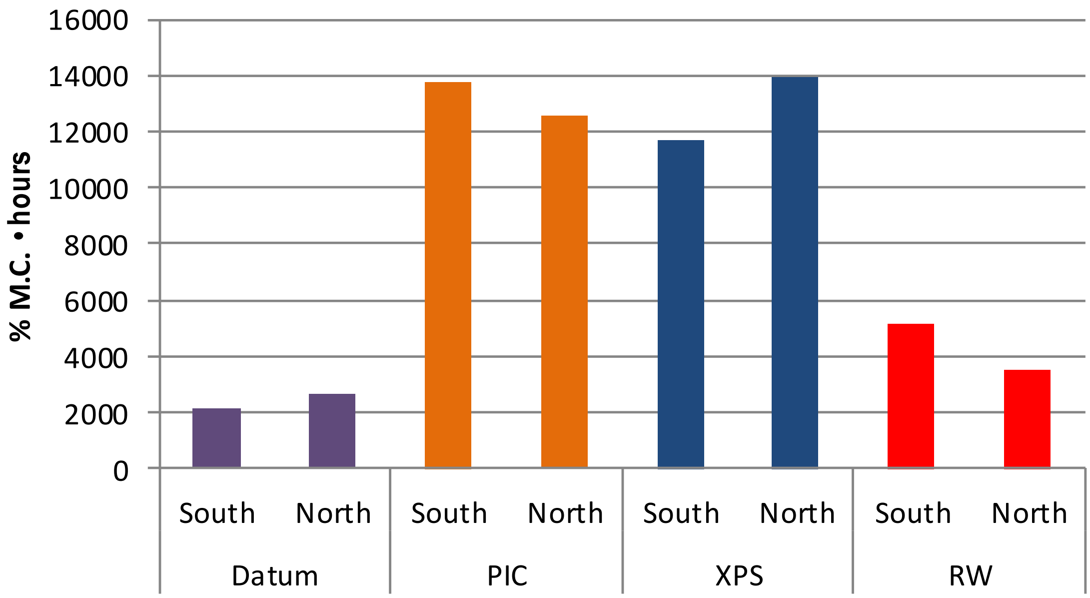

Figure 79- Integration values of the of the normalized M.C. plots during wetting and drying

5.2.4 Summary

The results show that the addition of insulation exterior to the sheathing can have both positive and negative effects on moisture performance. All of the exterior insulated walls tested showed a significant improvement in resisting air leakage condensation compared to the walls with no exterior insulation. The drying capabilities of the exterior insulated walls however, varied considerably between the exterior insulation types. The insulations with low vapour permeance (PIC and XPS) showed summertime drying rates as much as 6 times less than the walls with no exterior insulation, while the highly vapour permeable Rockwool dried approximately 2 times slower.

Although not demonstrated here, because of the well ventilated cladding used, inward vapor drives were not a factor in these results. If a moisture storage cladding such as brick, stucco, or stone were used, the vapor resistance of the PIC and XPS insulating sheathing would have been a major benefit.

6 Discussion

6.1 Thermal Performance

6.1.1 Effective R-Value

One of the main benefits touted by those who have developed and promoted exterior insulation strategies is increased cold-weather sheathing temperatures. Hourly sheathing temperature data from the experimental portion of this study clearly showed that walls with exterior insulation had warmer sheathing during winter conditions than walls without. While sheathing temperature was not a reliable predictor of sheathing condensation due to vapour flow, it was a very good predictor when air exfiltration was present. The hourly sheathing temperature data also showed that the thermal performance of the different exterior insulations varied between the exterior insulation types and also changed with exterior temperature conditions.

To calculate the effective thermal resistance of the exterior insulations under different temperature conditions, two examples of 6 consecutive hours of relatively constant cold, moderate and hot exterior temperature conditions were chosen. North elevation walls were chosen to avoid direct solar radiation. An excel-driven model was created to predict the temperature drop across each layer of the wall assembly based on standard material thermal conductivities (Straube and Burnett, 2005) and known thicknesses. For the exterior air gap, the equivalent conductance was adjusted for exterior temperature (Straube and Burnett, 2005). For the interstitial fiberglass batt insulation, thermal conductivity was adjusted for temperature, based on ASHRAE (1985) 23.17. Measured temperature conditions for exterior and interior ambient air and for wall sheathing were used to drive the model. The thermal conductivity of the exterior insulation layer was adjusted iteratively to reproduce the measured sheathing temperature. These conductivities were then converted to R-values.

Figure 80 plots the, effective R-values for each insulation type for three exterior temperature conditions. Figure 81 shows the same results, in the form of R-value per inch. Horizontal lines indicate the rated nominal R-value.

The polyisocyanurate (PIC) insulation was labeled with a nominal R-value of R-6 (RSI 1.06) per inch. Using the method described above, the calculated effective R-value of the PIC insulation increased from R-4 (RSI 0.7) per inch at -15 °C, to R-5 (RSI 0.9) per inch at 3.5 °C and to R-6.5 (RSI 1.1) per inch at 30 °C. These values fall within the ranges found in other studies of PIC insulation including studies by the National Roofing Contractors Association (Graham, 2010) and Building Science Corporation (BSC, 2013).

The extruded polystyrene (XPS) was labeled with a nominal R-value of R-5 (RSI .90) per inch. Using the described method, the calculated effective R-value of the XPS insulation decreased from R-4.5 (RSI 0.79) per inch at both -15 °C and at 3.5 °C, to only R-3.3 (RSI .58) per inch at 30 °C. These values are a little lower than the values reported for European XPS (nominally rated at R4.5/inch) by Ochs and Müller-Steinhagen (2005), but are significantly lower than reported for North American-made XPS (Schumacher, Grin and Ober, 2012). The reason for these low values was not determined.

The Rockwool insulated sheathing was labeled with a nominal R-value of R-4 (RSI .71) per inch. Using the described method, the calculated effective R-value decreased slightly as the exterior temperature increased from R-4.4 (RSI .78) at -15 °C to R-4.2 (RSI .74) at 3.5 °C to R-4.0 (RSI .71) at 30 °C. These values are very similar to the values reported by Roxul for their Top Rock product – which has a similar composition and density as the Roxul IS product tested.

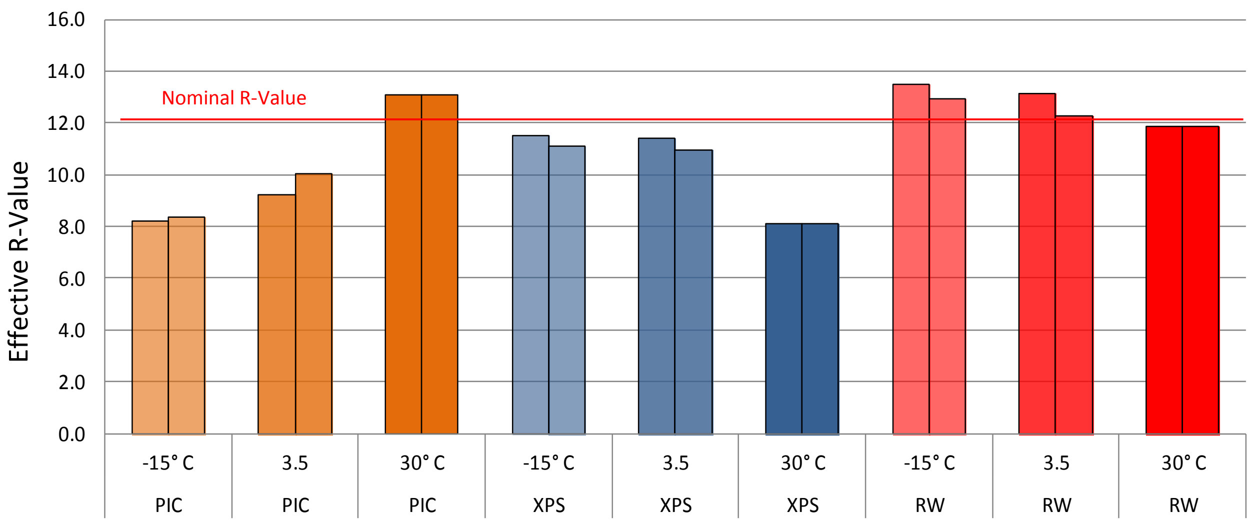

Figure 80- Effective installed R-values calculated from measured temperature data

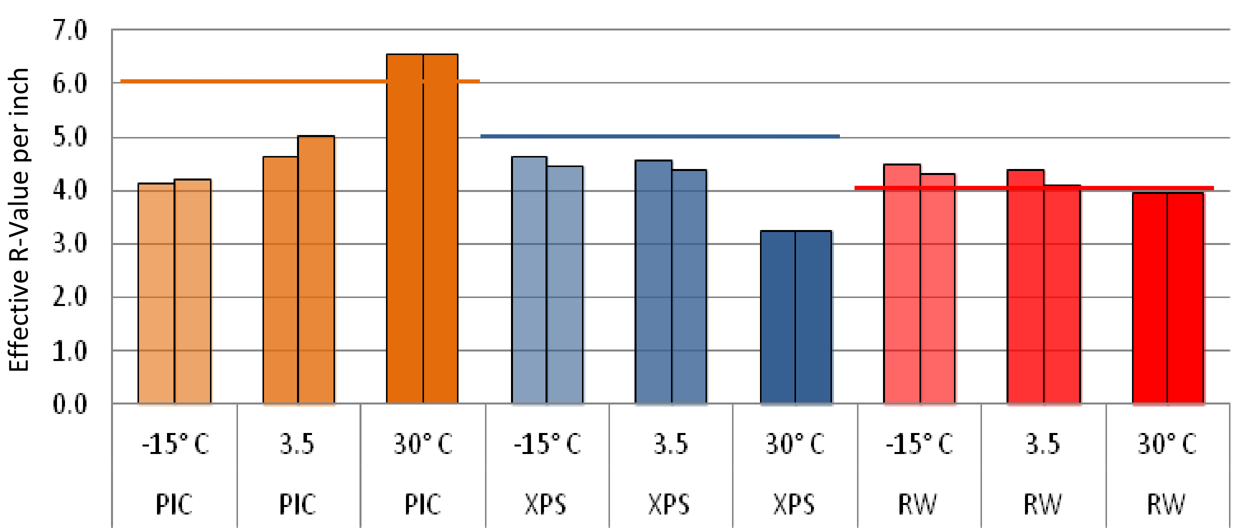

Figure 81 – Effective R-value per inch calculated from temperature data

The analysis performed above reveals some significant differences in the thermal performance of the three exterior insulation types tested. The PIC insulation performs above its rated R-value at high temperatures, but much lower than its rated value at moderate and low temperatures. The XPS insulation performs slightly above its rated R-value at low and moderate temperatures and much below its rated value at high temperatures, while the Rockwool insulation performs slightly better than its rated R-value at cold and moderate temperatures and equal to its rated R-value at hot temperatures.

These performance differences may have a significant impact on wall assembly design decisions. For example, an exterior layer of PIC insulation will be more effective in a hot climate than in a cold climate, where XPS or Rockwool would be more effective. Rockwool also performs more consistently across realistic temperature ranges, which may make it a good choice for mixed (heating and cooling) climates.

6.1.2 Air Leakage Warming Effect

As described in Section 3.2.3, Ojanen and Kumaran (1996) used computer modeling to study interstitial moisture accumulation due to air leakage condensation in a typical residential wall assembly. They reported that moisture accumulation increased with increased air flow until air flow exceeded 1 $l/s/m^2$. Above this level, moisture accumulation began to drop off due to the warming effects of the exfiltrating air on the sheathing directly adjacent to the air leakage location. Despite the fact that the air flow used in the experimental portion of this study was only ¼ of this rate, the same effect was observed, but only for the exterior insulated walls.

The change in moisture content due to air leakage for all test walls can be seen in Figure 82. The air flow rate used in the current experiment was only .24 $l/s/m^2$ and, as predicted by Ojanen and Kumaran's model, moisture content increased directly across from the air injection site for the two walls without exterior insulation (the Datum wall and the Double stud wall). The three exterior insulated walls however showed no change in moisture content directly across from the air injection site even though the surrounding sensor locations did show a small increase. This data shows that for the exterior insulated walls, even smaller air flows can raise the sheathing temperature above the dew point of the exfiltrating air and reduce sheathing condensation.

To quantify this warming effect, the theoretical sheathing temperature of the north side Datum and Rockwool walls were calculated on an hourly basis using a simple approach based on the percentage of thermal resistance interior and exterior to the sheathing. This approach is commonly referred to as a temperature profile analysis.

For the Datum wall with no exterior insulation: $T_{sheathing} = T_{exterior}$

For the Rockwool wall with 1/3 of its thermal resistance exterior to the sheathing:

$$T_{sheathing} = T_{interior} - ((T_{interior} - T_{exterior}) * 2/3)$$

This predicted value was then compared to the hourly measured temperature at the lower sheathing location. A plot of the measured and predicted sheathing temperatures for the Rockwool wall can be seen in Figure 82. During the air sealed condition, the modeled temperatures agreed closely with the measured data. The predicted sheathing temperature averaged 0.5 ° C and 0.1 ° C lower than the actual measured value for the Datum wall and the Rockwool walls respectively. During the air injection phase of testing however, the predicted sheathing temperature averaged 6.2 ° C and 6.8 ° C lower than the actual measured value for the Datum wall and the Rockwool wall respectively. This simple analysis shows the significant warming effect of the exfiltrating air on the sheathing. Since the exterior insulated walls started at a higher temperature, the relatively small amount of air leakage in this study provided enough heat energy to raise the sheathing temperature above the dew point of the interior air.

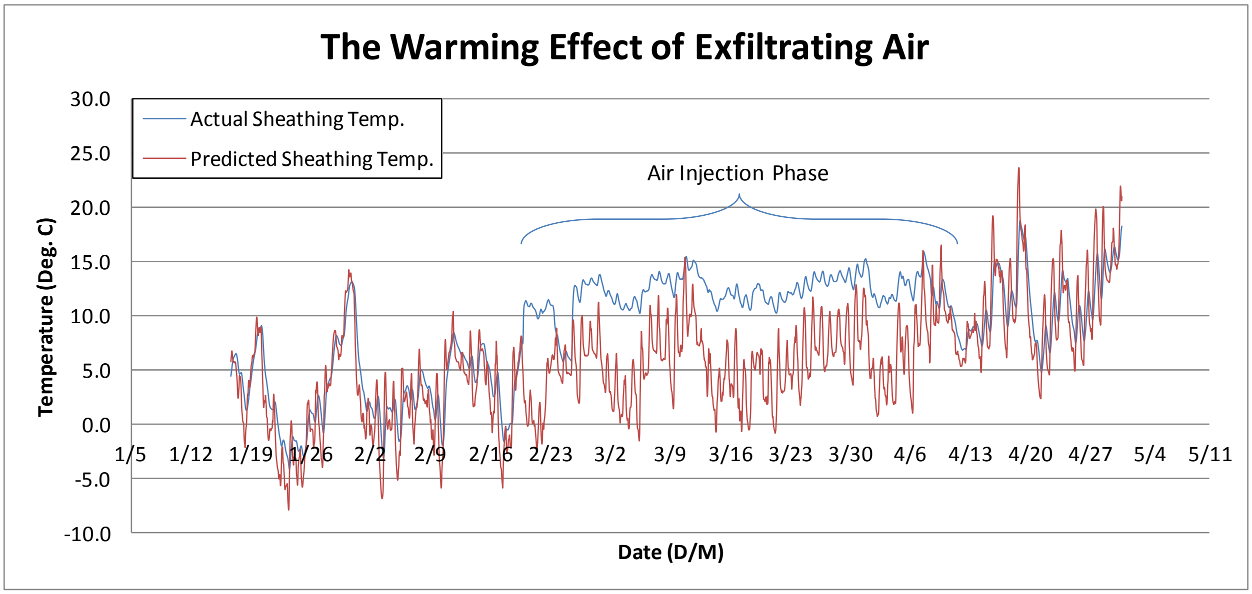

Figure 82 - The warming effect of exfiltrating air on the lower sheathing position on the Rockwool wall

The significance of this effect is that the simple temperature profile calculation above will significantly under-predict sheathing temperature where air leakage is occurring. This means that the exterior temperature conditions need to be lower than the theoretical value (as calculated above) for the sheathing to reach the dew point temperature. This can significantly reduce the actual the number of condensation hours resulting from a point source air leak compared to the prediction resulting from a simple dew point analysis.

6.2 Moisture Performance

6.2.1 Air Leakage Condensation

To demonstrate the warming effect of exfiltrating air on the prediction of condensation in both conventional and exterior insulated wall systems, a simple analysis was performed. Assuming interior air at 21 ° C and 30% RH, a psychrometric analysis shows a dew point of 2.8 ° C. If we first ignore the warming effects of the exfiltrating air, the simple temperature profile formulas above can be used to calculate the exterior temperature required to produce a sheathing temperature of 2.8 °. Inserting $T_{sheathing}$ = 2.8 ° C and $T_{interior}$ = 21 ° C, the exterior air temperature that will result in condensation is calculated to be 2.8 ° C for the Datum wall and – 6.3 ° C for the Rockwool wall.

Accounting for the warming effects of the exfiltrating air produces a much different answer. Adding 6.5 ° C (the average increase in temperature due to air leakage as discussed in Section 6.1.2) to the sheathing temperature changes the above equations to:

Datum Wall: $T_{exterior} = T_{sheathing} - 6.5$

Rockwool Wall: $T_{exterior} = 3/2\ (T_{sheathing} - 6.5) - ½\ (T_{exterior})$

Assuming that $T_{sheathing}$ = 2.8 ° C and $T_{interior}$ = 21 ° C, this results in a safe exterior air temperature of -3.7 ° C for the datum wall and – 16.0 ° C for the Rockwool wall. Because of the thermal resistance exterior to the sheathing in the Rockwool wall, the warming effect of the exfiltrating air had a much greater effect on the acceptable exterior temperature, decreasing it by 18.8 ° C.

Using the Rockwool wall as an example, and hourly temperature data for Toronto, Ontario, the importance of accounting for air leakage warming can be seen. If the warming effects of the exfiltrating air are ignored, the simple dew point analysis shows 230 hours of condensation per year. Accounting for the warming effects of the air, the number of condensation hours is reduced to 2 hours.

6.2.2 Air Leakage Condensation Performance Under Other Conditions

As discussed in Section 3.2, previous studies of air leakage condensation have identified exterior sheathing temperature and interior RH as two important factors related to the accumulation of air leakage condensation within a wall system. In the experimental portion of the current study, the exterior insulated wall systems were effective at reducing air leakage condensation under the conditions tested. To investigate the effectiveness of exterior insulation in controlling air leakage condensation under different interior RH and sheathing temperature conditions, a simple simulation study was performed. The goal of this simulation was to address the interaction of the interior/exterior insulation ratio, exterior temperature conditions, and interior RH.

The basis of the simulation was the dew point analysis, modified for the warming effects of exfilatrating air as described in Section 6.2.1 above. The simulations are based on hourly temperature data for four Canadian cities, representing the full range of temperature variation found in populated areas of the country:

1) Vancouver, BC (2130 HDD)
2) Toronto, ON (2970 HDD)
3) Edmonton, AB (5080 HDD)
4) Yellow Knife, NWT (7050 HDD)

The modified dew point analyses were performed on four theoretical R-35 walls with different interior/exterior insulation ratios:

1) No exterior insulation
2) $^{1}/_{3}$ of thermal resistance on the exterior
3) ½ of thermal resistance on the exterior
4) $^{2}/_{3}$ of thermal resistance on the exterior

The analyses were also performed under 3 different interior RH conditions:

1) 30%
2) 40%
3) 50%

The results of this simulation, expressed in condensation hours, can be seen in Figure 83 below. The different coloured bars represent the different Canadian cities. The blue horizontal line represents 10% of the total hours for coldest three months of the year (January, February and December). While there are many factors that contribute to the acceptable number of condensation hours, based on the results from the vapour pressure analysis and the moisture content measurements, 10% of winter hours seems to be a safe level to avoid moisture accumulation in these types of wall systems. For the purpose of this discussion, 10% of winter hours (220 hours) is used as the maximum acceptable level of condensation, although higher or lower values might prove to be more approporiate.

The grouping of bars to the left side of the chart represents a wall system with no exterior insulation. If an interior RH of 40% or lower is maintained, this wall system would result in acceptable levels of air leakage condensation in Vancouver but not in Toronto, Edmonton or Yellowknife. At an interior RH of 50%, this wall design poses a risk of air leakage condensation-related durability issues anywhere in Canada. As the climate gets colder, the interior winter RH tends to be lower. Attempting to maintain even 30%RH during the winter in Yellowknife, for example, is difficult, and will result in significant quantities of condensation even on triple-glazed windows and insulated door hardware. Conversely, 50%RH in Vancouver is quite a common level, although lower interior RH is possible with good ventilation.

The second grouping from the left represents an exterior insulated wall system with 1/3 of its thermal resistance exterior to the sheathing (similar to the exterior insulated walls in the experimental portion of this thesis). At any interior RH of 50% or less, this wall design results in acceptable condensation resistance in Vancouver and Toronto, but will pose a significant condensation risk in Edmonton and Yellow Knife.

The next grouping represents an exterior insulated wall design with 1/2 of its thermal resistance exterior to the sheathing. At 30% interior RH, this wall system will provide acceptable condensation resistance in Vancouver, Toronto and Edmonton, but still poses a significant condensation risk in Yellowknife. At 40% and 50% RH, this wall system will pose condensation risk in both Edmonton and Yellowknife.

The final grouping, on the far right, represents an exterior insulated wall system with 2/3 of its thermal resistance exterior to the sheathing. This wall system will perform well under all interior RH conditions tested at any location in Canada.

The analysis above demonstrates the need for condition-specific design, and gives design guidelines for various locations in Canada. As exterior temperature decreases and/or interior RH increases, more exterior insulation is required to limit air leakage condensation.

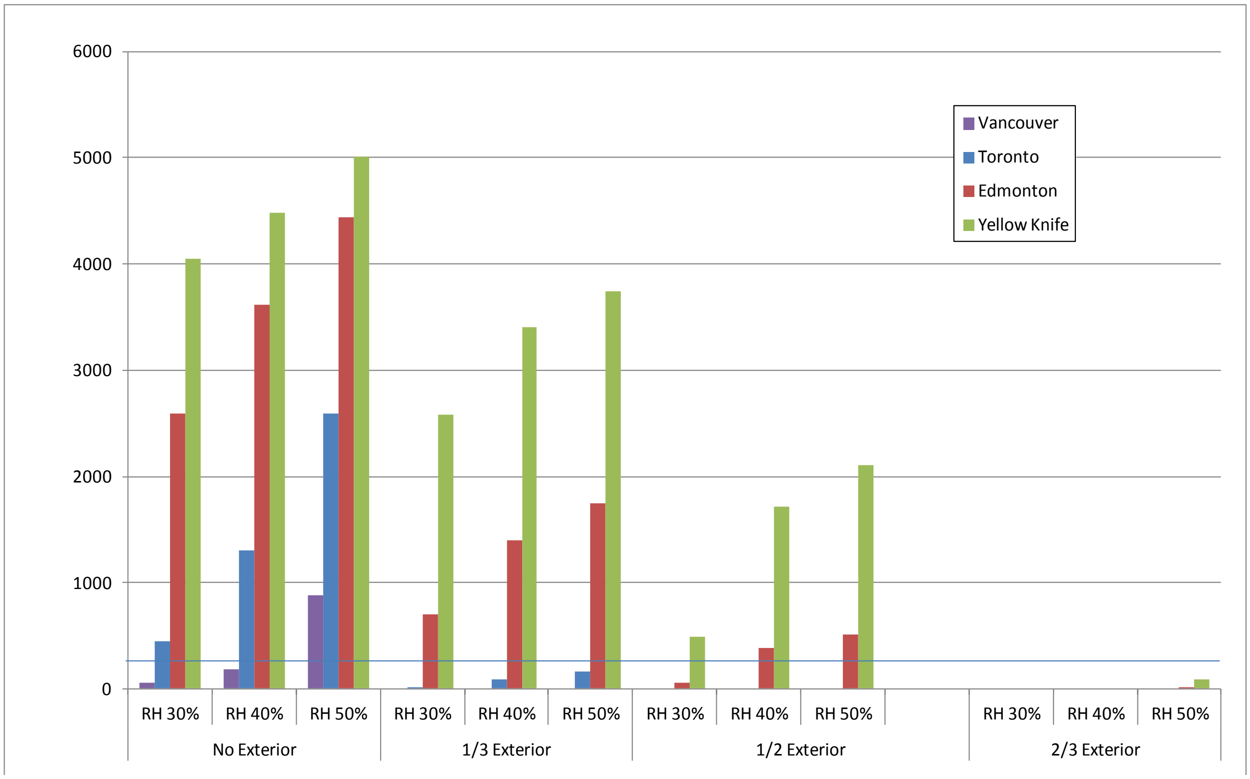

Figure 83- Results of modified dew point analysis under different conditions

6.2.3 Drying Potential

While the proponents of exterior insulation strategies have discussed and studied the reduced condensation potential of these types of wall systems, there is limited discussion of the potential reduction of drying capacity. Air leakage condensation is not the only source of moisture encountered by a wall system. The most important source of moisture in many areas of the country is precipitation. The penetration of water from the exterior is likely in all wall system designs, especially at penetrations such as windows and doors. For this reason, the ability of the wall system to dry is an important factor in long term durability.

The results of previous studies have shown that the vapour permeance of the materials exterior to the sheathing directly affect the drying capacity of the assembly. Janssens and Hens (2003) found that using a vapour permeable underlay and a ventilated air gap significantly increased the ability of the roof system to dry to the exterior. Simulations performed by Ojanen and Kumaran (1996) showed an inverse relationship between moisture accumulation and vapour permeance. Due to the asymptotic relationship, it would take a 25 X increase in permeance to get a 50% reduction in moisture accumulation

The experimental portion of the current study confirmed that wall assembles with high vapour permeance (V.P.) exterior to the sheathing accumulated less moisture and dry more quickly than assemblies with low V.P. materials exterior to the sheathing all things being equal. Compared to the Datum and Double stud walls (with Tyvek of a permeance of 3300 ng/(s•m^2•Pa) or 58 US perms exterior to the sheathing), the Rockwool wall (with 1700 ng/(s•m^2•Pa) or 30 US perms exterior to the sheathing), accumulated approximately 40 % less moisture and dried 78 % faster.

Calculations show that if sufficient insulation is provided exterior to the sheathing, the temperature can rise high enough that significant drying to the inside can occur, even during cool weather. In the extreme, placing all of the insulation outboard of the wood components of a wall enclosure will mean that almost all drying will occur to the inside, and this drying rate will be almost the same during all times of the year.

While a layer of low vapour permeance insulation exterior to the sheathing slows the rate of drying to the exterior, there are some situations in which this layer may improve moisture management. In assemblies that use moisture-storing cladding systems such as brick, stone or stucco, solar-driven vapour drives can be a powerful wetting mechanism (Straube et. al, 2009; Lepage and Lstiburek, 2012). Direct solar exposure can result in very high vapour pressures behind the cladding, which can drive moisture into the sheathing from the exterior.

Even in the current experiment with light-weight, ventilated cladding this effect can be observed during the wetting mat testing phase. As shown in Figure 76 and Figure 77**Error! Reference source not found.**, for the Datum and Rockwool walls, the increase in moisture content due to the wetting mat was two times greater on the south elevation (where solar exposure was high), compared to the north elevation. This discrepancy between the elevations was not observed in the XPS or PIC walls. While the low V.P. walls still out performed the high V.P. walls on the south elevation, this data does demonstrate the potential vulnerability of low V.P. wall systems behind moisture storage cladding.

7 Conclusions

Nearly 1/3 of all energy consumed in Canada is used to operate the buildings in which we live and work. Due to the increased financial and environmental cost of harvesting, delivering and consuming this energy, promoting the development of low-energy buildings has become the focus of both governmentally mandated building codes and voluntary certification programs. Since heating and cooling energy accounts for more than half of the energy consumed by buildings, it represents the largest opportunity for improvement. The development of durable, highly-insulated wall systems has been identified as one of the top priorities in the pursuit of low energy buildings.

One solution to durable highly-insulated wall systems is the addition of insulation to the exterior of the structural framing. This can have many benefits, including:

1) Allowing for the application air and vapour control layers to the exterior of the structure where they can be applied continuously, with few obstructions.
2) Protecting the air, vapour and rain control layers and the structural framing from temperature extremes and reducing temperature cycling, thereby increasing the durability of these layers.
3) Allowing for a continuous application of insulation, reducing thermal bridging from structural elements and increasing the effective thermal resistance of the assembly significantly.
4) Increasing the temperature of the sheathing during cold weather, thereby reducing the condensation potential of the wall assembly and increasing durability.

The experimental portion of this thesis showed that placing 1/3 of the thermal resistance exterior to the wall sheathing was very effective at reducing air leakage condensation in the Waterloo, ON climate. Modeling, based on this data showed that no exterior insulation is required in Vancouver, BC when low interior humidities are maintained, a higher proportion of exterior insulation would be required in colder climates. For example, a climate such as Edmonton, AB, would require ½ of the total insulation exterior to the sheathing, while Yellowknife, NWT would require 2/3 to minimize the risk of air leakage condensation.

It was found that the addition of insulation to the exterior of the structure may also have some potential disadvantages including:

1) Increased cost due to more expensive insulation materials and increased labour
2) Increased detailing at window and door openings may be required to prevent water intrusion
3) Decreased drying potential to the exterior if the insulation materials has low vapor permeance

The field measurements showed that low permeability exterior insulations, such as extruded polystyrene and foil-faced polyisocyanurate significantly reduced the summer drying capacity of the wall system and thus could negatively affect the moisture-related durability. The application of high permeability exterior insulation, such as rockwool had little effect on the drying capacity.

To take full advantage of the benefits of exterior insulation and to minimize the potential disadvantages, a high-R wall system must be designed to perform under the conditions to which it will be exposed. Based on the results of the literature review and the experimental portion of this thesis, some broad guidelines on appropriate exterior/interior insulation ratios for different areas of Canada were developed. The first step is to understand the stresses that the wall system must resist. The most critical variables to assess include:

1) Exterior Climatic Conditions

Clearly, a wall system will not provide the same performance in Vancouver as it will in Yellowknife. Exterior temperature conditions have a direct effect on sheathing temperature and therefore condensation potential. As the climate becomes colder, a higher ratio of exterior insulation to interstitial insulation is required to keep sheathing above the dew point for a larger percentage of the year and minimize air-leakage condensation potential.

2) Interior Vapour Pressure

The interior temperature and relative humidity (RH) conditions determine the interior vapour pressure. As the interior vapour pressure increases, so does the dew point of the exfiltrating air. Because of this, the sheathing must be kept at a higher temperature to minimize condensation. This can be accomplished by increasing the ratio of exterior insulation to interstitial insulation. Due to comfort limitations, winter-time interior temperature variation is usually quite small (18 to 22 ° C). Winter-time interior relative humidity however, can vary significantly from 20% to 50% or even higher in special-purpose buildings such as swimming pools. Interior RH is typically a function of ventilation rate, occupation density and moisture producing activities within the building.

3) Air Leakage Rate

The air leakage rate of any building is a function of the air-tightness of the construction and the magnitude of the forces driving air leakage. A high level of air-tightness should be a design goal in any building enclosure system and is especially important in low energy buildings. The review of the literature indicates that the use of exterior insulated wall systems help to facilitate the application of a continuous air barrier system by allowing the primary air control layer to be exterior to the structural framing. When developing any wall system, the designer should be aware of any conditions which may cause excessive exfiltration forces such as discontinuities in the air barrier, large stack effect pressures, mechanical pressurization or extremely windy exterior conditions. If one or more of these conditions is expected, higher than normal air exfiltration rates should be expected. This could result in more moisture available for deposition via condensation when the sheathing is below the dew point temperature. The experimental portion of this thesis showed that for exterior insulated wall systems, even small amounts of exfiltration can cause significant warming effects on the sheathing, which can significantly reduce the number of condensation hours. This warming effect should be accounted for when performing dew point analysis to accurately compare the air-leakage condensation potential of exterior insulated wall systems and other types of high-R walls.

4) Exterior wetting potential

Driving rain is the most significant source of moisture affecting the durability of wall systems. The annual exposure of a wall system to driving rain is a function of many factors including:

1) Total annual rain
2) Wind speed and direction during rain events
3) Wall orientation
4) Building height
5) Roof overhangs
6) Protection from surrounding buildings, trees and topographical features

A summary of research and a simplified method for predicting driving rain exposure is described in "Simplified Prediction of Driving Rain on Buildings: ASHRAE 160P and WUFI 4.0" (Straube, 2010).

The other factor related to exterior wetting that must be considered during the design of an exterior insulated high-R wall system is the risk of driving rain breaching the rain control layer and entering the assembly. Driving rain infiltration is unlikely in the plane surface of a wall, and is more likely at joints, junctions and penetrations such as window and door openings. The risk of water penetration can therefore be roughly predicted by the complexity the building geometry.

The driving rain exposure and risk of penetration should always be considered in the design of an exterior insulated high-R wall system. A building with higher exposure and/or high risk of penetration should also have a higher drying potential. This can be accomplished by avoiding exterior insulation materials with low vapour permeability and use vapour-open products such as rockwool.

Another form of exterior wetting is through solar vapour drive. If moisture-storage cladding such as brick, stone or stucco are used, this process can contribute significant amounts of moisture to the wall system and will need to be controlled using less vapour permeable layers between the cladding and the sheathing.

Recommendations for Future Research

Further research is recommended to expand the understanding of the hygrothermal performance of exterior insulated wall systems. Some areas that would benefit from further study include:

1) Modeling should be extended for a wide-range of exterior climates, interior climates, and ratios of interior to exterior insulation values. This could provide a more widely applicable series of recommendations for home builders.

2) The performance of exterior insulated wall systems in more extreme cold and hot climates as well as high interior RH buildings. While modeling can be an effective tool for expanding the

results of this study to different climate zones, further field testing in more extreme climates should be done to increase confidence in the modeling results.

3) The performance of different exterior insulation types when placed behind moisture-storing claddings and exposed to solar-driven inward vapour drives. The presence of a moisture-storing cladding system (such as brick and stucco) is expected to change the wetting potential and drying capacity of the wall systems tested.

4) The performance of other exterior insulations. Other insulating materials such as expanded polystyrene, cork, and foamglas have different vapour permeance characteristics and are expected to perform differently than the materials in this study.

5) The effects of lower air leakage rates on the accumulation of air leakage condensation. The air leakage rate used was near the high end of the range expected for modern residential buildings and the effects of lower air leakage rates are not well understood.

References

Agilent Technologies, Inc. (2012). *Practical Temperature Measurements* – Application Note 290

Aitken, D. (2011, December 19). Frank Lloyd Wright and the Solar Hemicycle (Jacobs ii). *Green Architecture Notes,* Retrieved from http://greenarchitecturenotes.com/2011/12/frank-lloyd-wright-and-the-solar-hemicycle-jacobs-ii/

Anderson , R., and Roberts, D. (2008). *Maximizing residential energy savings: Net zero energy home technology pathways.* National Renewable Energy Laboratory (NREL/TP-550-44547)

Andrews, S. (2001). Rotting sip roofs in Juneau. *SIPs Monitor*, *Special Edition*, Retrieved from http://www.greenbuildingtalk.com/buildcentral/sip/2001-10_juneau.pdf

Arena, L., Owens, P. and Mantha, P. (2013) Measured Performance of an R-40 Double-Stud Wall in Climate Zone 5A. *Thermal Performance of the Exterior Envelopes of Whole Buildings XII International Conference*. Clearwater, FL

American Society of Heating, Refrigerating and Air-Conditioning Engineers. (2009). *2009 ASHRAE handbook: Fundamentals*. Atlanta, GA

Baker, P., and Makepeace, C. (2000). Adapting PERSIST for the Prevention of Water Accumulation in Residential Wood-frame Construction. *Buildings VII - Wall Designs and Building Science*. Clearwater, Fl.

Ball, W., (1961). *Thermal bridges in buildings* (CBD-16), National Research Council of Canada

Barra, O., Artese, G., Franceschi, L., Joels, K., & Nicoletti, A. (1987). The Barra Thermosyphon Air System. *International Conference of Building Energy Management*. Lausanne, Switzerland.

Besant, R., Dumont, R., & Schoneau, G. (1979). The Saskatchewan Conservation House: Some Preliminary Performance Results. *Energy and Buildings*, (2), 163-174.

Brown, W., and Wilson, A. (1963). *Thermal bridges in buildings* (CBD-44) National Research Council of Canada

Caffey, G. (1979) Residential Air Infiltration, *ASHRAE Trans*, V85(9) pp 41-57

CMHC (2007). *Canadian Housing Observer- 2007: New Housing for a Changing World*. Retrieved from: http://www.cmhc-schl.gc.ca/en/corp/about/cahoob/upload/chapter2_new_housing_2007_en.pdf

Denzer, A. (2013). *Solar House History*. New York, NY: Rizzoli International Publications.

Derome, D. (2005) Moisture Accumulation in Cellulose Insulation Caused by Air Leakage in Flat Wood Frame Roofs. *Journal of Thermal Envelope and Building Science,* Vol. 28, No. 3

Desmarais, G, Derome, D. and Fazio, P. (2000) Mapping of Air Leakage in Exterior Wall Assemblies. *Journal of Thermal Envelope and Building Science*. *Vol. 24*

Dumont, R.S., Orr , H.W., Hedlin, C.P. and Makuhon, J.T. (1980) Measured Energy Consumption of *a* Group of Low Energy Houses. *Proceedings, 1980 Annual Meeting, Solar Energy Society of Canada.*

Dumont, R., Orr, H., & Hedlin, C. (1983). Low-Energy Houses: Measured Energy Consumption Figures. *ASHRAE Transactions*, *89*(1A), 264-274.

Fennell, H., & Haehnel, J. (2005). Setting Air Tightness Standards. *ASHRAE Journal*, *47*(9),

Fox, M (2013). *Hygrothermal Performance of Highly Insulated Woof Framed Walls with Air Leakage: Field Measurements and Simulations*. Unpublished Masters Thesis, Ryerson, University, Toronto, Canada

Graham, M. (2010). R-Value concerns. *Professional Roofing*, May 2010.

Building Science Corporation, (2013). *Temperature dependence of R-values in polyisocyanurate roof insulation* (Info-502). Retrieved from website: http://www.buildingscience.com/documents/information-sheets/info-502-temperature-dependent-r-value/?searchterm=temperature dependence

Hall, N., (N.D.) *Exterior Insulation and Finish Systems (and Other Problems with Building Envelopes).* Retrieved from website: http://www.largelossdrying.com/pdf/Exterior%20Insulation%20and%20Finish%20Systems%20(EIFS).pdf

Holladay, M. (2010). The History of Superinsulated Houses in North America. *British Columbia Building Envelope Council*, Vancouver, BC

Hörster, H.; Bergmann, G.; Bruno, R.; Hermann, H.; Kersten, R. Klinkenberg, K.& Steinmüller, B. (1980). Neue Wege zum energiesparenden Wohnhaus. *Hamburg: Philips Fachbuchverlag*.

Huange, J., Hanford, J., Yang, F., (1999). *Residential Heating and Cooling Loads Component Analysis.* Lawrence Berkeley National Laboratory. Retrieved from website: http://simulationresearch.lbl.gov/dirpubs/44636.pdf

Hukseflux. (n.d.). *Hfp01 heat flux plate/ heat flux sensor*. Retrieved from http://www.hukseflux.com/sites/default/files/product_brochure/HFP01 v1003.pdf

Hutcheon, N., (1964). *Principles applied to an insulated masonry wall* (CBD-50) National Research Council of Canada

Hygrometrix Inc., (2004). *A comparison of relative humidity sensing technologies* (Applications Note 2004-2). Retrieved from website: http://lawr.ucdavis.edu/faculty/gpast/hyd151/hyd151readings/hyd151_read13.pdf

Janssens, A. and Hens, H. (2003) Interstitial Condensation Due to Air Leakage: A Sensitivity Analysis. *Journal of Thermal Envelope and Building Science*., Vol. 27, No. 1—July 2003

Jokisalo, J., Kurnitski, J. Korpi, M., Kalamees, T., Vinha, J. (2009). Building Leakage, Infiltration, and Energy Performance Analyses for Finnish Detached Houses. *Building and Environment* 44 (2009) 377–387

Kachadorian (2006). *The Passive Solar House*. Chelsea Green Publishing

Kalamees, T., and Kurnitski, J. (2010). Moisture Convection Performance of External Walls and Roofs. *Journal of Building Physics*, Vol. 33, No. 3—January 2010

Keclik, G.B. and Maino, A.L. (2008). Lessons Learned for Exterior Insulation Finish Systems. AEI 2008: Building Integration Solutions. Denver, CO

Lea, K. (2010). Mesa Verde Cliff Dwellings. *Green Passive Solar Magazine*, Retrieved from http://greenpassivesolar.com/2010/04/mesa-verde-cliff-dwellings/

Latta and Garden, K. (1962). *Temperature gradients through building envelopes* (CBD-36) National Research Council of Canada

Lepage, R., & Lstiburek, J., (2012). *Moisture Durability with Vapor Permeable Insulating Sheathing-Building America Report 1313.* Retrieved from website: http://www.buildingscience.com/documents/bareports/ba-1313-moisture-durability-with-vapor-permeable-insulating-sheathing/

Lstiburek, J. (2008). *The Perfect Wall* (BSI-001). Building Science Corporation. Retrieved from website: http://www.buildingscience.com/documents/insights/bsi-001-the-perfect-wall/?searchterm=perfect wall

Lstiburek, J. (1999). *Air Leakage and Building Envelopes* (RR-9905). Building Science Corporation. Retrieved from website: http://www.buildingscience.com/documents/reports/rr-9905-air-pressure-and-building-envelopes

Lstiburek, J., (2006).*Increasing the Durability of Building Constructions* (BSD-144). Building Science Corporation. Retrieved from website: http://www.buildingscience.com/documents/digests/bsd-144-increasing-the-durability-of-building-constructions/

Makepeace, C., and Dennis, B. (1998). PERSIST - Pressure Equalized Rain Screen Insulated Structure Technique- Design Approach. *Thermal Envelopes VII- Performance of Air Barrier Systems.* Clearwater Beach, FL.

Marshall, B., & Argue, R. (1981). *The Super-Insulated Retrofit Book*. Bookpeople, Austin, TX.

Maxwell, R. (2005). *The REMOTE Wall System*. Alaska Energy Associates.

Mazria, E. (1979). *The Passive Solar Energy Book*. Emmaus, PA: Rodale Press.

McCulley, M. (2008). Pioneering Superinsulation and the Lo-Cal House: Design, Construction, Evaluation and Conclusions. *3rd Annual North American Passive House Conference*, Duluth, MN

MIT solar decathlon team - history. (n.d.). Retrieved from http://web.mit.edu/solardecathlon/solar1.htmlNatural Resources Canada. (n.d.). *Energy star homes*. Retrieved from https://www.nrcan.gc.ca/energy/efficiency/housing/new-homes/energy-star/5057

Nevrala, D. and Etherige, D., (1977). Natural Ventilation in Well-Insulated Houses. *UNESCO International Seminar, Heat Transfer in Buildings.* Dubrovnik, Croatia

NRCan (2011). *Energy Efficiency Trends in Canada 1990-2009*. Retrieved from http://oee.nrcan.gc.ca/publications/statistics/trends11/pdf/trends.pdf

NRCan (2012). *2012 R-2000 Standard*. Retrieved from website: http://www.nrcan.gc.ca/sites/www.nrcan.gc.ca/files/oee/files/pdf/2012 R2000 Standard EN.pdf

NRCan (2014). *Energy Star Homes*. Retrieved from https://www.nrcan.gc.ca/energy/efficiency/housing/new-homes/energy-star/5057

Nisson, N., & Dutt, G. (1985). *The Super Insulated Home Book*. John Wiley and Sons. New York, NY.

NIST (2013). A New Gravimetric Hygrometer for Verification of NIST Humidity Standards. (2013, 05 20). Retrieved from http://www.nist.gov/pml/div685/grp01/grav-hyg.cfm

Ochs,F. and Müller-Steinhagen, H. (2005). Temperature and Moisture Dependence of the Thermal Conductivity of Insulation Materials. *NATO Advanced Study Institute on Thermal Energy Storage for Sustainable Energy Consumption (TESSEC*). Izmir, Cesme.

Ojanen, T. and Kumuran, K. (1996). Effect of Exfiltration on the Hygrothermal Behaviour of a Residential Wall Assembly. *Journal of Thermal Insulation and Building Envelope*. Volume 19- January 1996.

Omega Engineering. (n.d.). *Introduction to thermocouples*. Retrieved from http://www.omega.ca/prodinfo/thermocouples.html

Onysko, D., Schumacher, C., & Garrahan, P. (2008). Field Measurements of Moisture in Building Materials and Assemblies: Pitfalls and Error Assessment. *Building Enclosure Science and Technology Conference*. Minneapolis, MN.

Orr, H. (2013). The Saskatchewan Conservation House in Retrospect. *Eco Home*. Retrieved from http://www.ecohome.net/news/latest/principal-designer-house-inspired-global-passivhaus-movement-reflects-project-started

Passivhaus Institute. (n.d.). *About Passive House - What is a Passive House?*. Retrieved from http://passiv.de/en/02_informations/01_whatisapassivehouse/01_whatisapassivehouse.htm

Passive House Institute (2013). Pioneer award for 1970s Zero-Energy House in Denmark. Retrieved from http://passiv.de/en/

Passive House Institute. (2014). *Passive house requirements*. Retrieved from http://www.passiv.de/en/02_informations/02_passive-house-requirements/02_passive-house-requirements.htm

Perlin, J. (2013). *Let it shine: The 6000 Year Story of Solar Energy*. New World Library. Novato, CA

Ralko, J. (n.d.). *Energy Efficient Houses*. Retrieved from http://esask.uregina.ca/entry/energy-efficient_houses.html

Rantala, J. and Leivo, V. (2009). Heat, Air and Moisture Control in Slab-on-Ground Structures. Journal of Building Physics 32.4 (2009): 335-353

RECS. U.S. Energy Information Administration, Consumption and Efficiency. (2012). *RECS Data Show Decreased Energy Consumption per Household*. Retrieved from website: http://www.eia.gov/consumption/residential/reports/2009/consumption-down.cfm

Ritschard, R.L., J.W. Hanford and A.O. Sezgen (1992). *Single-Family Heating and Cooling Requirements: Assumptions, Methods, and Summary Results*. Topical Report No. GRI-91/0236. Gas Research Institute, Chicago, IL.

Roxul (n.d.). *Roofing Insulation for Commercial Construction*. Retrieved from website: http://www.roxul.com/files/RX-NA_EN/pdf/Sell Sheets/BEDR Roofs Sell Sheet.pdf

Ruby, D. (1981). Super-Insulated Houses: Air-Tight Double Walls Mean Near-Zero Heat Loads. November, 1981. *Popular Science*

Sherman M.H. and Dickerhoff D. (1998). Air-Tightness of U.S. Dwellings. *ASHRAE Transactions*, Vol. 104 (2), 1998, pp. 1359-1367

Schneiders, J. (2003). CEPHEUS – Measurement Results from More than 100 Dwelling Units in Passive Houses". *Eceee 2003 Summer Study – Time to Turn Down Energy Demand*.

Schumacher, C, Grin. A. Ober, D. (2012). Thermal Metric Project- A Year of Progress. *16th Annual Westford Symposium*. Westford, MA.

Shurcliff, W. (1978). *Solar Heated Buildings of North America: 120 Outstanding Examples*. Brick House Publishing Company. Baltimore, MD.

Shurcliff, W. (1980). *Thermal shutters and shades: Over 100 schemes for reducing heat-loss through windows*. Brick House Publishing Company. Baltimore, MD.

Shurcliff, W. (1981). *Super insulated houses and double envelope houses: A survey of principles and practice*. Brick House Publishing Company. Baltimore, MD.

Steinmuller, B. (2007). Reducing Energy by a Factor of Ten: Sustainable Housing Approaches in Europe. *21st North American ACI Home Performance Conference*. Cleveland, OH. Retrieved from http://www.bsmc.info/ACI2007KeyNoteBSMC-Text-SlideSummary.pdf

Straube, J.F., Smegal, J., Schumacher, C.J., Jablonka, M. (2009) Adhered Veneers and Inward Vapor Drives: Significance, Problems, and Solutions. *Proc. of Can. Bldg. Sci. & Tech. Conference*, Montreal, May 6-8, 2009, pp. 303-312.

Straube, J., and Burnett, E. 1995. Moisture Movement in Building Enclosure Wall Systems. *Proc. of Thermal Performance of the Exterior Envelopes of Buildings VI*. Atlanta, GA.

Straube, J., (2006). *The Building Enclosure* (BSD-018). Building Science Corporation Retrieved from website: http://www.buildingscience.com/documents/digests/bsd-018-the-building-enclosure_revised

Straube, J., Smegal, J. (2009) B*uilding America Special Research Project- High-R Walls Case Study Analysis* (BA-0903). Retrieved from website: http://www.buildingscience.com/documents/bareports/ba-0903-building-america-special-research-project-high-r-walls/view?searchterm=smegal

Straube, J., (2006). *Thermal Control in Buildings* (BSD-011). Building Science Corporation Retrieved from website: http://www.buildingscience.com/documents/digests/bsd-011-thermal-control-in-buildings/

Tenwold, A., Carll, C., Malinauskas, V. (2012). Air Pressures in Wood Framed Walls. *Thermal Envelopes VII. Clearwater, FL.*

U.S. Department of Energy, Energy Efficiency and Renewable Energy. (n.d.). *History of the Weatherization Assistance Program*. Retrieved from website: http://www1.eere.energy.gov/wip/wap_history.html

Ueno, K and Lstiburek, J (2015). Field Monitoring of Cold Climate Double Stud Walls with Cellulose and Low-Density Foam Insulation (DRAFT). *Fourth Building Enclosure Science and Technology Conference* (BEST 4)/. Kansas City, MO.

Walker, I. and Less, B. (2013). An Assessment of Envelope Measures in Mild-Climate Deep Energy Retrofits. *Thermal Performance of the Exterior Envelopes of Whole Buildings XII Conference*. Clearwater FL.

Wilson, A. (1961). *Air Leakage in Buildings* (CBD-23). National Research Council of Canada

Zonkel, P. (1998, December 5th). Cold and Dreary Chicago was an Early Sun City. *Chicago Tribune*. Retrieved from http://articles.chicagotribune.com/1998-12-05/news/9812050146_1_solar-park-solar-architecture-solar-energy

Appendix A: Measuring Heat, Moisture and Air Movement in Assemblies

Measuring Temperature

Thermocouple- A thermocouple is created by joining two wires made of dissimilar metals at both ends to create a circuit. A measurable current naturally flows between the materials in the circuit when there is a temperature difference between the two junctions. The net circuit voltage is a function of the junction temperature and the composition of the two metals. This phenomenon is known as the 'Seebeck Effect'.

The thermocouple is a simple and robust device that works over a large temperature range. They are also self-powered and require no external excitation. The main drawback to using thermocouples in building science applications is low sensitivity. The error for a typical thermocouple is between 1 and 2 ° C.

Thermistor- A thermistor is a special type of resistor whose resistance changes significantly with changes in temperature. They are generally composed of semi-conductor materials and have a negative temperature coefficient (ie. resistance increases with decreasing temperature) ("NTC Thermistors". Micro-chip Technologies. 2010). Compared to a thermo couple or a resistance temperature detector (RTD), the thermistor has a relatively small operational range (-90 to 130 ° C), but is also significantly more sensitive with changes of several percent per degree C. They can be made very small, making them unobtrusive and giving them a small thermal mass for a fast response time. These properties make the thermistor ideal for measuring temperature in most building science applications.

The price for this sensitivity however, is poor linearity. The resistance of a thermistor is extremely non-linear with changing temperature and is highly dependent on process parameters. An individual thermistor curve can be approximated using the Steinhart-Hart Equation:

$$1/T = A + B (\ln R) + C (\ln R)^3$$

Where: T = Temperature (in K)
R = resistance (on ohms)
A,B,C – curve fitting constants

A, B and C are found by selecting 3 points on the published data curve and solving the three simultaneous equations.

By applying a known voltage to the thermistor, the resistance can be measured and temperature calculated using the formula above. The resistance of a typical thermistor at 25 ° C is 5000 ohms. The typical resistance of the wiring to the thermistor is 10 ohms resulting in an error of only .05 ° C. (Agilent Technologies, Inc. 2012)

Measuring Heat Flow – The Heat Flux Transducer

A heat flux transducer is designed to measure the heat energy flowing though the object in which it is attached or incorporated. The transducer is made up of a series of thermocouples (known as a thermopile). The voltage output of a thermopile is not related to absolute temperature, but to the temperature difference across the device (Huxiflux).

Measuring Moisture

Relative Humidity Measures

The gold standard for measuring relative humidity is the gravimetric hygrometer. This device works by separating the water from the gas in a sample of air. The mass of the gas and water can then be measured separately to accurately determine moisture content. Other humidity quantities such as vapour pressure and relative humidity can then be calculated (NIST, 2013). Although extremely accurate, the gravimetric hygrometer is not practical for use as a research tool, but is useful for calibrating other instruments.

Hygrometers based on the physical characteristics of a hygroscopic material such as paper or a strand of hair. While cheap and readily available, these devices are large, inaccurate and more appropriate for amateur meteorology than research.

The best combination of accuracy, size and price can be found in electronic humidity sensors. The most common types of electronic humidity sensors are capacitance-based systems. These sensors consist of a hygroscopic dielectric material placed between a pair of electrodes, to form a small capacitor. The dielectric material used in most capacitive sensors is a polymer or plastic material. In the absence of moisture, the dielectric constant of the hygroscopic dielectric material and the sensor geometry determine the value of capacitance. At normal room temperature, the dielectric constant of water vapor has a value of about 80, a value much larger than the constant of the sensor dielectric material. Therefore, absorption of water vapor by the sensor results in an increase in sensor capacitance. The amount of moisture present in the hygroscopic dielectric material depends on both the ambient temperature and the ambient water vapor pressure. Since relative humidity is a function of both the ambient temperature and water vapor pressure, there is a relationship between relative humidity, the amount of moisture present in the sensor, and sensor capacitance. This relationship governs the operation of a capacitive humidity sensor (Hygrometrix Inc., 2004)

Measuring Moisture Content in Wood

Gravimetric Measurement

The gold standard for measuring moisture content in wood is the oven dry method. Wood samples are weighed before and after an oven drying procedure whereby the sample is placed in a ventilated oven at a standard temperature and weighed repeatedly at a specific time interval. When the sample is no longer losing mass, it is considered completely dry (ie. 0% moisture content). Its original moisture content is then expressed as a ratio of the difference between the original and the dry mass and the dry mass. This is the percent moisture content of the sample. This method is considered the most accurate method available and is used to calibrate all other methods.

There are two major limitations of this method that limit it to laboratory work. The first is that moisture content can not be measured in situ. The second is that it is quite time consuming.

Resistance Measurement

The search for a quick method to measure moisture content, that can be used in situ, lead to the study of the electrical properties of wood (Stamm, A. J., 1927). It was discovered the electrical resistance of wood could be correlated to its moisture content. This lead to the development of special ohm meters that were tuned to accurately measure the range of direct current resistances found in wood.

The electrical resistance of a material is the property that impedes the flow of electrical current through the material. This requires that an electric potential difference (voltage) exists between the two points, to cause the current to flow. The magnitude of the resistance, the voltage and the current are related by a fundamental equation known as Ohm's Law. This law states that the voltage across an ideal conductor is proportional to the current through it, and is expressed as:

$$V = I R$$

Where: V = electric potential in volts
I = electric current in amps
R = electric resistance in Ohms

The basis of resistance-based moisture measurement is that an electric circuit is created with the wood fibers completing the circuit. Two metal pins are driven into the wood and a power source of known voltage is used to apply an electric potential between the pins. A current meter is used to measure the current flowing through the circuit. Since the resistance of the other elements of the circuit is trivial, the total resistance of the circuit can be attributed to the wood fibers. With a known voltage and a measured current, Ohms law can be used to determine the resistance of the wood fibers.

The Effect of Moisture Content

Between the fiber saturation point (approx. 30% moisture content) and 0% moisture content the resistance of the wood fibers increases by a factor of over 10 million. Within this range, a rough linear inverse relationship exists between the logarithm of the resistance and the logarithm of the moisture content. Based on early studies, the baseline relationship between resistance and moisture content was determined using Douglas fir at a temperature of 73 deg. F. Although the relationship between resistance and moisture content is by far the most powerful, other factors also affect wood fiber resistance and must be used as correction factors to obtain accurate estimates of moisture content.

The Effect of Species.

The electric resistance of wood varies a small, but measureable amount between different wood species. It is believed that these differences are related to electrolyte concentrations and the physical structure and available surface area within the wood fibers. These relationships have been studied quite extensively and tables relating measurements of various species to doulas fir are widely available. Some modern handheld moisture meters have built-in conversion factors for common wood species.

The Effect of Temperature

The effect of temperature on the resistance of wood is also a small, but important factor for accurate moisture content measurements. At moisture levels above 10 percent, the resistance of the wood fibers is reduced by about a factor of 2, for every 10 ° increase in temperature. Temperature correction factor tables are also widely available.

Other Important Effects

Some degree of moisture gradation will exist in all wood members. For lumber that has been allowed to dry under relatively constant conditions, the approximate average moisture content can be measured at a depth of ¼ to 1/5 of its total thickness. Moisture gradation will be especially pronounced in unseasoned wood or in lumber that is part of an assembly that separates interior and exterior conditions. This moisture gradient will be changing constantly and will be most pronounced during extreme hot and cold exterior conditions. When measuring moisture content in lumber with a pronounced moisture gradient, insulated pins must be used and measurements made a various depths to understand the moisture profile. Whenever uninsulated pins are used, the moisture content being measured will be the wettest layer in contact with the pins, due to the lower resistance of the fibers in that layer.

The resistance of wood parallel to the grain is half of that perpendicular to the grain. When using resistance-based moisture meters, it is important that the probes are inserted parallel to the wood grain for accurate measurements.

Wood that has been impregnated with inorganic salts for fire or rot resistance, or has seen prolonged exposure to sea water, will have lower resistance than untreated wood. The effect of these salts will become greater as moisture content increases.

Oriented Strand Board (OSB)

OSB is an engineered wood panel product that is manufactured by laying parallel and cross mats of wood strands mixed with wax and adhesive. The panels are formed under high heat and pressure, creating a product with a higher density than the wood it was made from. OSB is commonly used as a sheathing material in modern buildings. Because of location on the exterior of the structure, it is vulnerable to wetting via leakage from the exterior and in cold climes, air leakage condensation from the interior. Because it is manufactured of small strands of wood, the amount of moisture it can safely store is less than solid lumber. For these reasons, the long term, in situ moisture content of OSB is a critical factor in building durability and its measurement has become an important analysis technique.

Due to the manufacturing process, the moisture content of OSB is typically 3-4% lower than for solid lumber of the same species, under the same conditions. Correction factors have been developed for OSB based on limited testing by Forintek.

Continuous Moisture Monitoring

The use of hand-held meters is useful and common practice for moisture measurement of wood that is easily accessible. Once buried into a wall or roof assembly however, hand-held meters are very limited in their usefulness. In order to perform long-term monitoring of wood members in an assembly, pairs of moisture pins, with lead wires are installed during construction of the assembly, with lead wires routed to an accessible location. A thermistor can also be set into the wood member near the moisture pins for temperature calibration. For repeated measures, the lead wires can be hooked up to the hand held moisture meter, but this requires someone to be present for each measure.

For repeated measurements and recordings, an automated moisture meter can be made using a data logger. The data logger can be programmed to provide a known voltage difference across the pins and determine the wood fiber resistance by comparing the voltage drop across the wood fibers to the voltage drop across a known resistor. The data logger can be programmed to take measurements and regular intervals and record the results in a database file. To monitor many moisture pin pairs, a multiplexer can be used in conjunction with the data logger.

The resulting resistance measurements can be converted into moisture content (for Douglas fir at 73 deg. F) using the following equation developed by the U.S. Forest Products Laboratory:

$$\log MC_u = 2.99 - 2.113\ X\ ((\log(\log R_w)))$$

Where : MC_u is uncorrected moisture content in %
R_w is the measured resistance of wood in Ohms

To correct for species and temperature a correlation equation has been developed, including an input for temperature and species correction.

$$MC_c = \left[\frac{R + 0.567 - 0.260\ T + 0.000051 T^2}{0.881\ (1.065)^T} - b\right]\frac{1}{a}$$

Where:
MC = corrected meter reading
R = meter reading
T = wood temperature in Deg. C
a and b = species correction coefficients

Using these two equations, temperature data and the correct species correlation coefficients, raw resistance measures can be converted into moisture content readings.

Air Tightness and Air Flow Measurements

In order to understand the air leakage characteristics of a specific building, it must first be measured. Given the complex nature of a building, including its geometry and the many components that make up the building enclosure, this is not a simple task. The two methods that have been developed are tracer gas measurement and blower door testing

Tracer Gas Measurement

One method of determining the natural air flow through the enclosure of a building is through the use of tracer gas measurements. An inert gas or vapour that is easily measurable can be introduced into a building and measured using several strategies. One strategy involves introducing the gas to the building until it reaches a known concentration and then measuring the rate of decay of the gas concentration over time. A second method involves the constant injection of the gas at a known rate measuring the increased concentration of the gas over time until equilibrium is obtained. A third method involves varying the rate of gas injection until the minimum rate is found that can maintain a concentration equilibrium.

Several major disadvantages make tracer gas testing impractical for most situations. First, testing is slow due to long equilibrium times and the fact that several measurements are required, spanning a range of weather conditions to get a representative average. Secondly, a thorough mixing of the tracer gas and interior air is required for accurate results, which requires many application heads and mixing fans. This equipment is large and cumbersome to transport, set-up and store when not in use. Due to these issues, tracer gas testing is not typically used for field testing.

Blower Door Testing

Most of the information currently available about air leakage in buildings has come from field pressurization testing using a blower door apparatus. This technology was first developed as a window-mounted unit in Sweden in the mid- 1970s to test the tightness of building enclosures (Blomsterbrg, 1977). The technology was then brought to the North America where it was further developed by a group of Canadian researchers in Saskatchewan lead by Harold Orr and independently, by researchers at Princeton University including Ken Gadsby, Gautam Dutt, David Harrje, and Frank Sinden.

The early use of blower doors in Sweden, Princeton and Saskatchewan uncovered the diagnostic potential of whole building pressurization testing. Blower Door could be used to uncover hidden leakage paths which lead to remediation techniques and design solutions for future buildings. Since the development of the technology, several standardized test procedures and reporting methods have been developed. The most commonly used testing standards are the ASTM Standard E779-87 (1991) and the Canadian standard - CGSB Standard 149 (1986).

One common metric used to determine relative air-tightness is the 'ACH 50' value. This value is determined by pressurizing (and/or depressurizing) the building to various levels between 10 and 60 Pa and recording the fan flow required to maintain pressure. The result is a curve relating air flow and pressure. The air flow required to maintain the building at 50 Pa pressure is then divided by the interior volume of the building to determine the number of air changes per hour (ACH) induced by the 50 Pa of pressure. Due to the relatively simple nature of the testing methods and equipment, and the repeatability of the results, blower door pressurization testing and the ACH50 value have become the 'gold' standard of whole building air leakage testing. This metric is commonly used in home energy certification programs such as R-2000, Energy Star and Passivhaus and can even be found in the national building codes of Sweden and Norway. While it is now well understood that blower door testing can be used to measure relative air tightness, the data could not be used to directly determine the most useful parameter- air leakage occurring under natural conditions.

In an attempt to use blower door pressurization data to determine a more useful 'natural' air leakage rate, many numerical methods and complex models have been developed.

In its simplest form, the relationship between whole building air leakage at 50 Pa pressure, and whole building air leakage in a natural state can be expressed as a power law (Baker et al. 1987).

$Q = C * (\text{delta } P)^n$ where C is the flow coefficient and n is the flow exponent

The flow exponent is an expression of the air flow path and is considered a combination of turbulent (n = 0.5) and laminar (n = 1.0) flow. Jokisalo et al. (2009) determined the flow exponents for new residential buildings in Finland and found that they vary between 0.6 and 0.9 with an average of 0.72. Orme et al. (1994) summarized 1,758 flow exponent measurements from Canada, Netherlands, New Zealand, the UK and the US. The distribution of flow exponent is roughly normal with a mean value of approximately 0.66. Based on this study, a value of 0.65 is typically used, unless further information is available.

since the flow coefficient is unknown and is a property of the enclosure, we solve for C

At 50 Pascal (blower door test): $C = (50 \text{ Pa})^{.65}/Q_{50}$

In situ, the pressure difference across the building enclosure is a function of wind, stack effect and the mechanical ventilation system. The pressure caused by these effects fluctuates constantly. To determine annual average infiltration rate, average pressure differences are used. Studies of low rise residential buildings in Finland reported typical negative and positive pressures of 5–10 Pa (Kalamees et al., 2007. (OTHER REFERENCES?) 4 Pa is commonly used to estimate annual air leakage from blower door data. Using the power law above and an average 4 Pa pressure difference:

At 4 Pascal (natural air leakage): $C = (4 \text{ Pa})^{.65}/Q_4$

Since leakage occurs through the same building enclosure the flow coefficient (C) in both of the equations above are equal. Therefore the equation can be expressed as:

$(50)^{.65}/Q_{50} = (4)^{.65}/Q_4$

solving for Q_4:

$Q_4 = Q_{50} * (4/50)^{.65}$

This simple power law is commonly used to estimate natural building air leakage based on the results of blower door testing. Other, more complex models and mathematical techniques are available, such as the Lawrence Berkely Laboratory (LBL) model. The LBL model attempts to determine hourly leakage rates based on the leakage characteristics of the building (as determined by blower door testing), temperature, wind and stack pressure effects. The hourly leakage estimates are then used with a weighted averaging method to determine the 'effective air change rate'.

Typical Air Leakage Rates

Several surveys of air leakage rates for residential building have been conducted in various areas of the world. A summary of these surveys can be seen in Table 1.

1) A study of 433 homes throughout the United Kingdom built over a 100 year period (pre 1900 to 1993) by the Building Research Establishment (Stephen, R.K., 1998) showed an average ACH_{50} of 11.5. These measurements had a large range from 3 to 28 with an average of 11.5. The average air tightness of the 80 homes built after 1987 was only slightly better than the average, at 9.6.
2) A survey of 32 cavity brick homes build in the 1950's in Scotland showed air leakage rates of 10 to 24 $ACH_{50,}$ with an average of 18 (Galbraith, et al., 1988).
3) A survey of 24 houses in three northern areas of Canada, build mostly in the 1970 and 1980s showed a range of ACH 50 values from 3.6 to 19, with an average ACH 50 of 8.5 (Rousseau et al. 2007).
4) A survey of 100 newly built, wood framed houses in Finland showed an average ACH 50 of 3.9 (Jokisalo et al. 2009).

Air Tightness Standards

As the importance of air tightness to building performance has been more fully understood, different standards have been developed by both mandatory building code agencies and voluntary energy rating certification groups.

Both Finland and Norway have included the concept of whole building air tightness into the national building code since the 1970s. Sweden's current code requires ACH_{50} values of 3.0 for detached homes, 2.0 for low rise multi-unit dwellings and 1.0 for high rise multi-unit buildings.

Several voluntary low energy building certification programs also have strict air tightness requirements. Canada's R2000 program requires an ACH_{50} value of 1.5, while the Energy Star for new homes program, which can be found in Canada and the United States requires and ACH_{50} value of 2.5. Several European programs including the French Effinerie program and the Swiss Minergie program have even higher standards for air tightness. These programs are mostly based on the German Passivhaus standard, which requires an ACH_{50} value of 0.6.

Appendix B: Exterior Insulation Options

Polyisocyanurate (PIC)

PIC is a thermoset plastic, based on cross-linked polymers. This structure allows it to remain more stable under high temperature conditions. The PIC insulation is created by reacting isocyanurate with blowing agents, additives and surfactants. The blowing agent is typically pentane, which has a low global warming potential (GWP). The commercially available versions are typically a blend of polyurethane foam and polyisocyanurate. The result is a closed cell foam with greater strength, better fire resistance and higher R-value than either foam individually. PIC sheet products typically have a facer for rigidity. Fiberglass mesh and aluminum foil are two typical facer materials.

Due to its stability at high temperatures, PIC is commonly used in roofing applications. When faced with aluminum foil, the foil acts as a radiant barrier, improving the R-value of the product under certain circumstances. PIC is less resistant to taking on liquid water than XPS, and does not allow water to drain and dry out quickly, like EPS. For this reason, PIC is usually not appropriate for below grade applications. PIC typically has an R-value of approximately R-7 per inch, however thermal resistance has been shown to decrease at low temperatures and over time as the blowing agent contained in the material is slowly replaced with air. The vapour permeability of PIC foam itself is approximately 3.0 perm per inch however fibreglass faced PIC boards are much lower at less than 1.0 perm., while foil faced boards are much lower again at 0.03 perm.

Extruded Polystyrene (XPS)

XPS is thermoplastic, based on linear or slightly branched (non-cross linked) polymers. It is manufactured by mixing molten polystyrene with a blowing agent under high temperature and high pressure. The blowing agent typically used is HFC 134a, which has a much higher global warming potential than pentane. The foam is the extruded through a die to form panels. This process results in a more regular cell structure and a final product this is stronger and more resistant to taking on water than EPS. The density of the product can be varied to create greater compressive strength, however a density of 2 pounds per square foot is most common.

Common uses of XPS in residential construction include insulated sheathing for above grade walls, below grade wall and slab insulation and insulating the interior surface of foundation walls. XPS is more resistant to taking on liquid water than EPS, but is also less able to allow drying via vapour flow than EPS. XPS typically has an R-value of approximately R-5 per inch and a vapour permeability of approximately 1.0 perm per inch.

Expanded Polystyrene (EPS)

EPS is thermoplastic, based on linear or slightly branched (non-cross linked) polymers. It is manufactured by expanding beads of polystyrene to fill a mold. The blowing agent used to form the beads is typically pentane, which has a low global warming potential. The density of the beads can be controlled, with an increased density resulting in increased thermal resistance, vapour resistance and compressive strength. Although the EPS beads are formed from closed cell foam, the gaps between the beads can allow liquid water and water vapour to pass into and through the material, making the product act like an open cell foam. The most common variants of EPS are Type I EPS which has a density of 1 pound per cubic foot (16 kg/m^3), Type II EPS which has a density of 1.5 pounds per cubic foot (24 kg/m^3) and Type IV EPS which has a density of 2 pounds per square foot (32 kg/m^2). The more dense products are more appropriate for below grade applications since its higher density makes it more durable.

Common uses of EPS in residential construction include insulated concrete forms (ICF), the core of Structural Insulated Panels (SIP) and as under slab insulation. Although EPS can take in liquid water, it can also drain and dry out quickly. Type II EPS has an R-value of approximately R-4 per inch and a vapour permeability of approximately 3.5 perm per inch.

Rockwool Insulated Sheathing

Rockwool is manufactured using a molten mixture of slag, coke, volcanic rock and recycled rockwool. The molten mixture is spun to form strands and the strands are laid down in layers with varying orientations with oil and a binding agent sprayed between the layers. Once laid to an appropriate thickness, the layers are compressed to the desired density and the product passes through an oven to cure the binding agent. The product id then cooled and cut to the desired size of panel. For exterior insulating applications, the density is set between 8 and 12 pounds per square foot, creating a stiff board-like product. The boards have some water resistance due to their density and oil content, however water vapour can readily pass through the rockwool boards.

Common uses for rockwool sheathing products include above and below grade wall insulation, and roofing applications. Rockwool insulated sheathing has an R-value of approximately R-4 per inch and a vapour permeability of approximately 30 perm per inch.

Appendix C: Determining Experimental Air Flow Rate

To simulate air exfilatration during cold weather, an air injection system was designed (see Section 4.7.3.2). This system was designed to simulate a common point source of air leakage such as an electrical outlet in an exterior wall. Previous studies of air leakage condensation produced exfilatration by applying pressure differences across a flaw in the air barrier such as an unsealed joint. The limitation of this method is that the air flow rate is only estimated. For the current study, we chose to control air flow rate directly using adjustable flow rate rotameters at each test wall. This way, we could be assured that all walls were receiving the same amount of air flow and therefore were being exposed to the same amount of moisture.

To determine an appropriate air flow rate, the following steps were followed:

1) The current Energy Star for New Homes limit for air leakage was used as the starting point. This program requires a maximum normalized air leakage rate of 0.2 CFM per sq. foot of building enclosure (1.02 l/s/m2) at 50 Pa pressurization.
2) It was assumed that air leakage is not completely diffuse, but occurs at multiple flaws in the air barrier system, which are relatively evenly distributed across all areas of the building enclosure.
3) This pressurized leakage rate was then converted to the air leakage rate expected under natural conditions. This was done using the power law (Laddament, 1987). This method has been commonly accepted and used by several national standards associations in North America (ASTM Standard E779, (1982), CGSB Standard 149.10-M86, (1986), ISO Standard 9972, (1995)) for calculating air flow through building enclosure based on blower door pressurization testing.

   The power law states:

   $Q = C * (\text{delta } P)^n$:

   where Q = air flow rate
   C = flow coefficient
   P = pressure
   n = flow exponent

   i. Since the flow coefficient is unknown and is a property of the building enclosure, we solve for C under both pressurized and natural conditions.

   ii. Based on previous studies of pressures in low rise residential buildings in cold climate (Kalamees et al., 2007; Jokasalo et al., 2008), a natural average pressure of 4 Pa is commonly used.
   iii. The flow exponent is an expression of the air flow path and is considered a combination of turbulent (n = 0.5) and laminar (n = 1.0) flow. Jokisalo et

al. (2009) determined that the flow exponents for new residential buildings in Finland vary between 0.6 and 0.9 with an average of 0.72. Orme et al. (1994) summarized 1,758 flow exponent measurements from Canada, Netherlands, New Zealand, the UK and the US. The distribution of flow exponent is roughly normal with a mean value of approximately 0.66. Based on this study, a value of 0.65 is typically used, unless further information is available.

Based on these assumed values, the power law was applied under both pressurized and natural conditions. Since the flow coefficient is unknown, and is a constant property of a given building enclosure, the power law is solved for C.

$C = (50\ Pa)^{.65}/Q_{50}$ and $C = (4\ pa)^{.65}/Q_4$

Therefore

$(50)^{.65}/Q_{50} = (4)^{.65}/Q_4$

solving for Q_4:

$Q_4 = Q_{50} * (4/50)^{.65}$

Q_4 = natural leakage = .039 CFM per sq. ft = .198 $l/s/m^2$

4) Applying this natural leakage rate to the wall test panels requires an assumption about the distribution of the air leakage locations in an average building. We chose to consider the center test bay of each wall an average representative sample of the building enclosure. At 2 feet wide by 8 feet high, the test bay has an area of 16 square feet. Applying a leakage rate of .039 CFM per sq. ft to this natural leakage rate:

Wall leakage rate = normalized natural leakage rate * area
= .039 CFM * 16 sq. ft
= .642 CFM per test wall
or 37.4 CFH per test wall

5) Due to the accuracy of the air flow rotameters, we chose to inject 40 CFH into each test wall.

Appendix D: Schematic Diagrams of Data Acquisition System

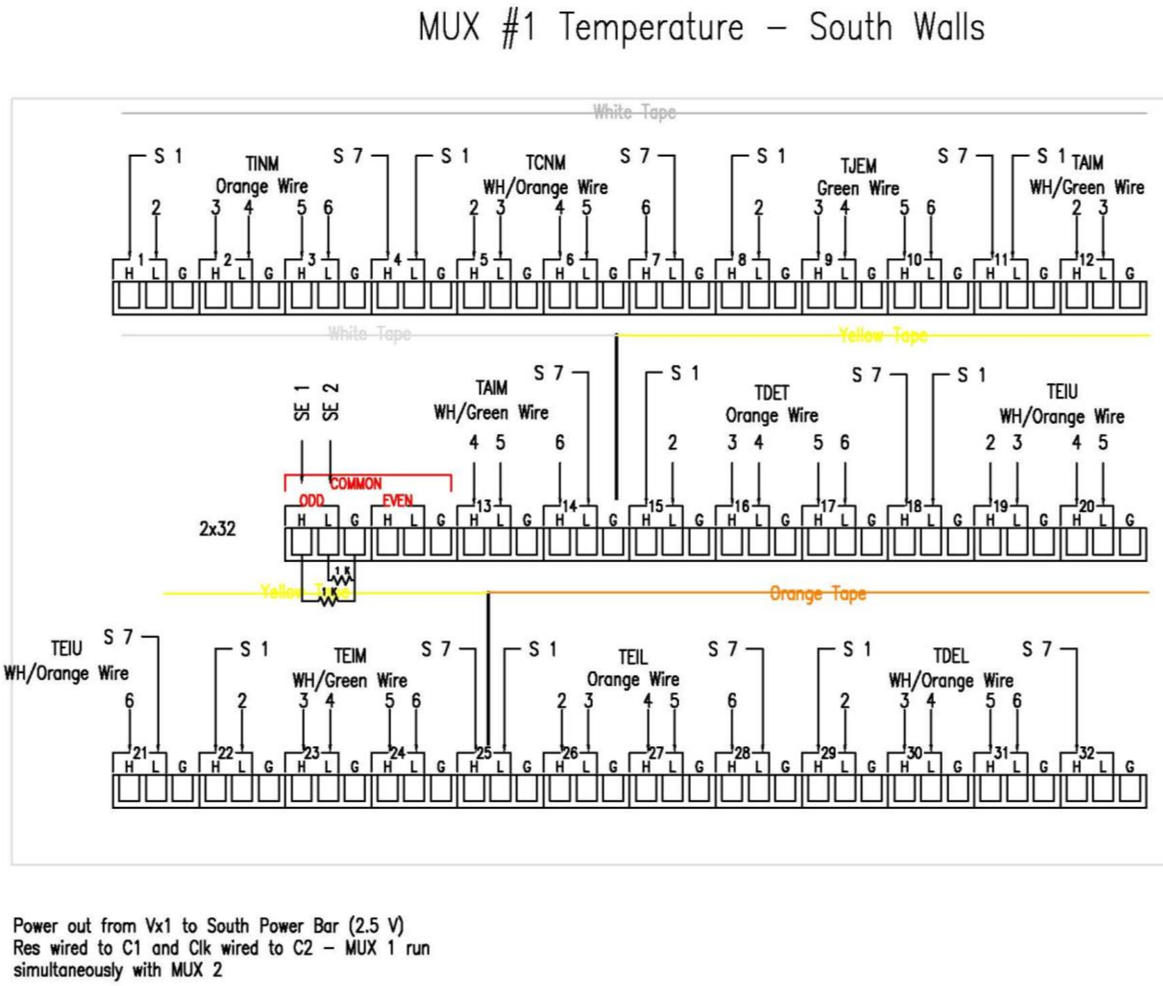

Figure 84- Wiring diagram for MUX #1 – South wall temperature sensors

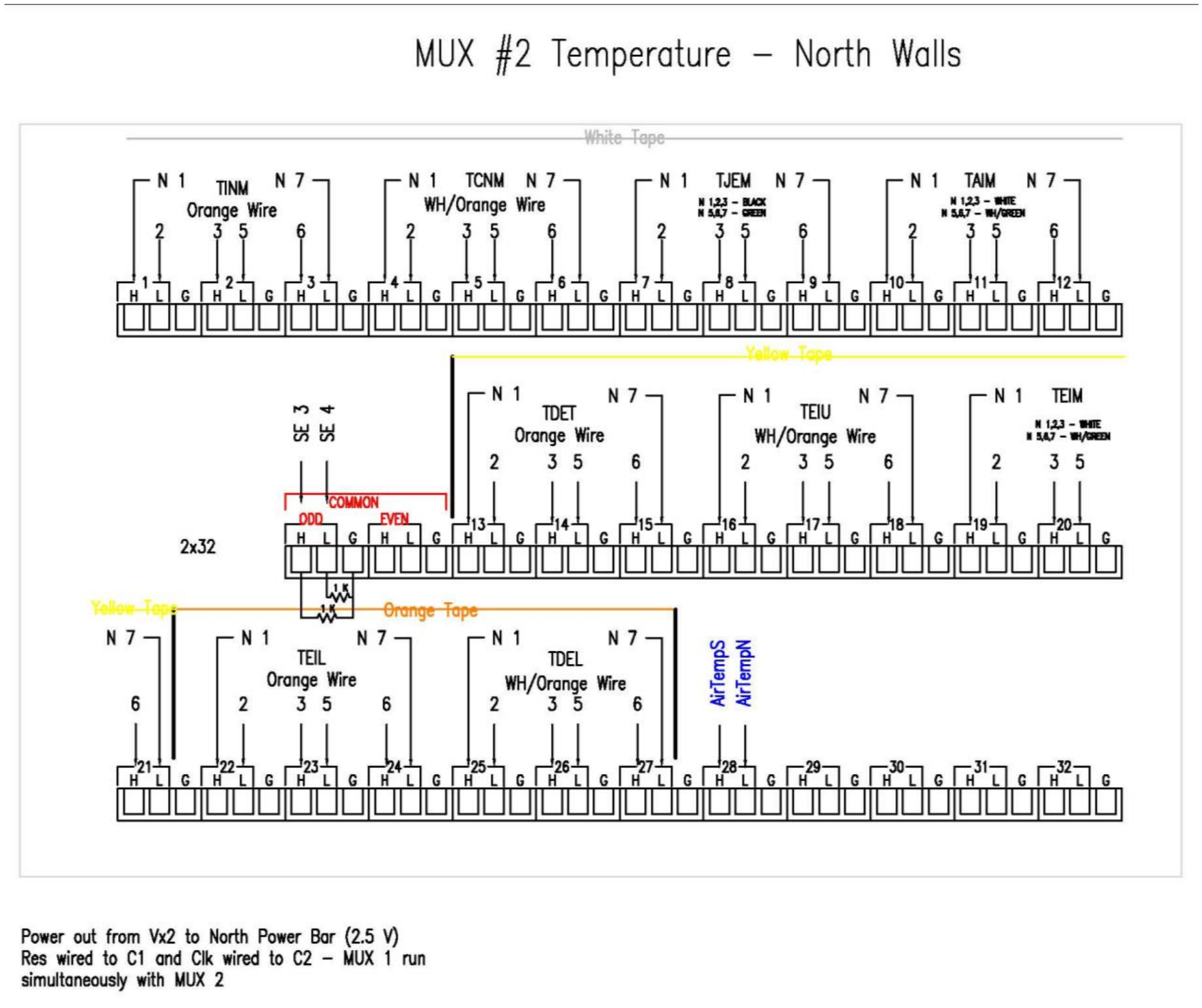

Figure 85- Wiring diagram for MUX#2 - North wall temperature sensors

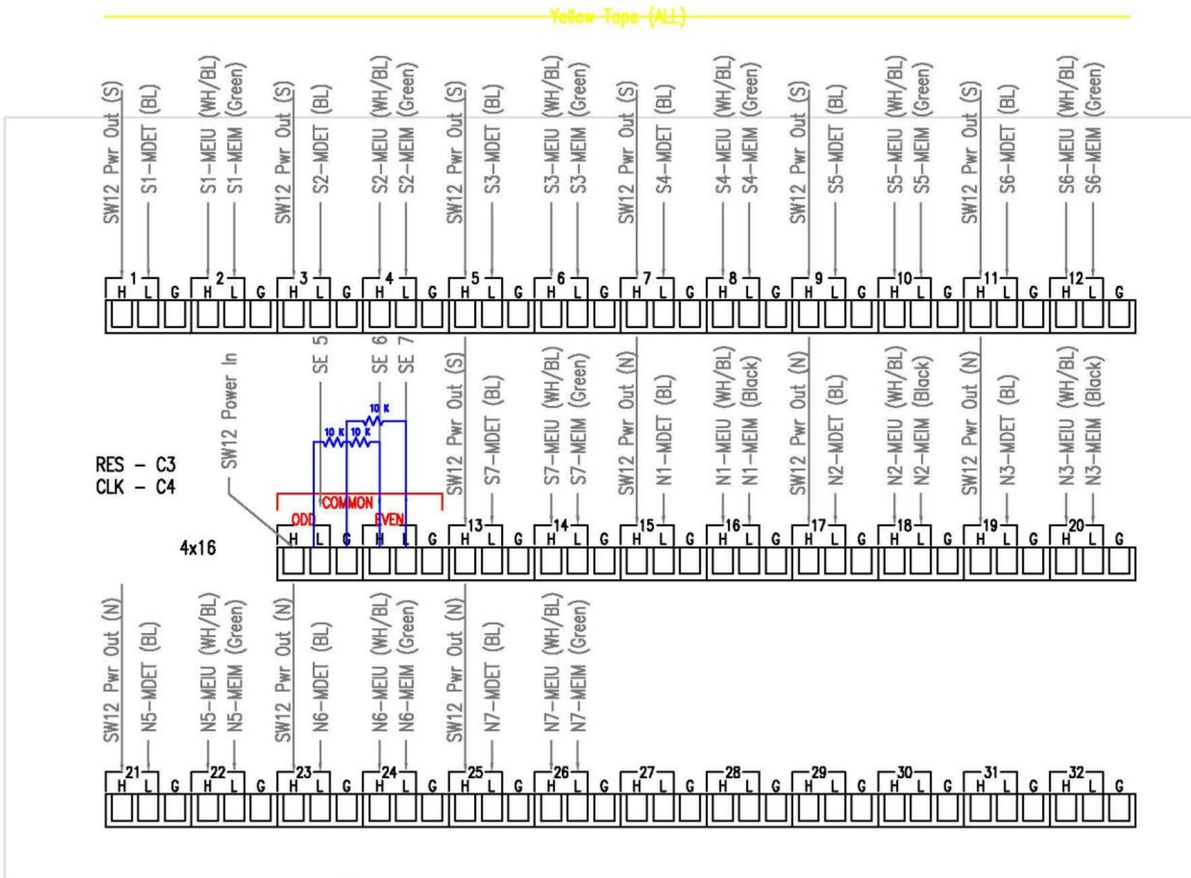

MUX #3 Moisture Content – Top 3 pin sets

7 – SW12 Power wires out to S Power Bar – CH 1–13 (ODD H) Blue {Bundled or individual as necessary}
6 – SW12 Power wires out to N Power Bar – CH 15–25 (ODD H) Blue {Bundled or individual as necessary}

Figure 86- Wiring diagram for MUX #3 – Upper 3 moisture content sensors

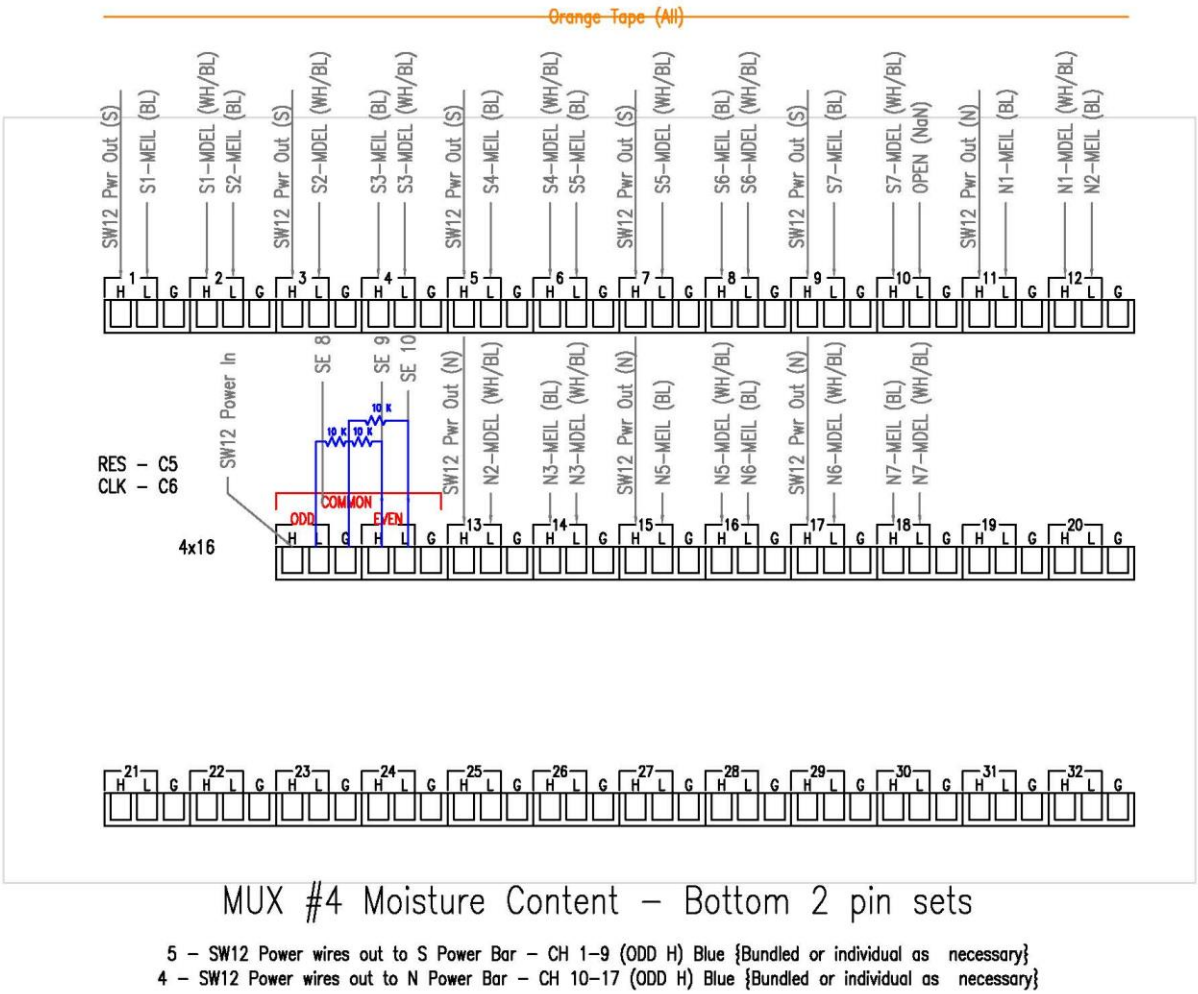

Figure 87- Wiring diagram for MUX #4 – bottom two moisture content sensors

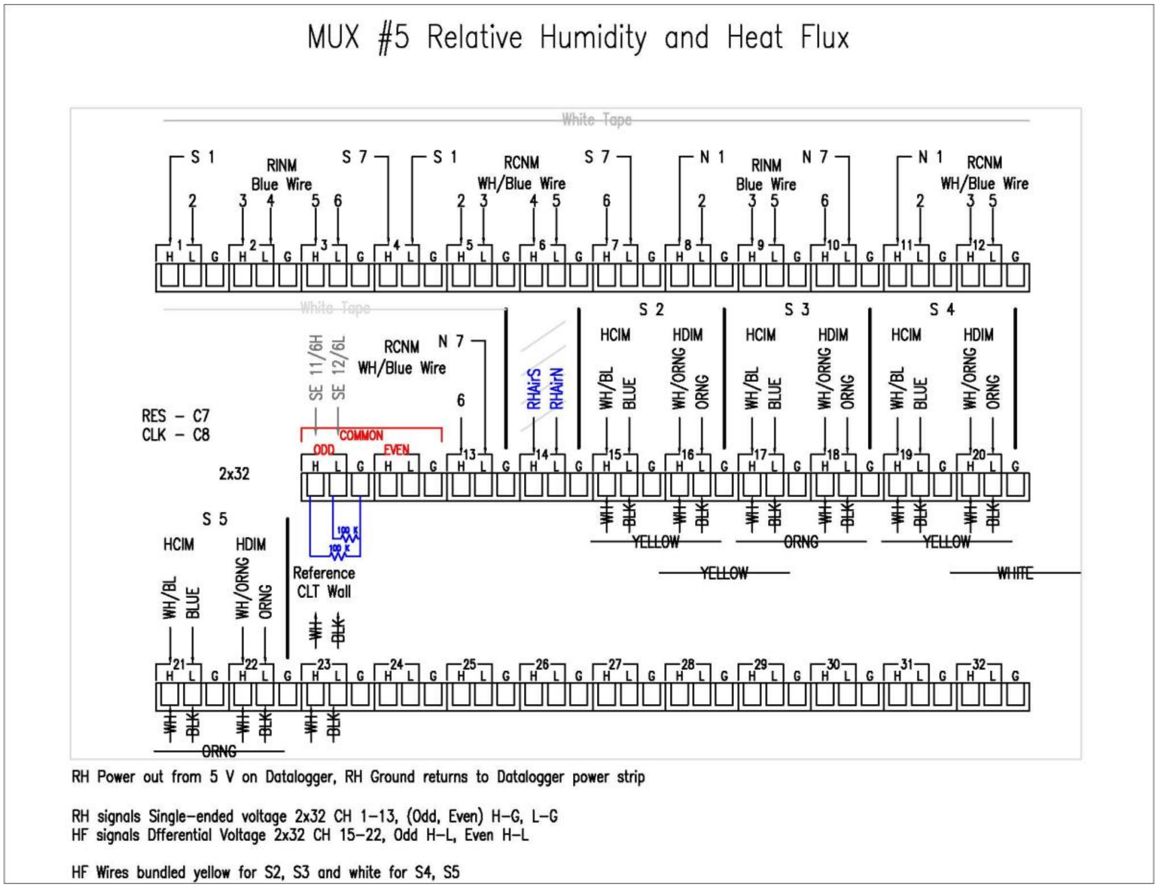

Figure 88- Wiring diagram for MUX #5 – RH and heat flux sensors